



Czech Technical University in Prague
Faculty of Nuclear Sciences and
Physical Engineering

DOCTORAL THESIS

**General Framework for
Classification at the Top**



Prague, 2023

Ing. Václav Mácha

Acknowledgements:

Thanks thanks thanks thanks thanks thanks thanks thanks thanks thanks thanks
thanks thanks thanks thanks thanks thanks thanks thanks thanks thanks thanks
thanks

Declaration:

Thanks thanks thanks thanks thanks thanks thanks thanks thanks thanks thanks
thanks thanks thanks thanks thanks thanks thanks thanks thanks thanks thanks
thanks

V Praze dne 1. prosince 2022

.....
Ing. Václav Mácha

Bibliografický záznam

Autor:	Ing. Václav Mácha, České vysoké učení technické v Praze, Fakulta jaderná a fyzikálně inženýrská, Katedra matematiky
Název práce:	Title title title title title title
Studijní program:	Aplikace přírodních věd
Studijní obor:	Matematické inženýrství
Školitel:	doc. Ing Václav Šmídl, Ph.D., České vysoké učení technické v Praze, Fakulta elektrotechnická, Katedra počítačů
Školitel specialista:	Mgr. Lukáš Adam, Ph.D., České vysoké učení technické v Praze, Fakulta elektrotechnická, Katedra počítačů
Akademický rok:	2022/2023
Počet stran:	137
Klíčová slova:	Keywords keywords keywords keywords keywords keywords key- words keywords keywords keywords keywords keywords keywords key- words

Abstrakt

[illegible]

Bibliographic Entry

Author:	Ing. Václav Mácha, Czech Technical University in Prague, Faculty of Nuclear Sciences and Physical Engineering, Department of Mathematics
Title of Dissertation:	General Framework for Classification at the Top
Degree Programme:	Application of Natural Sciences
Field of Study:	Mathematical Engineering
Supervisor:	doc. Ing Václav Šmídl, Ph.D., Czech Technical University in Prague, Faculty of Electrical Engineering, Department of Computer Science
Supervisor Specialist:	Mgr. Lukáš Adam, Ph.D., Czech Technical University in Prague, Faculty of Electrical Engineering, Department of Computer Science
Academic Year:	2022/2023
Number of Pages:	137
Keywords:	Binary classification, ranking, accuracy at the top, Neyman-Pearson, hypothesis testing

Abstract

In standard binary classification, the goal is to classify all samples with the lowest possible error. However, in many applications, the error for one class is more severe than the other, especially if the classes are not balanced. A typical example is cancer detection. Classifying a sick patient as healthy is a more serious error than the other way around. However, we still want to minimize both errors since trying to cure a healthy patient is also not ideal. Therefore the ultimate goal is to minimize the number of sick patients classified as healthy with some constraint on the number of healthy patients classified as sick. This formulation belongs to the class of problems where the performance is evaluated only on a small number of relevant (top) samples. We call this class classification at the top, and it is the main object of this work.

Many well-known categories of problems, such as ranking, accuracy at the top, or hypothesis testing, are closely related to classification at the top. In this work, we introduce a unified framework for classification at the top, show that several known formulations fall into the framework, and propose entirely new formulations (*Pat&Mat*, *Pat&Mat-NP*) that fall into the framework. We provide a theoretical analysis of the framework for the primal form when a linear model is used. We also discuss the theoretical properties of individual formulations and potential pitfalls that some formulations may encounter. Besides that, we show the convergence of the stochastic gradient descent for selected formulations even though the gradient estimate is inherently biased. Moreover, we derive dual forms of selected formulations, show how to incorporate non-linear kernels into these forms, and derive an efficient coordinate descent algorithm to solve them. We also study the primal forms with non-linear models. We show that when we use a non-linear model, the resulting formulations are non-decomposable. This property prevents us from using stochastic gradient descent in a standard way. We introduce modified stochastic gradient descent and show that this modification leads to a biased estimate of the true gradient. To mitigate this issue, we propose a new formulation *DeepTop-Push*. Lastly, we demonstrate the performance of proposed formulations on visual recognition datasets and real-world applications on steganalysis and malware detection datasets.

Contents

Introduction	1
1 Introduction to Classification at the Top	3
1.1 Binary Classification	3
1.2 Performance Evaluation	5
1.2.1 Confusion Matrix	5
1.2.2 ROC Analysis	7
1.3 Classification at the Top	9
1.3.1 Ranking Problems	10
1.3.2 Accuracy at the Top	12
1.3.3 Hypothesis Testing	13
1.4 Summary	14
2 Framework for Classification at the Top	15
2.1 Surrogate Formulation	15
2.2 Ranking Problems	17
2.3 Accuracy at the Top	18
2.3.1 Threshold Comparison	20
2.3.2 Efficient Computing of the Threshold for <i>Pat&Mat</i>	20
2.4 Neyman-Pearson Problem	21
2.4.1 Threshold Comparison	23
2.5 Summary	24
3 Primal Formulation: Linear Model	27
3.1 Convexity	27
3.2 Differentiability	28
3.3 Stability	29
3.4 Stochastic Gradient Descent	32
3.5 Summary	34
4 Dual Formulation: Linear Model	37
4.1 Derivation of Dual Problems	37
4.1.1 Family of <i>TopPushK</i> Formulations	39
4.1.2 Family of <i>Pat&Mat</i> Formulations	40
4.2 Kernels	41
4.3 Coordinate Descent Algorithm	42
4.3.1 Update Rules	42
4.3.2 Initialization	44
4.4 Summary	46

5	Primal Formulation: Non-Linear Model	49
5.1	Bias of Sampled Gradient	50
5.2	<i>DeepTopPush</i>	52
5.3	Theoretical Justification	53
6	Numerical Experiments	55
6.1	Settings	55
6.1.1	Formulations	55
6.1.2	Hyper-parameters	57
6.1.3	Datasets	58
6.1.4	Performance Criteria	59
6.1.5	Critical Difference Diagrams	60
6.1.6	Implementation	60
6.2	Image Recognition	60
6.2.1	Primal Formulation: Linear Model	61
6.2.2	Dual Formulation: Linear Model	64
6.2.3	Primal Formulation: Non-Linear Model	65
6.3	Steganalysis	70
6.3.1	Nsf5	70
6.3.2	JMiPOD	71
6.4	Malware Detection	73
	Conclusion	75
	Appendices	77
A	Appendix for Chapter 2	79
B	Appendix for Chapter 3	81
B.1	Convexity	81
B.2	Differentiability	82
B.3	Stability	83
B.4	Stochastic Gradient Descent	88
B.4.1	General Results	88
B.4.2	Proof of Theorem 3.9	89
B.4.3	Auxiliary Results	94
C	Appendix for Chapter 4	97
C.1	Derivation of Dual Problems	97
C.1.1	Family of <i>TopPushK</i> Formulations	97
C.1.2	Family of <i>Pat&Mat</i> Formulations	100
C.2	Coordinate Descent Algorithm	101
C.2.1	Family of <i>TopPushK</i> Formulations	101
C.2.2	Family of <i>Pat&Mat</i> Formulations	110
D	Appendix for Chapter 5	121
	Bibliography	123

Introduction

The modern world is a world of information. In the past few decades, we have witnessed the rapid spread of computers, the internet, smart devices, sensors, etc., to every possible aspect of our lives. All these new technologies provide us with valuable data. But the amount of data is enormous, and the time when it was possible to process all the data manually is long gone. Thus, the need for methods that can process data automatically without explicitly being programmed for specific tasks has grown significantly. The field devoted to such methods is machine learning and covers many different approaches to achieving such goals [1]. In this work, we focus on one specific subcategory of machine learning called classification [2].

Classification can be easily described on autonomous cars. Autonomous cars are getting more and more popular these days. One problem that they must solve is the recognition of road signs. Let's say that we have a lot of images of road signs. All these signs can be grouped into a finite number of classes based on their meaning. Classification aims to find a function that returns the corresponding class to which the road sign from the image belongs [3]. Such a function is usually called a classifier, and the process of finding a classifier is called training.

In most cases, the classifier is a parameterized function. In such a case, training is the process of finding parameter values for which the classification is most accurate. To be able to train the best parameter values, we need a so-called training set. In the case of classification, each data point in the training set consists of features and a corresponding label. The features describe the object of interest in a way understandable for computers. The label is the identifier of the class to which the object of interest belongs. Problems that assume a labeled training set are called supervised learning problems [2]. In our example, the features are individual pixels of the image of the road sign, and the label is its type. The labels in the training set are essential because they allow us to determine which classifier parameters provide the most accurate predictions. However, they are usually challenging and expensive to obtain, as the labeling process must be done manually by a person with experience in the corresponding field. Notably, the labels are only used during training. Once the training is finished, only the features are needed to use the classifier.

The problem of classification is very important, and many real-world problems can be formulated as classification problems:

- **Autonomous Cars:** As we have already mentioned, the classification can be used for autonomous cars, for example for road sign recognition [3].
- **Medical Diagnosis:** In medicine, classification is often used to improve disease diagnosis. In such a case, the features are medical records such as the patient's blood tests, temperature, or x-ray images. The classes are whether the patient has some disease or not. As an example, we can mention the classification of mammogram images. In such a case, the goal is to detect whether the patient has cancer [4, 5].
- **Spam Detection:** Another use of classification can be found in detecting spam emails based on the content of the email [6].
- **Internet Security:** These days, the internet is a crucial part of our lives. With its increasing usage, the number of attacks also increases. An essential part of the defense are

intrusion detection systems [7, 8] that search for malicious activities (network attacks) in network traffic. Classification can be used to improve such systems, as shown in [9, 10].

- **Marketing:** In marketing, the task can be to classify customers based on their buying interests. Such information can be used to build a personalized recommendation system for customers and therefore increase income [11, 12].

From the previous examples, it is clear that classification is a problem present in many sectors. We can also see that many classification problems contained only two classes. For example, we want to detect whether the patient has some disease or not in medical diagnosis. Or in spam detection, we have a class of clear and spam emails. Such problems are usually called binary classification. The rest of the work focuses only on binary classification problems and is organized as follows:

- Chapter 1 introduces the general formulation for binary classification and discussed how to measure the performance of binary classifiers. Furthermore, we show that standard binary classification optimizes overall performance. However, many problems closely tied to binary classification only focus on the performance of the most relevant samples. We introduce three categories of such problems and discuss their relation to binary classification.
- Chapter 2 introduces a general optimization framework for classification at the top. Many problems fall into this framework even though they are usually considered separate problems. We describe Ranking problems, Accuracy at the Top, and the Neyman-Pearson problem in more detail and show that many formulations from these three categories fall into the framework. Moreover, we derive two new formulations closely related to the existing one. Finally, we discussed the basic properties and relations between introduced formulations. All formulations are introduced in a general form with arbitrary model f , even though many of them have been initially designed only for a linear model. Theoretical properties of the formulations with different models are discussed later.
- Chapter 3 is dedicated to the linear model and formulations in their primal form, i.e., in the form presented in this chapter. This chapter shows that some formulations have nice properties such as convexity, differentiability, or stability. We derive some theoretical guarantees for the optimal solution based on these properties.
- Chapter 4 is dedicated to the dual forms of formulations from Table 2.1. In this chapter, we again assume a linear model only and show that all formulations can be split into two families based on their similarities. Then we derive dual formulations for these two families and show that these formulations are very similar to standard SVM. Using this observation, we use the kernel trick to employ non-linearity into the formulations. Finally, we derive an efficient algorithm for solving the formulations.
- In Chapter 5, we assume a nonlinear model. A prototypical example of such a model can be a neural network. The resulting formulations are not decomposable since the decision threshold is always a function of all classification scores. Therefore, it is impossible to use the stochastic descent algorithm directly to solve them. In Chapter 5, we present two approaches for dealing with this problem.
- Chapter 6 is dedicated to all numerical experiments.

Chapters 1 and 2 are crucial for the whole work since they introduce all formulations that are studied in the rest of the work. On the other hand, Chapters 3, 4, and 5 study the properties of these formulations in three different settings. Therefore, these three chapters can be read separately.

Introduction to Classification at the Top

In the previous chapter, we briefly introduced binary classification and what it is suitable for. In this chapter, we introduce binary classification more formally and define the notation used in the rest of the work. Moreover, we discuss several approaches that can be used to measure the performance of binary classifiers. Finally, we present the problem of classification at the top, which is closely related to binary classification. This problem is the main topic of the entire work.

1.1 Binary Classification

As we discussed before, binary classification is the special case of classification in which the total number of classes is two. Although these classes can have arbitrary names, we call the class we are interested in the *positive class* and the other class the *negative class*. Moreover, we use the label $y = 1$ to denote the positive class and $y = 0$ to denote the negative class. The notation used in the rest of the work is summarized in Notation 1.1.

Notation 1.1: Dataset

In this work, we use label 0 to encode the negative class and label 1 to encode the positive class. By a dataset of size $n \in \mathbb{N}$ we mean a set of pairs in the following form

$$\mathcal{D} = \{(\mathbf{x}_i, y_i)\}_{i=1}^n,$$

where $\mathbf{x}_i \in \mathbb{R}^d$ represents samples and $y_i \in \{0, 1\}$ corresponding labels. To simplify future notation, we denote a set of all indices of dataset \mathcal{D} as $\mathcal{I} = \mathcal{I}_- \cup \mathcal{I}_+$, where

$$\mathcal{I}_- = \{i \mid i \in \{1, 2, \dots, n\} \wedge y_i = 0\},$$

$$\mathcal{I}_+ = \{i \mid i \in \{1, 2, \dots, n\} \wedge y_i = 1\}.$$

We also denote the number of negative samples in \mathcal{D} as $n_- = |\mathcal{I}_-|$ and the number of positive samples in \mathcal{D} as $n_+ = |\mathcal{I}_+|$. The total number of samples is $n = n_- + n_+$.

The goal of any classification problem is to classify given samples with the highest possible accuracy or, in other words, with the lowest possible error. In the case of binary classification, there are two types of error: a positive sample is classified as negative, and vice versa. Formally, using the Notation 1.1, the minimization of these two types of errors can be written as follows

$$\begin{aligned} & \underset{\mathbf{w}, t}{\text{minimize}} && C_1 \sum_{i \in \mathcal{I}_-} \mathbb{1}_{[s_i \geq t]} + C_2 \sum_{i \in \mathcal{I}_+} \mathbb{1}_{[s_i < t]} \\ & \text{subject to} && s_i = f(\mathbf{x}_i; \mathbf{w}), \quad i \in \mathcal{I}, \end{aligned} \tag{1.1}$$

where $C_1, C_2 \in \mathbb{R}$, the function $f: \mathbb{R}^d \rightarrow \mathbb{R}$ is further referenced as a model and $\mathbb{1}_{[\cdot]}$ is the Iverson function which is used to count misclassified samples and is defined as

$$\mathbb{1}_{[x]} = \begin{cases} 0 & \text{if } x \text{ is false,} \\ 1 & \text{if } x \text{ is true.} \end{cases} \quad (1.2)$$

Moreover, the vector $w \in \mathbb{R}^d$ represents trainable parameters (weights) of the model f and $t \in \mathbb{R}$ represents a decision threshold. The parameters w are determined from the training set. Although the decision threshold t can also be determined from the training data, in many cases, it is fixed. For example, many training algorithms assume that the classification score $s_i = f(x_i; w)$ given by the model f represents the probability that the sample x_i belongs to the positive class. Therefore, the decision threshold is set to $t = 0.5$, and the sample is classified as positive if its classification score is larger than this threshold. In Notation 1.2, we summarize the notation used in the rest of the work.

Notation 1.2: Classifier

By classifier, we always mean a pair of a model f and a corresponding decision threshold t . By model, we mean a function $f: \mathbb{R}^d \rightarrow \mathbb{R}$ which maps samples x to its classification scores s , i.e. for all $i \in \mathcal{I}$ the classification score is defined as

$$s_i = f(x_i; w),$$

where w represents trainable parameters (weights) of the model f . Predictions are defined for all $i \in \mathcal{I}$ in the following way

$$\hat{y}_i = \begin{cases} 1 & \text{if } s_i \geq t, \\ 0 & \text{otherwise.} \end{cases} \quad (1.3)$$

In the introduction, we briefly described how to find the best classifier. However, this process is more complicated in the real world. The whole process can be split into the four phases:

- **Training:** The first phase is the actual training of the classifier. In this phase, we use some algorithm to find the trainable parameters of the classifier based on the provided training set. Returning to the formulation of binary classification 1.1, in this phase, we want to find weights w and the threshold t . However, most formulations have some hyperparameters, such as C_1 and C_2 in 1.1. These hyperparameters are fixed for training. Multiple classifiers with different hyperparameter values are typically trained in the training phase.
- **Validation:** The validation phase selects the best hyper-parameter values that lead to the most performant and robust classifier. In this phase, the performance of classifiers from the training phase is evaluated on the so-called validation set. The validation set has the same structure as the training set but contains different samples.
- **Testing:** In the testing phase, the classifier with the best performing values of hyperparameters is tested against different classifiers. For the testing, the testing set is used. The testing set also has the same structure as the training set (it contains the labels) but contains different samples.
- **Inference:** In the previous phases, we trained multiple classifiers and selected the best one for our specific task. In the inference phase, we apply this classifier to real unlabeled data.

1.2 Performance Evaluation

In the previous section, we defined general binary classification problem (1.1). However, we did not discuss how to measure the performance of the resulting classifier. In this section, we introduce basic performance metrics that are used to measure the performance of binary classifiers.

1.2.1 Confusion Matrix

Based on the prediction \hat{y}_i from (1.3) and the actual label y_i of the sample \mathbf{x}_i , each sample can be assigned to one of the four following categories:

- **True negative:** sample \mathbf{x}_i is negative and is classified as negative, i.e. $y_i = 0 \wedge \hat{y}_i = 0$.
- **False positive:** sample \mathbf{x}_i is negative and is classified as positive, i.e. $y_i = 0 \wedge \hat{y}_i = 1$.
- **False negative:** sample \mathbf{x}_i is positive and is classified as negative, i.e. $y_i = 1 \wedge \hat{y}_i = 0$.
- **True positive:** sample \mathbf{x}_i is positive and is classified as positive, i.e. $y_i = 1 \wedge \hat{y}_i = 1$.

If we assign each sample from dataset \mathcal{D} to one of the categories above and count the number of samples in each of these four categories, we get the confusion matrix (sometimes also called contingency table) [13], see Figure 1.1. A confusion matrix consists of four fields that contains number of true-negative (**tn**), false-positive (**fp**), false-negative (**fn**), and true-positive (**tp**) samples in the whole dataset. More formally, using the prediction rule (1.3) we can compute all fields of the confusion matrix as follows

$$\begin{aligned} \text{tp}(\mathbf{s}, t) &= \sum_{i \in \mathcal{I}_+} \mathbb{1}_{[s_i \geq t]}, & \text{fn}(\mathbf{s}, t) &= \sum_{i \in \mathcal{I}_+} \mathbb{1}_{[s_i < t]}, \\ \text{tn}(\mathbf{s}, t) &= \sum_{i \in \mathcal{I}_-} \mathbb{1}_{[s_i < t]}, & \text{fp}(\mathbf{s}, t) &= \sum_{i \in \mathcal{I}_-} \mathbb{1}_{[s_i \geq t]}, \end{aligned} \quad (1.4)$$

where \mathbf{s} is the vector of classification scores given by model f , and $\mathbb{1}_{[\cdot]}$ is the Iverson function (1.2). In the following text, we sometimes use a simplified notation $\text{tp} = \text{tp}(\mathbf{s}, t)$ (and similar notation for other counts). In such cases, the vector of classification scores and decision threshold is fixed and is known from the context. Using the simplified notation, we can define true-positive, false-positive, true-negative, and false-negative rates as follows

$$\text{tpr} = \frac{\text{tp}}{n_+}, \quad \text{fnr} = \frac{\text{fn}}{n_+}, \quad \text{tnr} = \frac{\text{tn}}{n_-}, \quad \text{fpr} = \frac{\text{fp}}{n_-}. \quad (1.5)$$

Figure 1.2 shows the relation between classification rates and the decision threshold. The blue and red curves represent the theoretical distribution of the scores of negative and positive samples, respectively. If we increase the value of the threshold t , we decrease the false-positive rate, but at the same time, we also increase the false-negative rate. On the other hand, if we decrease the value of t , we decrease the false-negative rate, but at the same time, we also increase the false-positive rate. In other words, it is not possible to decrease the false-positive rate only by moving the threshold t without increasing the false-negative rate and vice versa. Therefore, we always have to find some balance between these two types of errors.

If we look at the general definition of the binary classification problem (1.1), the objective function is only the weighted sum of false-positive and false-negative samples. Therefore, we can use the notation (1.5) and rewrite the problem (1.1) to

$$\begin{aligned} &\underset{\mathbf{w}, t}{\text{minimize}} && C_1 \cdot \text{fp}(\mathbf{s}, t) + C_2 \cdot \text{fn}(\mathbf{s}, t) \\ &\text{subject to} && s_i = f(\mathbf{x}_i; \mathbf{w}), \quad i \in \mathcal{I}. \end{aligned} \quad (1.6)$$

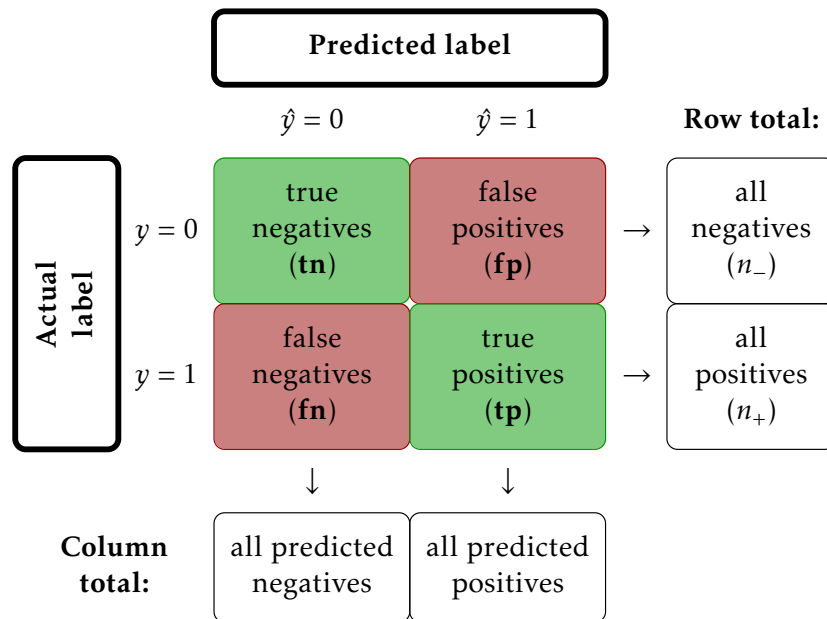


Figure 1.1: The confusion matrix for the binary classification problem, where the negative class has the label 0 and the positive class has the label 1. The true (target) label is denoted by y and the predicted label is denoted by \hat{y} .

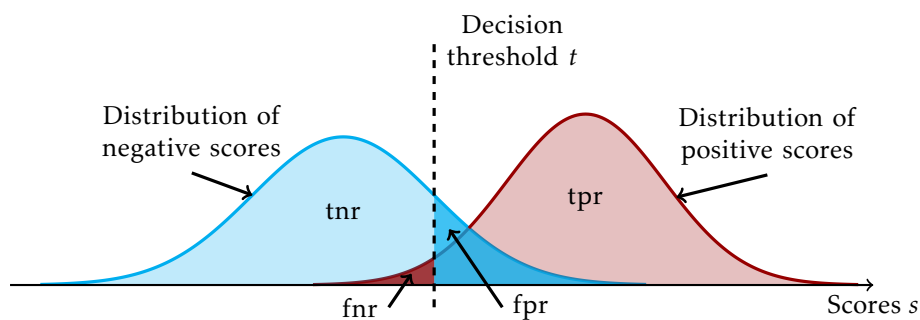


Figure 1.2: The relation between classification scores and rates. The blue/red curve is the theoretical distribution of the scores of negative/positive samples, respectively. The area between the blue line and the x-axis is divided by the decision threshold t . The left part represents the true-negative rate, while the right part represents the false-positive rate. The area between the red line and the x-axis is also divided by t . The left part represents a false-negative rate, and a right represents the true-positive rate.

Name	Aliases	Formula
true negatives	correct rejection	tn
false positives	Type I error, false alarm	fp = $n_- - \text{tn}$
true positives	hit	tp
false negatives	Type II error	fn = $n_+ - \text{tp}$
true negative rate	specificity, selectivity	$\text{tnr} = \frac{\text{tn}}{n_-}$
false positive rate	fall-out	$\text{fpr} = \frac{\text{fp}}{n_-} = 1 - \text{tnr}$
true positive rate	sensitivity, recall, hit rate	$\text{tpr} = \frac{\text{tp}}{n_+}$
false negative rate	miss rate	$\text{fnr} = \frac{\text{fn}}{n_+} = 1 - \text{tpr}$
accuracy	—	$\text{acc} = \frac{\text{tp} + \text{tn}}{n}$
balanced accuracy	—	$\text{bacc} = \frac{\text{tpr} + \text{tnr}}{2}$
precision	positive predictive value	$\text{precision} = \frac{\text{tp}}{\text{tp} + \text{fp}}$

Table 1.1: Summary of classification metrics derived from confusion matrix. The first column shows the name used in this work, while the second column shows alternative names that can be found in the literature. The last column shows the formula based on the confusion matrix.

Parameters $C_1, C_2 \in \mathbb{R}$ are used to specify which error is more serious for the particular classification task.

The confusion matrix is not the only way to measure the performance of binary classifiers. For example, there are many different classification matrices, and many of them are derived directly from the confusion matrix [13, 14, 15, 16]. As an example, we can mention accuracy and balanced accuracy defined as

$$\text{acc} = \frac{1}{n}(\text{tp} + \text{tn}), \quad \text{bacc} = \frac{1}{2}(\text{tpr} + \text{tnr}).$$

Note that the objective function in (1.6) is accuracy if $C_1 = C_2 = \frac{1}{n}$. Moreover, for $C_1 = \frac{1}{2n_-}$ and $C_2 = \frac{1}{2n_+}$, the objective function is balanced accuracy. This shows the importance of these two performance matrices for standard binary classification. More performance metrics derived from the confusion matrix can be found in Table 1.1. Moreover, in the following section, we introduce a different approach for the performance evaluation of binary classifiers.

1.2.2 ROC Analysis

In the previous section, we defined a general binary classification formulation (1.6) that minimizes a weighted sum of false-positive and false-negative counts. Therefore, we always have to find some trade-off between the false-positive and false-negative counts and select the best hyperparameters C_1, C_2 , for given tasks. There is no universal truth which of these two errors is worse. For example, it is probably better to classify a healthy patient as sick and do additional tests than the other way around. On the other hand, in computer security, an antivirus program with a lot of false-positive alerts is useless since it is disruptive to the user. The Receiver Operating Characteristic (ROC) space [17, 13] is one way to visualize the trade-off between false-positive and false-negative errors.



Figure 1.3: A basic representation of the ROC space with five different classifiers. **(left)** A comparison of ROC curves for two different classifiers. **(right)**

ROC space is a two-dimensional space with the x-axis equal to the false-positive rate and the y-axis to the true-positive rate. The left-hand side of Figure 1.3 shows the ROC space with five highlighted points. Each point in the ROC space represents one fixed classifier, i.e., one pair consisting of a model f and a decision threshold t . There are several important points in the ROC space. The point (0,0) represents a classifier classifying all samples as negative, while (1,1) is a classifier classifying all samples as positive. Both these classifiers are useless. On the other hand, the point (0, 1) represents the perfect classifier that classifies all samples correctly since $\text{fpr} = 0$ and $\text{tpr} = 1$.

ROC representation allows us to decide whether one classifier is better than another, only in some cases. For example, in Figure 1.3, classifier **B** is better than classifier **C** since **B** has a higher true-positive rate and at the same time a lower false-positive rate. On the other hand, it is impossible to say which classifier is better if one has a higher true-positive rate and the other has a lower false-positive rate. We can see this situation for classifier **B** and **A**. In such a case, the preference depends on the given problem, as discussed at the beginning of this section.

Another important part of the ROC space is the diagonal line highlighted in red in Figure 1.3. Any classifier that appears on this diagonal provides the same performance as a random classifier. For example, classifier **C** is represented in ROC space by point (0.7,0.7). Such classifier randomly classifies 70% of samples as positive. Therefore, any classifier that appears in ROC space in the lower right triangle is worse than a random classifier. There are usually no classifiers in this area since any classifier from the lower right triangle can be easily improved. If we negate the prediction of such a classifier for every sample, we get its negated version in the upper left triangle. Such a situation is in Figure 1.3 for classifiers **E** and **B**. Since classifier **E** has a false-negative rate of $1 - \text{tpr} = 0.8$, we can deduce that negated classifier will have a true-positive rate of 0.8. Similarly, since classifier **E** has a true-negative rate of $1 - \text{fpr} = 0.4$, its negated version will have a false-positive rate of 0.4. Therefore the negated version of classifier **E** is represented in ROC space by point (0.4,0.8), which is classifier **B**.

Many classifiers only predict whether samples are positive or negative. As an example, we can mention decision trees. Such classifiers are always represented as a single point in the ROC space. In this text, we consider only classifier from Notation 1.2, which predict a continuous score instead of a hard prediction. We assume that the classifier consists of the model f that produces classification scores and the decision threshold t . Many standard classifiers such as neural networks or logistic regression fall into this setting. Even though the decision threshold is determined during the training process, it is possible to change it and obtain different

predictions. This possibility is very often used to produce so-called ROC curves [13].

ROC curve shows how model f behaves for different thresholds t varying from $-\infty$ to $+\infty$. Right-hand side of Figure 1.3 provides an example of two ROC curves for two different classifiers. **Classifier 1** provides accuracy 95% and is represented by the blue dot, while the blue line represents its ROC curve. **Classifier 2** represented by the green dot provides accuracy 76%, and the green dashed line represents its ROC curve. A standard method for comparing two classifiers is to compare the corresponding areas under the ROC curves (AUC) [18, 19]. Such an approach is a simple way to reduce the curve to one number. In the case of standard binary classification, the larger the AUC, the better. In Figure 1.3 we can see that the blue classifier has AUC 95% while the green one has only 77%. Therefore, for most classification problems, the blue classifier is better. Even though we get almost the same values of accuracy and AUC for both classifiers, the accuracy is not equivalent to AUC. The similarity is only a consequence of the used example.

Since both false-positive and true-positive rates are non-increasing functions of threshold t , we can efficiently compute the ROC curve from sorted classification scores. Moreover, the AUC of a classifier is equivalent to the probability that the classifier will rank a randomly chosen positive sample higher than a randomly chosen negative sample [13]. By comparing the classifiers from the right-hand side of Figure 1.3, we can deduce that **Classifier 1** is generally better at a false-positive rate larger than 0.01. Otherwise, **Classifier 2** is the better one. Therefore, there is a specific region of the ROC space where **Classifier 2** outperforms **Classifier 1**. In the next section, we discuss multiple different problems which focus on the performance only at low false-positive rates.

1.3 Classification at the Top

As discussed above, **Classifier 1** focuses on the overall performance, while the **Classifier 2** on the performance on low false-positive rates, see Figure 1.3. The latter classifier can be handy for search engines such as Google or DuckDuckGo, where the goal is to have all relevant results on the first few pages. The results on page 50 are usually of no interest to anyone, so it is crucial to move the most relevant results to the few first pages [20]. Therefore, it is essential to push as many positive samples above some small portion of the worst negative samples (negative samples with the largest classification scores). In this section, we use two different visual representations for the performance of classifiers from the right-hand side of Figure 1.3 to show the difference and emphasize their advantages.

Figure 1.4 shows the difference between the standard classifier (**Classifier 1**) that maximizes the accuracy and the classifier that focuses only on the classification at the top (**Classifier 2**). In this particular case, **Classifier 2** maximizes the number of positive samples that are ranked higher or equal than the worst negative sample. In other words, **Classifier 2** maximizes true-positive rate at the smallest possible false-positive rate. If we go back to the example with search engines, the goal of **Classifier 2** is to push as many relevant results before the first irrelevant. Formally, **Classifier 2** maximizes the following metric

$$\text{pos@top}(s) = \frac{1}{n_+} \sum_{i \in \mathcal{I}_+} \mathbb{1}_{[s_i \geq \max_{j \in \mathcal{I}_-} s_j]}. \quad (1.7)$$

For both classifiers, Figure 1.4 shows two different decision thresholds. The black threshold is the one for which the classifier was trained, while the green one represents the worst negative sample. For **Classifier 2** these two thresholds coincide. We can observe that **Classifier 1** provides a much better separation of positive and negative samples. Only a few samples above the black threshold ruin perfect separation. On the other hand, the separation provided by **Classifier 2** is much worse since half of the positive samples are mixed with negative ones. Therefore, the accuracy of **Classifier 1** is 95% while the accuracy of **Classifier 2** is only 76%.



Figure 1.4: Difference between standard classifiers (**Classifier 1**) and classifiers maximizing pos@top metric (**Classifier 2**). While the former has a good total accuracy, the latter has a good pos@top metric.

However, in terms of metric (1.7) the situation is quite different. Since there are few negative outliers, there is only 19% of positive samples above the worst negative for **Classifier 1**, but 53% for **Classifier 2**.

The same behavior can also be demonstrated using ROC curves. Figure 1.5 shows ROC curves for both classifier with (right) and without (left) logarithmic scaling of x-axis. The blue line represents ROC curve for **Classifier 1** and the green dashed one for **Classifier 2**. Moreover, There are two important points for **Classifier 2**. The blue filled circle corresponds to the black threshold and the blue filled square to the green threshold from Figure 1.4. Since for **Classifier 2** both thresholds coincide, there is only one point in Figure 1.5 highlighted by a green square. The superiority of **Classifier 1** in the overall performance is evident from the left-hand side of the figure, since there is only a small region of ROC space, where **Classifier 2** provides a higher true-positive rate. However, this region is very interesting. The right-hand side of Figure 1.5 allows us to concentrate on very low false-positive rates. If the false-positive rate is lower than $7 \cdot 10^{-1}$, then **Classifier 2** provides better true-positive rate than **Classifier 1**. Finally, the value of metric (1.7) is highlighted using squares for both classifiers and it is clear, that **Classifier 2** provides higher value of this metric.

The rest of the chapter presents three main categories of problems that focus only on a small number of the most relevant samples. Moreover, in Chapter 2, we show that at least some formulations from these three categories are closely related to binary classification.

1.3.1 Ranking Problems

The first category is the category of ranking problems. The ranking algorithms play a crucial role in many information retrieval problems:

- **Document (Text) retrieval systems** are used for obtaining relevant documents from the collection of documents based on the relevance to the user's query. Such systems are widely used for accessing books, journals, or any other documents. However, the most visible applications are search engines such as Google or DuckDuckGo.
- **Collaborative filtering** is one of the techniques used to predict a user's rating of a new product based on past ratings of users with similar rating patterns. Such systems can be used to generate music or video playlists automatically. Therefore, such systems are widely used in services such as Youtube or Spotify.

The two examples above show that ranking problems usually depend on users' feedback or preferences. In binary classification, we only have the labels that represent if the samples are

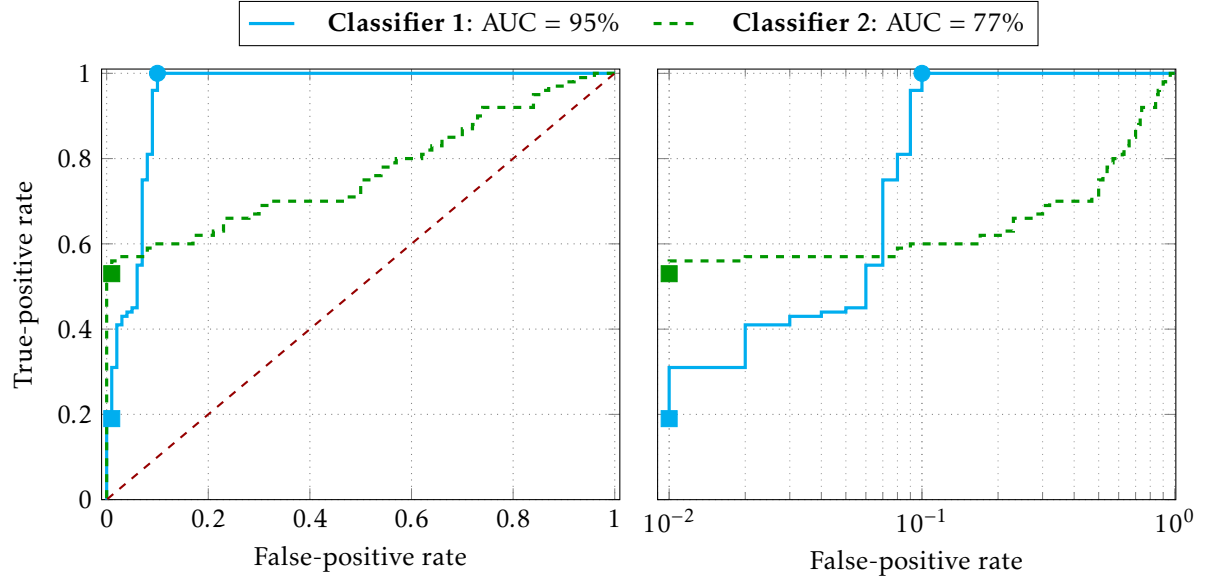


Figure 1.5: Difference between standard classifiers (**Classifier 1**) and classifiers maximizing pos@top metric (**Classifier 2**). While the former has a good total accuracy, the latter has a good pos@top metric.

positive or negative. On the other hand, ranking problems use multiple ways to describe the users' feedback. One approach uses the feedback function $\Phi : \mathbb{R}^d \times \mathbb{R}^d \rightarrow \mathbb{R}$ to represent the user's preferences [21]. In such a case, the feedback function can be defined for all pairs of samples $(\mathbf{x}_i, \mathbf{x}_j)$ in the following way

$$\Phi(\mathbf{x}_i, \mathbf{x}_j) \begin{cases} > 0 & \mathbf{x}_i \text{ is preferred over } \mathbf{x}_j, \\ = 0 & \text{no preference,} \\ < 0 & \mathbf{x}_j \text{ is preferred over } \mathbf{x}_i. \end{cases}$$

We can see, that the feedback function specifies if the user prefers \mathbf{x}_i over \mathbf{x}_j or not. Moreover, the feedback function also specifies how strong the preference is, i.e., the higher the volume $|\Phi(\mathbf{x}_i, \mathbf{x}_j)|$, the higher the preference. Many ranking algorithms try to find some ordering of all samples that minimizes the number of incorrectly ordered pairs of samples. Consider a ranking function $r : \mathbb{R}^d \rightarrow \mathbb{R}$. The sample \mathbf{x}_i is ranked higher than the sample \mathbf{x}_j if $r(\mathbf{x}_i) > r(\mathbf{x}_j)$. Then, the minimization of the number of misordered pairs can be formally written as follows

$$\underset{r}{\text{minimize}} \quad \sum_{i \in \mathcal{I}} \sum_{j \in \mathcal{I}} \mathbb{1}_{[r(\mathbf{x}_i) \leq r(\mathbf{x}_j)]} \cdot \max\{0, \Phi(\mathbf{x}_i, \mathbf{x}_j)\}. \quad (1.8)$$

This problem is computationally demanding since the objective function contains a pairwise comparison of all samples. Therefore, the problem is not suitable for large data. *RankBoost* [21] is a boosting algorithm based on the AdaBoost [22] that combines many weak ordering functions to obtain the final ranking. This approach leads to the maximization of the AUC [23]. Therefore, RankBoost focuses on the overall performance. However, as we discussed at the beginning of the section, we want to focus only on the small portion of the most relevant samples in many applications. In such a case, this approach is not ideal.

Consider movie recommendations. In such a case, we only care if the movie is good or not. It is not important if one bad movie is ranked higher than another bad movie. Both movies are still bad and therefore not relevant. Many ranking algorithms [23] use the so-called bipartite ranking to address this situation. In such a situation, each sample is positive (good)

or negative (bad), and the goal is to push positive samples above negative ones. The authors of [23] proposed the following formulation

$$\underset{r}{\text{minimize}} \quad \left(\sum_{j \in \mathcal{I}_-} \left(\sum_{i \in \mathcal{I}_+} \mathbb{1}[r(x_i) \leq r(x_j)] \right)^p \right)^{\frac{1}{p}}. \quad (1.9)$$

The authors of [23] also proposed boosting algorithm called ***p*-Norm Push** to solve the formulation above. Note that for $p = 1$, the formulation (1.9) is very similar to the RankBoost (1.8) and the resulting ranking function maximizes the AUC, therefore focusing on optimizing the overall ranking. On the other hand, for $p \rightarrow +\infty$, the formulation (1.9) minimizes the largest number of positive samples ranked below any negative sample

$$\underset{r}{\text{minimize}} \quad \max_{j \in \mathcal{I}_-} \sum_{i \in \mathcal{I}_+} \mathbb{1}[r(x_i) \leq r(x_j)].$$

In such a case, the resulting ranking function focuses only on the absolute top, i.e., it aims to push as many positive samples above the negative sample with the highest rank. Moreover, the formulation above can be equivalently rewritten as follows

$$\underset{r}{\text{minimize}} \quad \sum_{i \in \mathcal{I}_+} \mathbb{1}[r(x_i) \leq \max_{j \in \mathcal{I}_-} r(x_j)]. \quad (1.10)$$

Authors of [24] focus on this formulation and introduce a SVM (*Support Vector Machines* [25]) based algorithm called *Infinite Push* to solve it. Finally, authors of [26] proposed an even more efficient algorithm with the linear complexity in the number of samples called *TopPush*. Note that the objective function of the problem above is almost the same as the metric (1.7). Therefore, this **Classifier 2** from Figures 1.4 and 1.5 corresponds to the ranking function given by *TopPush* algorithm. It shows a close connection between binary classification and the bipartite ranking problems.

1.3.2 Accuracy at the Top

In the previous section, we introduced formulation (1.10), which focuses on maximizing the number of positive samples above the worst negative sample (the one with the highest rank or highest classification score). This formulation is very useful, as discussed at the beginning of this section. However, such a maximization problem can be unstable since the objective function does not allow false-positive errors. Therefore, if there is one negative outlier with a high score, the number of positive samples above this outlier can be tiny. The authors of [27] focus on a similar problem as *TopPush*, but use a different approach. They proposed the following formulation and called it **Accuracy at the Top**

$$\begin{aligned} \underset{w}{\text{minimize}} \quad & \frac{1}{n_-} \text{fp}(s, t) + \frac{1}{n_+} \text{fn}(s, t) \\ \text{subject to} \quad & s_i = f(x_i; w), \quad i \in \mathcal{I}, \\ & t = \max \left\{ t \mid \frac{1}{n} \sum_{i \in \mathcal{I}} \mathbb{1}[s_i \geq t] \geq \tau \right\}, \end{aligned} \quad (1.11)$$

where $f : \mathbb{R}^d \rightarrow \mathbb{R}$ is a model. This formulation focuses on the top τ -fraction of all samples and tries to maximize the number of positive samples and minimize the number of negative samples in it. Even though the goal is to maximize the number of positive samples above the top τ -quantile, the objective function contains false-positive and false-negative rates. It should be sufficient to include only one of them since the definition of the threshold implies

the minimization of the other one as well. However, this form of objective function should be more robust [7]. The problem of Accuracy at the Top is useful, for example, in applications where identified samples undergo expensive post-processing, such as human evaluation. For instance, in pharmaceuticals, potentially useful drugs must be preselected and manually investigated in drug development. Since the manual investigation is costly, we have to select only a fraction of drugs with the highest potential. However, it is precisely what Accuracy at the Top does.

There are many methods on how to solve Accuracy at the Top, since the formulation is complicated due to the top τ -quantile in the constraint. The early approaches aim at solving approximations. For example, the authors of [28] optimize a convex upper bound on the number of errors among the top samples. Due to exponentially many constraints, the method is computationally expensive. In [27] the authors presented a SVM-like formulation. They assume that the top τ -quantile is one of the samples, construct n unconstrained optimization problems with fixed thresholds, solve them and select the best solution. While this removes the necessity to handle the (difficult) quantile constraint, the algorithm is computationally infeasible for a large number of samples. The authors of [7] proposed the projected gradient descent method, where after each gradient step, the quantile is recomputed. In [29] authors suggested new formulations for various criteria and argued that they keep desired properties such as convexity. Finally, the authors of [30] showed that Accuracy at the Top is maximized by thresholding the posterior probability of the relevant class.

1.3.3 Hypothesis Testing

The hypothesis testing operates with null H_0 and alternative H_1 hypothesis. The goal is to either reject the null hypothesis in favor of the alternative or not to reject it. Since the problem is binary, two possible errors can occur. Type I occurs when H_0 is true but is rejected, and Type II error happens when H_0 is false but fails to be rejected. The Neyman-Pearson problem minimizes [31] Type II error while keeping Type I error smaller than some predefined bound. Using our notation for the Neyman-Pearson problem, the null hypothesis H_0 states that sample \mathbf{x} has a negative label. Then Type I error occurs when the sample is false-positive, while Type II error occurs when the sample is false-negative. Therefore, the Neyman-Pearson problem minimizes the false-negative rate with the prescribed level τ of the false-positive rate. Such constraint can be written in the form of quantile, i.e., the threshold is the top τ -quantile of scores of all negative samples.

$$\begin{aligned} & \underset{f}{\text{minimize}} && \frac{1}{n_+} \text{fn}(s, t) \\ & \text{subject to} && s_i = f(\mathbf{x}_i), \quad i \in \mathcal{I}, \\ & && t = \max \left\{ t \left| \frac{1}{n_-} \sum_{i \in \mathcal{I}_-} \mathbb{1}_{[s_i \geq t]} \geq \tau \right. \right\}, \end{aligned}$$

This formulation is very similar to the one for Accuracy at the Top (1.11). The main difference is that the quantile in the constraint is not computed from all but only from negative samples. Also, note one key difference in interpretation. The τ in Accuracy at the Top represents the total amount of samples we want to process with the smallest possible error. On the other hand, in the Neyman-Pearson problem τ represents the maximal acceptable false-positive rate. Therefore, the former approach is useful in situations where we can process only a certain number of samples. The latter is for situations where we have strict constraints on false-positive errors.

1.4 Summary

In this chapter, we introduced the general formulation (1.6) for binary classification and discussed how to measure the performance of binary classifiers. The first approach for performance evaluation is based on the confusion matrix. This approach is very straightforward. Moreover, it is possible to derive many different classification matrices from the confusion matrix. Table 1.1 summarizes classification matrices derived from the confusion matrix used in the upcoming chapters. The second approach introduced in this chapter uses the ROC space to visualize the ability of classifiers to rank positive samples above negative ones. Since standard binary classification focuses on optimizing the overall performance, we discussed that there are many problems closely tied to binary classification that focus on the performance of the most relevant samples. Such problems occur in many applications, from search engines to drug development. We also introduced Ranking problems, the problem of Accuracy at the Top, and the Neyman-Pearson problem and discussed their relation to the binary classification.

Note 1.3

To improve the readability of the main part of the work, we postpone many results into appendices. Main results are presented in the main part, but all auxiliary results and proofs are located in appendices.

Framework for Classification at the Top

In the previous chapter, we introduced the general formulation (1.6) and fundamental evaluation matrices for the binary classification problems. Furthermore, in Section 1.3, we introduced three problems closely related to binary classification but focused on specific performance criteria, namely: *Accuracy at the top* problem, *Ranking problems*, and the problem of *Hypothesis testing*. Even though these problems are usually considered separately, they all aim to minimize the number of misclassified samples below (or above) a certain threshold. In the rest of the chapter, we focus on this common property and show that all these problems fall into the following unified framework for binary classification at the top

$$\begin{aligned} & \underset{w}{\text{minimize}} && C_1 \cdot \text{fp}(s, t) + C_2 \cdot \text{fn}(s, t) \\ & \text{subject to} && s_i = f(\mathbf{x}_i; w), \quad i \in \mathcal{I}, \\ & && t = G(s, y), \end{aligned} \tag{2.1}$$

where function $G: \mathbb{R}^n \times \{0, 1\}^n \rightarrow \mathbb{R}$ takes the scores and labels of all samples and computes the decision threshold. The concrete form of the function G that defines the decision threshold depends on the used problem. As we show later in the chapter, all problems mentioned above differ only in the definition of the function G . Note the important distinction from the standard binary classification (1.6): the decision threshold is no longer fixed (as in the case of neural networks) or trained independently (as in SVM) but is a function of scores of all samples. Therefore, the minimization in problem (2.1) is performed only concerning the one variable w .

2.1 Surrogate Formulation

The objective function in (2.1) is a weighted sum of false-positive and false-negative counts. Since these counts are discontinuous due to the presence of the Iverson function (see (1.4)), the whole objective function is discontinuous too. Therefore, problem (2.1) is difficult to solve. One way how to simplify the problem is to derive its continuous approximation. The usual approach is to employ a surrogate function to replace the Iverson function [26, 7].

Notation 2.1: Surrogate function

To approximate the Iverson function (1.2), we use any surrogate function l that is convex, non-negative, and non-decreasing with $l(0) = 1$, and $l(s) \rightarrow 0$ as $s \rightarrow -\infty$. As examples of such function, we can mention the hinge loss or the quadratic hinge loss defined by

$$l_{\text{hinge}}(s) = \max\{0, 1 + s\}, \quad l_{\text{quadratic}}(s) = (\max\{0, 1 + s\})^2.$$

Figure 2.1 compares the Iverson function with the hinge and quadratic hinge loss with scaled inputs by $\vartheta = 2$ and without scaling. We use $\vartheta > 0$ to denote any scaling parameter.



Figure 2.1: Comparison of the approximation quality of the Iverson function using different surrogate functions and scaling parameters.

Notation 2.1 summarizes all assumptions that a proper surrogate function must fulfill and introduces the two most often used surrogate functions: hinge and quadratic hinge loss functions. Moreover, Figure 2.1 compares these two surrogate functions with the Iverson function. It is clear that the surrogate function always provides an upper approximation of the Iverson function. In other words, if a surrogate function l satisfies assumptions from Notation 2.1, then $l(s) \geq \mathbb{1}_{[s \geq 0]}$ holds for any $s \in \mathbb{R}$. Besides that, Figure 2.1 shows how the scaling parameter ϑ affects the approximation quality of the surrogate function. If the scaling parameter is greater, the surrogate function approximates the Iverson function better on interval $(-\infty, 0)$. In the opposite case, the approximation is better on interval $(0, \infty)$. The usual choice of scaling parameter is $\vartheta = 1$, and we used this choice for all surrogate functions used in the objective functions. However, we also use surrogate functions for approximation of the decision threshold. In such a case, the scaling parameter plays a crucial role for some theoretical guaranties, as shown in upcoming chapters.

With a properly defined surrogate function, we can define the surrogate approximation of the objective function of problem (2.1). To follow the notation from the previous chapter, we first replace the Iverson function in (2.1). Using any surrogate function l that satisfies assumptions from Notation 2.1, the true counts (2.1) may be approximated by their surrogate counterparts defined by

$$\begin{aligned} \overline{\text{tp}}(s, t) &= \sum_{i \in \mathcal{I}_+} l(s_i - t), & \overline{\text{fn}}(s, t) &= \sum_{i \in \mathcal{I}_+} l(t - s_i), \\ \overline{\text{tn}}(s, t) &= \sum_{i \in \mathcal{I}_-} l(t - s_i), & \overline{\text{fp}}(s, t) &= \sum_{i \in \mathcal{I}_-} l(s_i - t). \end{aligned} \quad (2.2)$$

Since the surrogate function provides upper approximation of the Iverson function, the surrogate counts (2.2) provide upper approximations of the true counts (1.4). By replacing the true counts in the objective function of (2.1) with their surrogate counterparts and adding a regularization for better numerical stability, we get

$$\begin{aligned} \underset{\mathbf{w}}{\text{minimize}} \quad & \frac{\lambda}{2} \|\mathbf{w}\|^2 + C_1 \cdot \overline{\text{fp}}(s, t) + C_2 \cdot \overline{\text{fn}}(s, t) \\ \text{subject to} \quad & s_i = f(\mathbf{x}_i; \mathbf{w}), \quad i \in \mathcal{I}, \\ & t = G(s, \mathbf{y}). \end{aligned} \quad (2.3)$$

The resulting objective function is continuous, and therefore the problem is easier to solve than the original problem (2.1). No additional theoretical properties can be derived without

knowing the concrete form of model f and function G . Therefore, the rest of the chapter is dedicated to problems that fall into the general framework (2.3) and concrete form of G for such problems. More precisely, we focus on the three problems introduced in Section 1.3 and show how to rewrite them to our general formulation (2.3). Most of these problems are defined originally only for the linear model since this choice allows to derive nice theoretical properties and efficient solving algorithms. However, this chapter focuses on the problem formulation itself rather than on how to solve it. Therefore for all problems, we derive their version with general model f . The discussion of the theoretical properties for specific forms of f is provided in Chapter 3, 4, and 5.

Notation 2.2: Classification scores

In Notation 1.2, we defined vector $\mathbf{s} \in \mathbb{R}^n$ of scores of all samples with components defined for any $i \in \mathcal{I}$ as

$$s_i = f(\mathbf{x}_i; \mathbf{w}), \quad i \in \mathcal{I},$$

where $f: \mathbb{R}^d \rightarrow \mathbb{R}$ represents an arbitrary model. To simplify the upcoming sections, we define a sorted version of vector \mathbf{s} with non-increasing components and denote it as $\mathbf{s}_{[\cdot]}$. It means that components of $\mathbf{s}_{[\cdot]}$ fulfill

$$s_{[1]} \geq s_{[2]} \geq \dots \geq s_{[n-1]} \geq s_{[n]}.$$

Moreover, we denote negative samples as \mathbf{x}^- and positive samples as \mathbf{x}^+ . Finally, we define vectors $\mathbf{s}^- \in \mathbb{R}^{n_-}$, $\mathbf{s}^+ \in \mathbb{R}^{n_+}$ of scores of all positive and negative samples with components defined as

$$s_j^- = f(\mathbf{x}_j^-; \mathbf{w}), \quad j = 1, 2, \dots, n_-,$$

$$s_i^+ = f(\mathbf{x}_i^+; \mathbf{w}), \quad i = 1, 2, \dots, n_+,$$

and their sorted versions $\mathbf{s}_{[\cdot]}^-, \mathbf{s}_{[\cdot]}^+$ with non-increasing components.

Note 2.3

To improve the readability of the main part of the work, we present results only for hinge loss. Results for quadratic hinge loss are in appendix

2.2 Ranking Problems

The first category of problems from Section 1.3 is a category of ranking problems. The general goal of problems from this category is to rank positive (relevant) samples higher than negative ones. That can be achieved in many different ways, but we focus only on the problems that concentrate on the high-ranked negative samples and try to push as many positive samples as possible above them. The simplest case is to maximize the number of positive samples above the worst negative. Since the worst negative sample is the negative sample with the highest classification score, the decision threshold for such a case is the highest score corresponding to the negative sample. Then the aim is to maximize the number of true-positive samples above this threshold or, equivalently, minimize the number of false-negative negative below it, which may be written as

$$\begin{aligned} & \underset{\mathbf{w}}{\text{minimize}} && \frac{1}{n_+} \text{fn}(\mathbf{s}, t) \\ & \text{subject to} && s_i = f(\mathbf{x}_i; \mathbf{w}), \quad i \in \mathcal{I}, \\ & && t = s_{[1]}^-. \end{aligned} \tag{2.4}$$

Since the decision threshold t in the previous definition is computed from the sorted vector of negative scores $s_{[\cdot]}^-$, it is a function of all negative scores. Therefore, formulation (2.4) is just a special case of the general formulation (2.1) for $C_1 = 0$ and $C_2 = 1/n_+$. The authors in [26] proposed an efficient method to solve formulation (2.4) and called it *TopPush*. They replaced the true counts in the objective function of (2.4) with its surrogate counterpart in the same way as we did in Section 2.1. The resulting formulation has the following form

$$\begin{aligned} & \underset{\mathbf{w}}{\text{minimize}} && \frac{\lambda}{2} \|\mathbf{w}\|^2 + \frac{1}{n_+} \overline{\text{fn}}(\mathbf{s}, t) \\ & \text{subject to} && s_i = f(\mathbf{x}_i; \mathbf{w}), \quad i \in \mathcal{I}, \\ & && t = s_{[1]}^-, \end{aligned} \tag{2.5}$$

which again falls into our framework (2.3). To stress the origin of this formulation, we denote it as *TopPush*. Unfortunately, *TopPush* formulation can be very sensitive to outliers, especially when the linear model is used, as shown in Section 3.3. To robustify the formulation, we follow the idea presented in [32] and replace the highest negative score by the mean of K highest negative scores. The resulting formulation is as follows

$$\begin{aligned} & \underset{\mathbf{w}}{\text{minimize}} && \frac{\lambda}{2} \|\mathbf{w}\|^2 + \frac{1}{n_+} \overline{\text{fn}}(\mathbf{s}, t) \\ & \text{subject to} && s_i = f(\mathbf{x}_i; \mathbf{w}), \quad i \in \mathcal{I}, \\ & && t = \frac{1}{K} \sum_{i=1}^K s_{[i]}^-. \end{aligned} \tag{2.6}$$

To emphasize the similarity with the *TopPush*, we call this formulation *TopPushK*. It is also possible to use the value of K -th highest negative score as the threshold. Such a choice may be advantageous in some cases, and we will discuss it in Chapter 5. For now, we will stick to the formulation that uses the mean since it will allow us to derive some nice theoretical properties in Section 3.1.

2.3 Accuracy at the Top

The second problem from Section 1.3 is the problem of Accuracy at the Top [27]. This problem aims to find an ordering of samples so that samples whose scores are among the top τ -quantile are as relevant as possible. In statistics, the τ -quantile of all scores is defined as follows

$$t = \max \left\{ t \left| \frac{1}{n} \sum_{i \in \mathcal{I}} \mathbb{1}_{[s_i \geq t]} \geq \tau \right. \right\}. \tag{2.7}$$

All relevant samples should be ranked above the quantile t and all irrelevant samples below the quantile t in an ideal case. Thus, the main difference to the ranking problems is that the problem of Accuracy at the Top considers both classification errors and does not focus only on false-negative samples. The original formulation [27] considers a balanced dataset with the same number of positive and negative samples. Paper [7] reformulated the problem for the unbalanced dataset and derived the following formulation

$$\begin{aligned} & \underset{\mathbf{w}}{\text{minimize}} && \frac{1}{n_-} \text{fp}(\mathbf{s}, t) + \frac{1}{n_+} \text{fn}(\mathbf{s}, t) \\ & \text{subject to} && s_i = f(\mathbf{x}_i; \mathbf{w}), \quad i \in \mathcal{I}, \\ & && t = \max \left\{ t \left| \frac{1}{n} \sum_{i \in \mathcal{I}} \mathbb{1}_{[s_i \geq t]} \geq \tau \right. \right\}. \end{aligned} \tag{2.8}$$

This formulation already falls into our framework (2.1) for $C_1 = 1/n_-$ and $C_2 = 1/n_+$. Moreover, the authors of [27, 7] used the same surrogate trick to get rid of the discontinuous objective function, as we used in Section 2.1. Thus, by replacing false-positive and false-negative counts in the objective function with their surrogate counterparts we get

$$\begin{aligned} & \underset{w}{\text{minimize}} && \frac{\lambda}{2} \|w\|^2 + \frac{1}{n_-} \overline{\text{fp}}(s, t) + \frac{1}{n_+} \overline{\text{fn}}(s, t) \\ & \text{subject to} && s_i = f(x_i; w), \quad i \in \mathcal{I}, \\ & && t = \max \left\{ t \mid \frac{1}{n} \sum_{i \in \mathcal{I}} \mathbb{1}_{[s_i \geq t]} \geq \tau \right\}. \end{aligned} \quad (2.9)$$

This formulation falls into our framework (2.3) for $C_1 = 1/n_-$ and $C_2 = 1/n_+$. Even though the original formulation is presented in [27], we denote the previous formulation as *Grill* based on the name of the first author of [7]. There are two reasons for that. The first one is that we used an unbalanced dataset as in [7]. The second one is that we use an algorithm proposed in [7] for numerical experiments since the one from [27] is suitable only for a small dataset.

The *Grill* formulation (2.9) is still challenging to solve due to the form of the decision threshold (2.7). The authors of [27] removed the necessity to handle the difficult quantile constraint by setting quantile as one of the samples and solving n independent problems. However, such an approach is infeasible for a large number of samples. The authors of [7] proposed the projected gradient descent method, where after each gradient step, the quantile is recomputed. This approach is suitable for large data but lacks theoretical guarantees. In the following text, we propose two approximations of the true quantile (2.7) that can be used to simplify formulation (2.9). The first one is a simple approximation by the mean of $n\tau$ -th highest scores

$$t = \frac{1}{n\tau} \sum_{i=1}^{n\tau} s_{[i]}. \quad (2.10)$$

where for simplicity we assume, that $n\tau$ is an integer. The main purpose of (2.10) is to provide a convex approximation of the non-convex quantile (2.7). In fact, it is known that it is the tightest convex approximation of (2.7). Putting (2.10) into the constraint results in the following problem, which we call *TopMeanK*

$$\begin{aligned} & \underset{w}{\text{minimize}} && \frac{\lambda}{2} \|w\|^2 + \frac{1}{n_+} \overline{\text{fn}}(s, t) \\ & \text{subject to} && s_i = f(x_i; w), \quad i \in \mathcal{I}, \\ & && t = \frac{1}{K} \sum_{i=1}^K s_{[i]}, \end{aligned} \quad (2.11)$$

where $K = n\tau$. Besides changing the form of the decision threshold, we also simplified the objective function. This change allows preserving the convexity of the formulation for the linear model as shown in Section 3.1. Even though we start with a different optimization problem, we derived a very similar formulation to the *TopPushK* formulation (2.6) from the previous section. The only difference is that the threshold for *TopMeanK* is computed from scores of all samples and not only from the negative ones.

The second option how to approximate the true quantile is to use surrogate counterparts to replace true counts in (2.7) and solve the following equality

$$t \text{ solves } \frac{1}{n} \sum_{i \in \mathcal{I}} l(\vartheta(s_i - t)) = \tau, \quad (2.12)$$

where $\vartheta > 0$ is fixed scaling parameter. Due to the properties of the surrogate function l (see Notation 2.1), the problem above has a unique solution, and we do not have to use the maximum as in the case of true threshold (2.7). Since this threshold uses the surrogate approximation, we denote it as surrogate top τ -quantile. We get the following formulation by replacing the true quantile in the constrain and simplifying the objective function

$$\begin{aligned} & \underset{\mathbf{w}}{\text{minimize}} && \frac{\lambda}{2} \|\mathbf{w}\|^2 + \frac{1}{n_+} \overline{\text{fn}}(\mathbf{s}, t) \\ & \text{subject to} && s_i = f(\mathbf{x}_i; \mathbf{w}), \quad i \in \mathcal{I}, \\ & && t \text{ solves } \frac{1}{n} \sum_{i \in \mathcal{I}} l(\vartheta(s_i - t)) = \tau. \end{aligned} \tag{2.13}$$

This formulation also used only false negatives in the objective to preserve the convexity for the linear model. In such a case, the formulation is easily solvable due to the convexity and requires almost no tuning. Together with the fact that formulation (2.13) provides a good approximation to the Accuracy at the Top problem, we named it *Pat&Mat* (Precision At the Top & Mostly Automated Tuning).

2.3.1 Threshold Comparison

The previous section introduces three formulations *Grill*, *TopMeanK*, and *Pat&Mat*. While *Grill* formulations use true top τ -quantile (2.7) as a threshold, the remaining two formulations use only its approximations. The following lemma shows that the approximation used by *TopMeanK* is better than the one used by *Pat&Mat*.

Lemma 2.4: Thresholds relation [33]

Consider fixed vector of scores \mathbf{s} and thresholds for *Grill*, *TopMeanK*, and *Pat&Mat* defined by

$$t_1(\mathbf{s}) = \max \left\{ t \left| \frac{1}{n} \sum_{i \in \mathcal{I}} \mathbb{1}_{[s_i \geq t]} \geq \tau \right. \right\}, \quad t_2(\mathbf{s}) = \frac{1}{n\tau} \sum_{i=1}^{n\tau} s_{[i]}, \quad t_3(\mathbf{s}) \text{ solves } \frac{1}{n} \sum_{i \in \mathcal{I}} l(\vartheta(s_i - t)) = \tau.$$

Then the following inequalities hold

$$t_1(\mathbf{s}) \leq t_2(\mathbf{s}) \leq t_3(\mathbf{s}).$$

The previous lemma shows that for fixed scores \mathbf{s} , the threshold (2.10) for *TopPushK* is always lower or equal to the threshold (2.12) for *Pat&Mat*. These formulations use a surrogate approximation of the false-negative rate as an objective function. Since this approximation is a non-decreasing function of t , a lower threshold t means a lower objective function value. Therefore, *TopPushK* seems to be a better formulation since it uses a better approximation of the true quantile. Besides that, it is also easier to compute the threshold for *TopMeanK* than for *Pat&Mat*. However, Chapter 3 shows that *Pat&Mat* formulation has better properties than *TopMeanK*. Moreover, the following section shows how to efficiently compute the threshold for *Pat&Mat* with hinge loss as a surrogate function.

2.3.2 Efficient Computing of the Threshold for *Pat&Mat*

In this section, we show how to efficiently find the threshold (2.12) for *Pat&Mat* when the hinge loss is used as a surrogate. Consider function

$$h(t) = \sum_{i \in \mathcal{I}} l(\vartheta(s_i - t)) - n\tau,$$

then finding threshold (2.12) for *Pat&Mat* is equivalent to looking for \hat{t} such that $h(\hat{t}) = 0$. Function h is continuous and strictly decreasing until it hits the global minimum. Moreover, $h(t) \rightarrow \infty$ as $t \rightarrow -\infty$ and $h(t) \rightarrow -n\tau$ as $t \rightarrow \infty$. Thus, there is a unique solution to the equation $h(t) = 0$. For sorted data, the following lemma advises how to solve this equation. For better readability, the proof of the lemma is in Appendix A.

Lemma 2.5

Consider vector of scores s and its sorted version $s_{[.]}$ with non-increasing elements as defined in Notation 2.2, and threshold for *Pat&Mat* formulation

$$h(t) = \sum_{i \in \mathcal{I}} l(\vartheta(s_i - t)) - n\tau, \quad (2.14)$$

where $\vartheta > 0$ and l is the hinge loss from Notation 2.1. For all $i \in \mathcal{I}$ define $t_i = s_{[i]} + \frac{1}{\vartheta}$. Then for all $i = 2, 3, \dots, n$ we have

$$h(t_i) = h(t_{i-1}) + (i-1)\vartheta(t_{i-1} - t_i), \quad (2.15)$$

with the initial condition $h(t_1) = -n\tau$.

The previous lemma shows how to compute the values of the function (2.14) from the sorted vector of classification scores. Therefore, to solve equation $h(t) = 0$, we can start from initial point $h(t_1) = -n\tau$ and use the recurrent relation (2.15) until we find the first threshold for which the function value of h is non-negative. Denote this threshold as t_i . Then, the threshold \hat{t} can be found using linear interpolation as follows

$$\hat{t} = t_{i-1} - h(t_{i-1}) \frac{t_i - t_{i-1}}{h(t_i) - h(t_{i-1})} = t_{i-1} - h(t_{i-1}) \frac{t_i - t_{i-1}}{(i-1)\vartheta(t_{i-1} - t_i)} = t_{i-1} + \frac{1}{(i-1)\vartheta} h(t_{i-1}),$$

where the second equality follows from (2.15). The whole procedure of finding \hat{t} is summarized in Algorithm 1.

Algorithm 1 An efficient algorithm for computing threshold (2.12) for *Pat&Mat* formulation.

Require: vector s sorted into $s_{[.]}$ and

- 1: Set $t_1 \leftarrow s_{[1]} + \frac{1}{\vartheta}$, $h(t_1) \leftarrow -n\tau$, and $i \leftarrow 2$
 - 2: **while** $h(t_i) < 0$ **do**
 - 3: $t_i \leftarrow s_{[i]} + \frac{1}{\vartheta}$
 - 4: $h(t_i) \leftarrow h(t_{i-1}) + (i-1)\vartheta(s_{[i-1]} - s_{[i]})$
 - 5: $i \leftarrow i + 1$
 - 6: **end while**
 - 7: **return** $\hat{t} \leftarrow t_{i-1} + \frac{1}{(i-1)\vartheta} h(t_{i-1})$
-

2.4 Neyman-Pearson Problem

The last problem from Section 1.3 is the Neyman-Pearson problem, which is closely related to hypothesis testing. The hypothesis testing operates with null H_0 and alternative H_1 hypothesis. The goal is to either reject the null hypothesis in favor of the alternative or not to reject it. Since this problem is binary, two possible errors can occur. Type I occurs when H_0 is true but is rejected, and Type II error happens when H_0 is false but fails to be rejected. The Neyman-Pearson problem [31] minimizes Type II error while keeping Type I error smaller than some predefined bound. Using our notation for the Neyman-Pearson problem, the null hypothesis H_0 states

that sample \mathbf{x} has a negative label. Then Type I error occurs when the sample is false-positive, while Type II error when the sample is false-negative, see Table 1.1. In other words, Type II error corresponds to the false-negative rate, and Type I error to false-positive rate. Therefore, if the bound on the Type I error is τ , we may write this as

$$t^{\text{NP}} = \max \left\{ t \left| \frac{1}{n_-} \sum_{i \in \mathcal{I}_-} \mathbb{1}_{[s_i \geq t]} \geq \tau \right. \right\}. \quad (2.16)$$

Note that we only count the false-positive samples in (2.16) instead of counting all positives in (2.7). Then, we may write the Neyman-Pearson problem as

$$\begin{aligned} & \underset{\mathbf{w}}{\text{minimize}} && \frac{1}{n_+} \text{fn}(\mathbf{s}, t) \\ & \text{subject to} && s_i = f(\mathbf{x}_i; \mathbf{w}), \quad i \in \mathcal{I}, \\ & && t = \max \left\{ t \left| \frac{1}{n_-} \sum_{i \in \mathcal{I}_-} \mathbb{1}_{[s_i \geq t]} \geq \tau \right. \right\}. \end{aligned} \quad (2.17)$$

This problem falls within our framework for (2.1) for $C_1 = 0$ and $C_2 = 1/n_+$. Moreover, formulation (2.17) differs from (2.8) by two things. The first one is the absence of a false-positive rate in the objective function. The second one is that the threshold is computed from negative samples only. Therefore, we can use the same techniques to approximate both objective function and the decision threshold.

To follow the previous section, we first derive the Neyman-Pearson alternative to the *Grill* formulation. We need to add false-positive counts in the objective function to do that. Moreover, we also need to replace true counts with their surrogate counterparts and add the regularization. The resulting formulation is as follows

$$\begin{aligned} & \underset{\mathbf{w}}{\text{minimize}} && \frac{\lambda}{2} \|\mathbf{w}\|^2 + \frac{1}{n_-} \overline{\text{fp}}(\mathbf{s}, t) + \frac{1}{n_+} \overline{\text{fn}}(\mathbf{s}, t) \\ & \text{subject to} && s_i = f(\mathbf{x}_i; \mathbf{w}), \quad i \in \mathcal{I}, \\ & && t = \max \left\{ t \left| \frac{1}{n_-} \sum_{i \in \mathcal{I}_-} \mathbb{1}_{[s_i \geq t]} \geq \tau \right. \right\}. \end{aligned} \quad (2.18)$$

We denote this formulation as *Grill-NP* to emphasize the relation with the original *Grill* formulation and the Neyman-Pearson problem.

The second formulation (2.11) from the previous section, uses mean of $n\tau$ highest scores to approximate true quantile (2.7). In the same way, we can approximate true quantile (2.16) by the mean of $n_- \tau$ highest of scores corresponding to the negative samples

$$t^{\text{NP}} = \frac{1}{n_- \tau} \sum_{i=1}^{n_- \tau} s_{[i]}^-. \quad (2.19)$$

For simplicity, we again assume that $n_- \tau$ is an integer. Putting (2.19) into the constraint results in the Neyman-Pearson alternative to *TopMeanK* defined as

$$\begin{aligned} & \underset{\mathbf{w}}{\text{minimize}} && \frac{\lambda}{2} \|\mathbf{w}\|^2 + \frac{1}{n_+} \overline{\text{fn}}(\mathbf{s}, t) \\ & \text{subject to} && s_i = f(\mathbf{x}_i; \mathbf{w}), \quad i \in \mathcal{I}, \\ & && t = \frac{1}{n_- \tau} \sum_{i=1}^{n_- \tau} s_{[i]}^-. \end{aligned} \quad (2.20)$$

This problem already appeared in [33] under the name τ -FPL. Formulation (2.20) has almost the same form as formulation (2.11). The only difference is that for τ -FPL we have $K = n_- \tau$ while for *TopPushK*, the value of K is small. Thus, even though we started from two different problems, we arrived at two approximations that differ only in the value of one parameter. This slight difference shows a close relationship between the ranking problems and the Neyman-Pearson problem and the need for a unified theory to handle these problems.

The last formulation (2.13) from the previous sections uses the surrogate approximation of the true quantile (2.7). The surrogate approximation of the true quantile (2.16) reads

$$t^{\text{NP}} \text{ solves } \frac{1}{n_-} \sum_{i \in \mathcal{I}_-} l(\vartheta(s_i - t)) = \tau. \quad (2.21)$$

Putting (2.21) into the constraint results in the Neyman-Pearson alternative to *Pat&Mat* in the following form

$$\begin{aligned} & \underset{w}{\text{minimize}} && \frac{\lambda}{2} \|w\|^2 + \frac{1}{n_+} \bar{\text{fn}}(s, t) \\ & \text{subject to} && s_i = f(x_i; w), \quad i \in \mathcal{I}, \\ & && t \text{ solves } \frac{1}{n_-} \sum_{i \in \mathcal{I}_-} l(\vartheta(s_i - t)) = \tau. \end{aligned} \quad (2.22)$$

We call this formulation *Pat&Mat-NP* to stress the similarity with *Pat&Mat*. The only difference between these two formulations is that only negative samples are involved in computing the decision threshold for *Pat&Mat-NP*, while *Pat&Mat* uses all samples. For *Pat&Mat* we derived and efficient algorithm (Algorithm 1) for finding the threshold if the hinge loss is used as surrogate. Similar algorithm can be derived for *Pat&Mat-NP*.

2.4.1 Threshold Comparison

In Section 2.3.1, we show that the threshold for *TopMeanK* provides a better approximation of the true top τ -quantile of all scores than the threshold for *Pat&Mat*. The only difference between τ -FPL and *TopMeanK* is that the former computes the threshold only from negative samples while the latter uses all samples. The same holds for *Pat&Mat-NP* and *Pat&Mat*. Therefore, we can show the same for τ -FPL and *Pat&Mat-NP* relations as showed in Section 2.3.1 for *TopMeanK* and *Pat&Mat*. The following lemma shows that the approximation used by τ -FPL is better than the one used by *Pat&Mat-NP*.

Lemma 2.6: Thresholds relation [33]

Consider fixed vector of scores s and thresholds for *Grill-NP*, τ -FPL, and *Pat&Mat-NP* defined by

$$\begin{aligned} t_1^{\text{NP}}(s) &= \max \left\{ t \left| \frac{1}{n_-} \sum_{i \in \mathcal{I}_-} \mathbb{1}_{[s_i \geq t]} \geq \tau \right. \right\}, & t_3^{\text{NP}}(s) & \text{ solves } \frac{1}{n_-} \sum_{i \in \mathcal{I}_-} l(\vartheta(s_i - t)) = \tau, \\ t_2^{\text{NP}}(s) &= \frac{1}{n_- \tau} \sum_{i=1}^{n_- \tau} s_{[i]}^-. \end{aligned}$$

Then the following inequalities hold

$$t_1^{\text{NP}}(s) \leq t_2^{\text{NP}}(s) \leq t_3^{\text{NP}}(s).$$

Using the same arguments as at the end of Section 2.3.1, τ -FPL is a better formulation in the sense that for the fixed vector of scores, it provides a lower threshold and lower objective

function value. However, Chapter 3 shows that *Pat&Mat-NP* formulation has better properties than τ -FPL.

Finally, Lemma 2.7 shows that *Grill* provides a larger threshold under some conditions than *Grill-NP*. In the same way, *TopMeanK* under some conditions provides a larger threshold than τ -FPL. Since the goal of the presented formulations is to push s^+ above s^- , we may expect that the conditions in Lemma 2.7 are satisfied. The importance of these properties is discussed in Section 3.3, where we show that the formulations with larger thresholds are in some sense more unstable.

Lemma 2.7

Consider *Grill*, *Grill-NP*, *TopMeanK* and τ -FPL formulations and Notation 2.2. If the following inequality holds

$$s_{[n_+\tau]}^+ > s_{[n_-\tau]}^-,$$

then *Grill* has larger threshold than *Grill-NP*. In the same way, if the following inequality holds

$$\frac{1}{n_+\tau} \sum_{i=1}^{n_+\tau} s_{[i]}^+ > \frac{1}{n_-\tau} \sum_{i=1}^{n_-\tau} s_{[i]}^-$$

then *TopMeanK* has larger threshold than τ -FPL.

2.5 Summary

In this chapter, we presented the general framework (2.1) and its surrogate approximation (2.3) to handle the problem of binary classification at the top. Moreover, we showed that many important problems might be formulated in a way that falls into the framework. In Table 2.1, we summarize all formulations introduced in this chapter and show their relation to the general framework (2.3). All these formulations were derived with general model f even though many of them have been initially designed only for the linear model. The reason for that is simple. This chapter aims only to emphasize the similarities between these formulations. The theoretical properties that follow from the concrete form of the model are discussed in the upcoming chapters.

In Section 2.3.1, we showed that the threshold for *TopMeanK* better approximates the true top τ -quantile than the threshold for *Pat&Mat*. Since both formulations use the same objective function, that is non-decreasing function of the threshold, *TopMeanK* provides a lower objective value for the fixed model. Furthermore, it is easier to compute the threshold for *TopMeanK* than for *Pat&Mat*. Therefore it seems that *TopMeanK* is a better formulation. To simplify the problem of finding the threshold for *Pat&Mat*, we derived an efficient algorithm for finding it when the hinge loss is used, see Section 2.3.2. Moreover, in the next chapter, we will show that *Pat&Mat* has better theoretical properties. A similar relation holds for the τ -FPL and *Pat&Mat-NP*, as discussed in Section 2.4.1.

Formulation	Label	Source	Ours	Hyper-parameters	C_1	C_2	Threshold
<i>TopPush</i>	(2.5)	[26]	✗	λ	0	$\frac{1}{n_+}$	$s_{[1]}^-$
<i>TopPushK</i>	(2.6)	[34]	✓	λ, K	0	$\frac{1}{n_+}$	$\frac{1}{K} \sum_{i=1}^K s_{[i]}^-$
<i>Grill</i>	(2.9)	[7]	✗	λ	$\frac{1}{n_-}$	$\frac{1}{n_+}$	$\max\left\{t \mid \frac{1}{n} \sum_{i \in \mathcal{I}} \mathbb{1}_{[s_i \geq t]} \geq \tau\right\}$
<i>TopMeanK</i>	(2.11)	—	✗	λ	0	$\frac{1}{n_+}$	$\frac{1}{K} \sum_{i=1}^K s_{[i]}^-$
<i>Pat&Mat</i>	(2.13)	[34]	✓	λ, ϑ	0	$\frac{1}{n_+}$	$\frac{1}{n} \sum_{i \in \mathcal{I}} l(\vartheta(s_i - t)) = \tau$
<i>Grill-NP</i>	(2.18)	—	✗	λ	$\frac{1}{n_-}$	$\frac{1}{n_+}$	$\max\left\{t \mid \frac{1}{n_-} \sum_{i \in \mathcal{I}_-} \mathbb{1}_{[s_i \geq t]} \geq \tau\right\}$
τ -FPL	(2.20)	[33]	✗	λ	0	$\frac{1}{n_+}$	$\frac{1}{n_- \tau} \sum_{i=1}^{n_- \tau} s_{[i]}^-$
<i>Pat&Mat-NP</i>	(2.22)	[34]	✓	λ, ϑ	0	$\frac{1}{n_+}$	$\frac{1}{n_-} \sum_{i \in \mathcal{I}_-} l(\vartheta(s_i - t)) = \tau$

Table 2.1: Summary of problem formulations that fall in the framework (2.3). Column **Formulation** shows the name of the formulation that we use in this work. Column **Label** represents the label of the formulation in this text. Column **Source** is the citation of the work where the formulation was introduced. Column **Ours** shows whether the formulation was introduced in any of our previous papers. Column **Hyperparameters** shows the hyperparameters available for each formulation. The last three columns show the values of parameters C_1 , C_2 and the form of the decision threshold for given framework (2.3).

Primal Formulation: Linear Model

In the previous chapter, we introduced the general framework for binary classification at the top. Table 2.1 summarizes all formulations that fall into this framework. In this chapter, we focus on the particular case when the model f is linear, i.e., the model is in the following form

$$f(\mathbf{x}; \mathbf{w}) = \mathbf{w}^\top \mathbf{x},$$

where $\mathbf{w} \in \mathbb{R}^d$ is the normal vector to the separating hyperplane. In such a case, framework (2.3) simplifies into the form below

$$\begin{aligned} & \underset{\mathbf{w}}{\text{minimize}} && \frac{\lambda}{2} \|\mathbf{w}\|^2 + C_1 \cdot \overline{\text{fp}}(s, t) + C_2 \cdot \overline{\text{fn}}(s, t) \\ & \text{subject to} && s_i = \mathbf{w}^\top \mathbf{x}_i, \quad i \in \mathcal{I}, \\ & && t = G(s, \mathbf{y}). \end{aligned}$$

In the upcoming sections, we provide a theoretical analysis of this unified framework using linear model. We consider the problem formulations from Chapter 2 and not individual algorithms which specify how to solve these formulations. The theoretical properties we mainly focus on are as follows:

- *Convexity* implies a guaranteed convergence for many optimization algorithms or their better convergence rates [35].
- *Differentiability* increases the speed of convergence.
- *Stability* is a general term, by which we mean that the global minimum is not at $\mathbf{w} = \mathbf{0}$. This actually is the case for many formulations from Table 2.1 and results in the situation where the separating hyperplane is degenerate and does not actually exist.

We show the results only for formulations from Section 2.2 and 2.3 for better readability. Formulations in Section 2.3 are mostly identical to the ones from Section 2.4. The only difference is that all formulations in Section 2.3 compute the decision threshold from all samples, while formulations in Section 2.4 use only negative samples. Therefore, the results for both sections are identical, and we show only the ones for Section 2.3.

3.1 Convexity

Convexity is one of the most important properties in numerical optimization. It ensures that the optimization problem has neither stationary points nor local minima. All points of interest are global minima. Moreover, it allows for faster convergence rates. This section shows that some of the formulations from Table 2.1 are convex and, therefore, easier to solve. The first result is summarized in the following proposition. Note that we denote the thresholds as functions of weights \mathbf{w} . This dependence holds since the thresholds are defined in Section 2.3 as functions of scores \mathbf{s} .

Proposition 3.1

Consider fixed vector of scores \mathbf{s} with elements defined as $s_i = \mathbf{w}^\top \mathbf{x}_i$ for all $i \in \mathcal{I}$. Moreover, consider thresholds for *TopPush*, *Grill*, *TopMeanK* and *Pat&Mat* from Section 2.2 and 2.3 defined as

$$\begin{aligned} t_0(\mathbf{w}) &= s_{[1]}, & t_1(\mathbf{w}) &= \max \left\{ t \mid \frac{1}{n} \sum_{i \in \mathcal{I}} \mathbb{1}_{[s_i \geq t]} \geq \tau \right\}, \\ t_2(\mathbf{w}) &= \frac{1}{K} \sum_{i=1}^K s_{[i]}, & t_3(\mathbf{w}) & \text{ solves } \frac{1}{n} \sum_{i \in \mathcal{I}} l(\vartheta(s_i - t)) = \tau, \end{aligned}$$

Then thresholds t_0 , t_2 and t_3 are convex functions of weights \mathbf{w} , while the threshold t_1 is non-convex.

The proposition says that *Grill* formulation uses non-convex threshold while *TopPush*, *TopMeanK*, and *Pat&Mat* use the convex ones. Moreover, the thresholds for τ -FPL and *TopPushK* are convex since both formulations use almost the same threshold as *TopMeanK*. The same holds for the thresholds of *Pat&Mat* and *Pat&Mat-NP* formulations. Notice that all formulations that have a convex threshold use the same objective function.

Theorem 3.2

If the threshold $t = t(\mathbf{w})$ is a convex function of weights \mathbf{w} , then function

$$L(\mathbf{w}) = \overline{\text{fn}}(\mathbf{s}, t) = \sum_{i \in \mathcal{I}_+} l(t - \mathbf{w}^\top \mathbf{x}_i)$$

is convex.

While the proof of Theorem 3.2 is simple, it points to the necessity of considering only false-negatives in the objective function. Due to this theorem, almost all formulations from Table 2.1 are convex optimization problems. There are only two exceptions: *Grill* and *Grill-NP* are not convex problems.

3.2 Differentiability

Similar to convexity, differentiability is crucial for improving the convergence rate. Moreover, differentiability can often be used to derive better termination criteria for numerical algorithms. The next theorem shows which formulations from Table 2.1 are differentiable.

Theorem 3.3

Consider thresholds from Proposition 3.1. Threshold t_0 , t_1 and t_2 are non-differentiable functions of weights \mathbf{w} . Moreover, if the surrogate function l is differentiable, threshold t_3 is a differentiable function of weights \mathbf{w} , and its derivative equals

$$\nabla t_3(\mathbf{w}) = \frac{\sum_{i \in \mathcal{I}} l'(\vartheta(\mathbf{w}^\top \mathbf{x}_i - t_3(\mathbf{w}))) \mathbf{x}_i}{\sum_{j \in \mathcal{I}} l'(\vartheta(\mathbf{w}^\top \mathbf{x}_j - t_3(\mathbf{w})))}.$$

Due to the previous theorem and Theorem 3.2, only *Pat&Mat*, and *Pat&Mat-NP* are convex and differentiable optimization problems. These properties allow us to prove the convergence of the stochastic gradient descent for these two formulations, as shown in Section 3.4.



Figure 3.1: Distribution of positive (red circles) and negative samples (blue circles) for the example from Example 3.4. **(left)** Contour plot of the objective function value for *TopPush* with hinge loss as a surrogate and no regularization and its convergence (orange lines) to the zero vector from 12 different initial points. **(right)**

3.3 Stability

We first provide a simple example and show that many formulations from Table 2.1 are degenerate for it. Then we analyze general conditions under which this degenerate behavior happens.

Example 3.4: Degenerate Behaviour

Consider n negative samples uniformly distributed in $[-1, 0] \times [-1, 1]$, n positive samples uniformly distributed in $[0, 1] \times [-1, 1]$ and one negative sample at $(2, 0)$. An illustration of such settings is provided in Figure 3.1 (left). If n is large enough, the point at $(2, 0)$ is an outlier and the problem is (almost) perfectly separable using the separating hyperplane with normal vector $w_1 = (1, 0)$.

There are two important solutions for Example 3.4. The first is the optimal solution $w_1 = (1, 0)$, which generates the optimal separating hyperplane. The second is $w_0 = (0, 0)$, a degenerate solution that does not generate any separating hyperplane. Since the dataset is perfectly separable by w_1 , we expect that w_1 provides a lower value of the objective function than w_0 for all formulations from Table 2.1. However, it is not happening. Table 3.1 shows the threshold t and the value of the objective function L for w_0 and w_1 . For the precise computation of the results, see Appendix B.3. By highlighting the better objective in Table 3.1 by green, we see that *TopPush* and *TopMeanK* has a better objective in w_0 . It can be shown that w_0 is even the global minimum for these two formulations. This situation raises the question whether some tricks, such as early stopping or excluding a small ball around zero, cannot overcome this difficulty. The answer is negative, as shown in Figure 3.1 (right). Here, we run *TopPush* with hinge loss as a surrogate and no regularization from several starting points. In all cases, *TopPush* converges to zero from one of the three possible directions, and all these directions are far from the normal vector to the separating hyperplane.

The convexity derived in the previous section guarantees that there are no local minima. However, as we showed in the example above, the global minimum may be at $w = 0$. Such

Formulation	Label	$w_0 = (0, 0)$		$w_1 = (1, 0)$	
		t	L	t	L
<i>TopPush</i>	(2.5)	0	1	2	$\frac{5}{2}$
<i>TopPushK</i>	(2.6)	0	1	$\frac{2}{K}$	$\frac{1}{2} + \frac{2}{K}$
<i>Grill</i>	(2.9)	0	2	$1 - 2\tau$	$\frac{3}{2} + 2\tau(1 - \tau)$
<i>TopMeanK</i>	(2.11)	0	1	$1 - \tau$	$\frac{3}{2} - \tau$
<i>Pat&Mat</i>	(2.13)	$\frac{1}{9}(1 - \tau)$	$1 + \frac{1}{9}(1 - \tau)$	$\frac{1}{9}(1 - \tau)$	$\frac{1}{2} + \frac{1}{9}(1 - \tau)$
<i>Grill-NP</i>	(2.18)	0	2	$-\tau$	$1 + \frac{1}{2}\tau^2$
τ -FPL	(2.20)	0	1	$-\frac{1}{2}\tau$	$\frac{1}{2} - \frac{1}{8}\tau(4 + \tau)$
<i>Pat&Mat-NP</i>	(2.22)	$\frac{1}{9}(1 - \tau)$	$1 + \frac{1}{9}(1 - \tau)$	$\frac{1}{9}(1 - \tau) - \frac{1}{2}$	$\frac{1}{9}(1 - \tau)$

Table 3.1: Comparison of formulations from Table 2.1 on the problem from Example 3.4. The table shows the threshold and the objective function value for two solutions: the optimal solution $w_1 = (1, 0)$ and degenerate solution $w_0 = (0, 0)$. Two formulations have the global minimum (denoted by green color) at w_0 , which does not generate any separating hyperplane.

a situation is highly undesirable since w is the normal vector to the separating hyperplane, and the zero vector provides no information. In the rest of the section, we analyze when this situation happens. Theorem 3.5 states that if the decision threshold $t = t(w)$ is above a certain value, then $\mathbf{0}$ has a better (lower) objective than w . If this happens for all w , then $\mathbf{0}$ is the global minimum.

Theorem 3.5

Consider any of these formulations: *TopPush*, *TopPushK*, *TopMeanK* or τ -FPL. Fix any w and denote the corresponding objective function $L(w)$ and threshold $t(w)$. If we have

$$t(w) \geq \frac{1}{n_+} \sum_{i \in \mathcal{I}_+} w^\top x_i, \quad (3.1)$$

then $L(\mathbf{0}) \leq L(w)$. Specifically, using Notation 2.2 we get the following implications

$$\begin{aligned} s_{[1]}^- &\geq \frac{1}{n_+} \sum_{i=1}^{n_+} s_i^+ &\implies L(\mathbf{0}) \leq L(w) \text{ for } TopPush, \\ \frac{1}{K} \sum_{i=1}^K s_{[i]}^- &\geq \frac{1}{n_+} \sum_{i=1}^{n_+} s_i^+ &\implies L(\mathbf{0}) \leq L(w) \text{ for } TopPushK, \\ \frac{1}{K} \sum_{i=1}^K s_{[i]}^- &\geq \frac{1}{n_+} \sum_{i=1}^{n_+} s_i^+ &\implies L(\mathbf{0}) \leq L(w) \text{ for } TopMeanK, \\ \frac{1}{n_- \tau} \sum_{i=1}^{n_- \tau} s_{[i]}^- &\geq \frac{1}{n_+} \sum_{i=1}^{n_+} s_i^+ &\implies L(\mathbf{0}) \leq L(w) \text{ for } \tau\text{-FPL}. \end{aligned}$$

The proof of Theorem 3.5 employs the fact that all formulations in the theorem statement have only false-negatives in the objective. If we use the zero solution $w_0 = \mathbf{0}$, all classification scores s_i are equal to zero, the threshold t equals zero, and the objective function L equals one. On the other hand, if the threshold t is large, many positive samples have scores below the threshold, and the false-negatives samples have the average surrogate value larger than one. In such a case, $w_0 = \mathbf{0}$ becomes the global minimum for some formulations. More specifically, *TopPush* fails if there are outliers, and *TopMeanK* fails whenever there are many positive samples.

Corollary 3.6

Consider the *TopPush* formulation. If positive samples lie in the convex hull of negative samples, then $w = \mathbf{0}$ is the global minimum.

Corollary 3.7

Consider the *TopMeanK* formulation. If $n_+ \geq n\tau$, then $w = \mathbf{0}$ is the global minimum.

There are two fixes to the situation described above:

- Include false-positives to the objective. This approach is taken by *Grill* and *Grill-NP* and necessarily results in the loss of convexity as shown in Section 3.1.
- Move the threshold away from zero even when all scores s are zero. This approach is taken by our formulations *Pat&Mat* and *Pat&Mat-NP* and keeps convexity.

The following theorem shows the advantage of the second approach.

Theorem 3.8

Consider the *Pat&Mat* or *Pat&Mat-NP* formulation with the hinge loss as a surrogate and no regularization. Assume that for some w we have

$$\frac{1}{n_+} \sum_{i \in \mathcal{I}_+} w^\top x_i > \frac{1}{n_-} \sum_{j \in \mathcal{I}_-} w^\top x_j. \quad (3.2)$$

Then there exists a scaling parameter ϑ_0 for the surrogate top τ -quantile (2.12) or (2.21) such that $L(w) < L(\mathbf{0})$ for all $\vartheta \in (0, \vartheta_0)$.

This theorem shed some light on the behavior of the formulations. Theorem 3.5 states that the stability of τ -FPL requires

$$\frac{1}{n_- \tau} \sum_{i=1}^{n_- \tau} s_{[i]}^- < \frac{1}{n_+} \sum_{i=1}^{n_+} s_i^+, \quad (3.3)$$

while Theorem 3.8 states that the stability of *Pat&Mat-NP* is ensured by

$$\frac{1}{n_-} \sum_{i=1}^{n_-} s_{[i]}^- < \frac{1}{n_+} \sum_{i=1}^{n_+} s_i^+. \quad (3.4)$$

Consequently, if τ -FPL is stable, then (3.3) is satisfied. The right-hand sides of (3.3) and (3.4) are the same, while the left-hand side of (3.4) is always smaller than the left-hand side of (3.3). This means that whenever (3.3) is satisfied, (3.4) is also satisfied. Thus, if τ -FPL is stable, *Pat&Mat-NP* is stable as well. At the same time, there may be a considerable difference

in the stability of both formulations. Since the scores of positive samples should be above the scores of negative samples, the scores s may be interpreted as performance. Then formula (3.3) states that if the mean performance of a small number of the worst negative samples is larger than the average performance of all positive samples, then τ -FPL fails. On the other hand, formula (3.4) states that if the average performance of all positive samples is better than the average performance of all negative samples, then *Pat&Mat-NP* is stable. The former may well happen as accuracy at the top is interested in a good performance of only a few positive samples.

In the same way, it can be shown that the stability of *TopMeanK* implies the stability of *Pat&Mat*.

3.4 Stochastic Gradient Descent

In the previous section, we analyzed the formulations from Table 2.1, but we did not consider any optimization algorithms. In this section we show a basic version of the stochastic gradient descent and then its convergent version. Due to considering the threshold, the gradient computed on a minibatch is a biased estimate of the true gradient. Therefore we need to use variance reduction techniques similar to SAG [36], and the proof is rather complex.

Many optimization algorithms for solving the formulations from Table 2.1 use primal-dual or purely dual formulations. Authors of [29] introduced dual variables and used alternating optimization to the resulting min-max problem. In [26, 33], authors dualized the problem and solved it with the steepest gradient ascent. Authors of [37] followed the same path but added kernels to handle non-linearity. We follow the ideas of [38] and [39] and solve the problems directly in their primal formulations. Therefore, even though we use the same formulation for *TopPush* as [26] or for τ -FPL as [33], our solution process is different. However, both algorithms should converge to the same point due to convexity.

For the convergence proof of stochastic gradient descent, we need differentiability. Due to Theorem 3.3, we have only two formulations that are differentiable: *Pat&Mat* and *Pat&Mat-NP*. Therefore, in the rest of the section, we consider only these two formulations. For simplicity, we show the proof only for *Pat&Mat*. The proof for *Pat&Mat-NP* is almost the same.

The decision in variable *Pat&Mat* formulation (2.13) is the normal vector of the separating hyperplane w . Therefore, the gradient descent algorithm uses the following rule

$$w^{k+1} \leftarrow w^k - \alpha^k \cdot \nabla L(w^k),$$

where $k \in \mathbb{N}$ denotes iteration, α^k is a step size, and ∇L is a gradient of the objective function. Since the decision threshold t depends on w , we need to use the chain rule to compute the gradient of the objective function. For each w , the threshold t can be computed uniquely as discussed in Section 2.3.2. We stress this dependence by writing $t(w)$ instead of t . Note that the convexity is preserved. Then we can compute the derivative via the chain rule

$$\begin{aligned} L(w) &= \frac{1}{2} \|w\|^2 + \frac{1}{n_+} \sum_{i \in \mathcal{I}_+} l(t(w) - w^\top x_i), \\ \nabla L(w) &= w + \frac{1}{n_+} \sum_{i \in \mathcal{I}_+} l'(t(w) - w^\top x_i) (\nabla t(w) - x_i), \end{aligned} \tag{3.5}$$

where we assume $\frac{\lambda}{2} = \frac{1}{2}$ for simplicity. The only unknown part is the computation of $\nabla t(w)$. Theorem 3.3 shows the computation for *Pat&Mat* with efficient computation method presented in Section 2.3.2. Since we derive the gradient for the objective function in (3.5), it is easy to derive how to apply the stochastic gradient descent. We only have to partition the dataset into minibatches and provide an update of the weights w based only on a minibatch, namely by replacing the mean over the whole dataset in (3.5) by a mean over the minibatch.

Even though we focus only on the *Pat&Mat* formulation, the relations (3.5) can be used for almost all formulations from Table 2.1. The only two exceptions are *Grill* and *Grill-NP*, which use a slightly different objective function. However, the form on the gradient of the objective function for these two formulations is very similar. Nevertheless, the rest of the section that shows the convergence of the stochastic gradient is applicable only for *Pat&Mat*.

Consider piecewise disjoint minibatches $\mathcal{I}_{\text{mb}}^1, \mathcal{I}_{\text{mb}}^2, \dots, \mathcal{I}_{\text{mb}}^m$ which cycle periodically, i.e., for all k we have $\mathcal{I}_{\text{mb}}^{k+m} = \mathcal{I}_{\text{mb}}^k$. At iteration k we have the decision variable \mathbf{w}^k and the active minibatch $\mathcal{I}_{\text{mb}}^k$. First, we update the vector of scores \mathbf{s}^k only on the active minibatch by setting

$$s_i^k = \begin{cases} \mathbf{x}_i^\top \mathbf{w}^k & \text{for all } i \in \mathcal{I}_{\text{mb}}^k, \\ s_i^{k-1} & \text{otherwise.} \end{cases} \quad (3.6)$$

We keep scores from previous minibatches intact. We use Section 2.3.2 to compute the surrogate quantile t^k as the unique solution of

$$\sum_{i \in \mathcal{I}} l(\vartheta(s_i^k - t^k)) = n\tau. \quad (3.7)$$

This is an approximation of the surrogate quantile $t(\mathbf{w}^k)$ from (2.12). The only difference from the true quantile is that we use delayed scores. Then we approximate the derivative $\nabla L(\mathbf{w}^k)$ from (3.5) by

$$g(\mathbf{w}^k) = \mathbf{w}^k + \frac{1}{n_{\text{mb},+}^k} \sum_{i \in \mathcal{I}_{\text{mb},+}^k} l'(t^k - s_i^k)(\nabla t^k - \mathbf{x}_i), \quad (3.8)$$

where ∇t^k is an approximation of $\nabla t(\mathbf{w}^k)$ from Theorem 3.3. To define the approximation ∇t^k , we first need to define an artificial variable

$$\mathbf{a}^k = \sum_{i \in \mathcal{I}_{\text{mb}}^k} l'(\vartheta(s_i^k - t^k)) \mathbf{x}_i. \quad (3.9)$$

Note that \mathbf{a}^k is an approximation of the numerator of $\nabla t(\mathbf{w}^k)$ from Theorem 3.3, but it uses only the current minibatch. Since our minibatches cycle periodically, we sum the last m variables \mathbf{a}^k and get the approximation of $\nabla t(\mathbf{w}^k)$ computed from all samples and delayed scores

$$\nabla t^k = \frac{\mathbf{a}^k + \mathbf{a}^{k-1} + \dots + \mathbf{a}^{k-m+1}}{\sum_{i \in \mathcal{I}} l'(\vartheta(s_i^k - t^k))}. \quad (3.10)$$

It would be easier to consider only \mathbf{a}^k in the numerator of (3.10). However, presented choice enables us to prove the convergence, and adds stability to the algorithm for small minibatches.

Theorem 3.9

Consider the *Pat&Mat* formulation, stepsizes $\alpha^k = \frac{1}{k+1} \alpha^0$, and piecewise disjoint minibatches $\mathcal{I}_{\text{mb}}^1, \mathcal{I}_{\text{mb}}^2, \dots, \mathcal{I}_{\text{mb}}^m$ which cycle periodically $\mathcal{I}_{\text{mb}}^{k+m} = \mathcal{I}_{\text{mb}}^k$. If l is the smoothened hinge function defined by

$$l(s) = \begin{cases} 0 & \text{for } s < -1 - \varepsilon, \\ \frac{1}{4\varepsilon}(1 + s + \varepsilon)^2 & \text{for } -1 - \varepsilon \leq s < -1 + \varepsilon, \\ 1 + s & \text{otherwise,} \end{cases} \quad (3.11)$$

where $\varepsilon > 0$, then Algorithm 2 converges to the global minimum of (2.13).

The whole procedure of the stochastic gradient descent for *Pat&Mat* formulation is summarized in Algorithm 2. Note that there are no vector operations outside of the current minibatch $\mathcal{I}_{\text{mb}}^k$. Moreover, note that a proper initialization for the first m iterations is needed.

Algorithm 2 Stochastic gradient descent for *Pat&Mat* formulation

Require: Dataset \mathcal{D} , minibatches $\mathcal{I}_{\text{mb}}^1, \mathcal{I}_{\text{mb}}^2, \dots, \mathcal{I}_{\text{mb}}^m$, and stepsize α^k

- 1: Initialize weights w^0
 - 2: **for** $k = 0, 1, \dots$ **do**
 - 3: Select a minibatch $\mathcal{I}_{\text{mb}}^k$
 - 4: Compute s_i^k for all $i \in \mathcal{I}_{\text{mb}}^k$ according to (3.6)
 - 5: Compute t^k according to (3.7)
 - 6: Compute a^k according to (3.9)
 - 7: Compute ∇t^k according to (3.10)
 - 8: Compute $g(w^k)$ according to (3.8)
 - 9: Set $w^{k+1} \leftarrow w^k - \alpha^k g(w^k)$
 - 10: **end for**
-

3.5 Summary

In this chapter, we derived theoretical properties for formulations from Table 2.1 with the linear model. We focused on the convexity, differentiability, and stability of formulations since these three properties are crucial for fast and proper convergence. All results are summarized in Table 3.2. We showed that *TopPush*, *TopPushK*, *TopMeanK*, and τ -FPL are convex, but all these formulations are vulnerable to having the global minimum at $w = 0$. On the other hand, *Grill* and *Grill-NP* are stable, but they are not convex or differentiable. Finally, our formulations *Pat&Mat* and *Pat&Mat-NP* satisfy all three theoretical properties.

A similar comparison is performed in Figure 3.2. Methods in green and yellow are convex, while formulations in red are non-convex. Based on Theorem 3.5, four formulations in yellow are vulnerable to having the global minimum at $w = 0$. This theorem states that the higher the threshold, the more vulnerable the formulation is. The full arrows depict this dependence. If it points from one formulation to another, the latter one has a smaller threshold and thus is less vulnerable to this undesired global minima. The dotted arrows indicate that this usually holds but not always. The precise formulation is provided in Appendix 2.3.1. This complies with Corollaries 3.6 and 3.7 which state that *TopPush* and *TopMeanK* are most vulnerable. At the same time, it says that τ -FPL is the best one from the yellow formulations. Finally, even though *Pat&Mat-NP* has a worse approximation of the true threshold than τ -FPL due to Lemma 2.6, it is more stable due to the discussion after Theorem 3.8. Similarly, *Pat&Mat* has a worse approximation of the true threshold than *TopMeanK* due to Lemma 2.4, but is more stable.

Formulation	Label	Convex	Differentiable	Stable
<i>TopPush</i>	(2.5)	✓	✗	✗
<i>TopPushK</i>	(2.6)	✓	✗	✗
<i>Grill</i>	(2.9)	✗	✗	✓
<i>TopMeanK</i>	(2.11)	✓	✗	✗
<i>Pat&Mat</i>	(2.13)	✓	✓	✓
<i>Grill-NP</i>	(2.18)	✗	✗	✓
τ -FPL	(2.20)	✓	✗	✗
<i>Pat&Mat-NP</i>	(2.22)	✓	✓	✓

Table 3.2: Summary of the formulations from Table 2.1. The last three columns show whether the formulation is differentiable, convex, and stable (in the sense of having global minimum in $w = 0$).

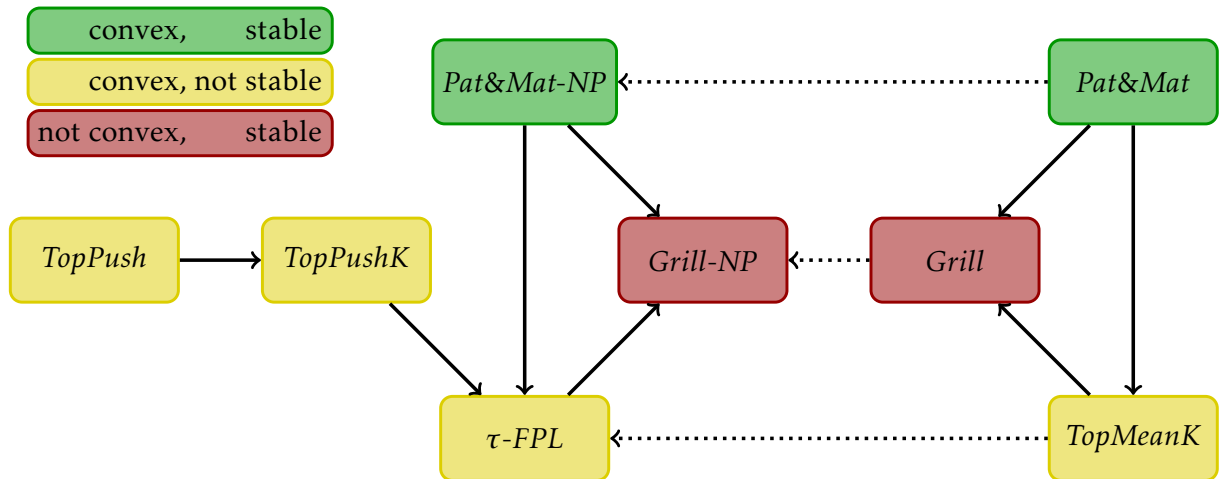


Figure 3.2: Summary of the formulations from Table 2.1. Methods in green and yellow are convex, while formulations in red are non-convex. Moreover, methods in yellow are vulnerable to having the global minimum at $w = 0$. A full (dotted) arrow pointing from one formulation to another shows that the latter formulation has (usually) a smaller threshold.

Dual Formulation: Linear Model

In Chapter 2, we introduced a general framework for binary classification at the top. Moreover, we showed that several problem classes, considered separate problems so far, fit into this framework. The summary of all formulations is provided in Table 2.1. In Chapter 3 we discussed a special case when the linear model is used. Then formulation (2.3) reads

$$\begin{aligned}
 & \underset{\mathbf{w}}{\text{minimize}} && \frac{\lambda}{2} \|\mathbf{w}\|^2 + C_1 \cdot \overline{\text{fp}}(\mathbf{s}, t) + C_2 \cdot \overline{\text{fn}}(\mathbf{s}, t) \\
 & \text{subject to} && s_i = \mathbf{w}^\top \mathbf{x}_i, \quad i \in \mathcal{I}, \\
 & && t = G(\mathbf{s}, \mathbf{y}).
 \end{aligned} \tag{4.1}$$

Many formulations have nice theoretical properties such as convexity or differentiability in this specific case. However, many real-world problems are not linearly separable, and in such cases, the approach from the previous section is not sufficient. In this chapter, we use the similarity of (4.1) to primal formulation of SVM [25] and derive dual forms for all formulations from Table 2.1. Then we use the kernel method [40] to introduce nonlinearity into the dual formulations. Moreover, as dual problems are generally computationally expensive, we propose an efficient method to solve them.

4.1 Derivation of Dual Problems

As discussed in the introduction, this section is dedicated to deriving dual forms for all formulations from Table 2.1. We do not discuss *Grill* and *Grill-NP* formulations in the following text since both formulations are not convex, and therefore their primal and dual formulations are not equivalent. Since many of the remaining formulations are very similar, we divide them into two families:

- **TopPushK family:** *TopPush*, *TopPushK*, *TopMeanK* and τ -FPL.
- **Pat&Mat family:** *Pat&Mat* and *Pat&Mat-NP*.

Both families use surrogate false-negative rate as an objective function. Moreover, all formulations from *TopPushK* family use the mean of K highest scores of all or negative samples as a threshold and differ only in the definition of K . Finally, both formulations from *Pat&Mat* family use a surrogate approximation of the top τ -quantile of scores of all or negative samples. In other words, we have two families of formulations that share the same objective function and the same form of the decision threshold. Therefore, we derive all results for the general form of these two families. Before we start, we need to introduce the concept of conjugate functions.

Definition 4.1: Conjugate function [35]

Let $l: \mathbb{R}^n \rightarrow \mathbb{R}$. The function $l^*: \mathbb{R}^n \rightarrow \mathbb{R}$, defined as

$$l^*(y) = \sup_{x \in \text{dom } l} \{y^\top x - l(x)\}.$$

is called the conjugate function of l . The domain of the conjugate function consists of $y \in \mathbb{R}^n$ for which the supremum is finite.

These functions will play a crucial role in the resulting form of dual problems. Recall the hinge loss and quadratic hinge loss function defined in Notation 2.1

$$l_{\text{hinge}}(s) = \max\{0, 1 + s\}, \quad l_{\text{quadratic}}(s) = (\max\{0, 1 + s\})^2.$$

The conjugate function for the hinge loss can be found in [41] and has the following form

$$l_{\text{hinge}}^*(y) = \begin{cases} -y & \text{if } y \in [0, 1], \\ \infty & \text{otherwise.} \end{cases} \quad (4.2)$$

Similarly, the conjugate function for the quadratic hinge was computed in [42] as

$$l_{\text{quadratic}}^*(y) = \begin{cases} \frac{y^2}{4} - y & \text{if } y \geq 0, \\ \infty & \text{otherwise.} \end{cases} \quad (4.3)$$

Notation 4.2: Kernel Matrix

To simplify the future notation, we introduce matrix \mathbb{X} of all samples. Each row of \mathbb{X} represents one sample and is defined for all $i \in \mathcal{I}$ as

$$\mathbb{X}_{i,\bullet} = \mathbf{x}_i^\top.$$

In the same way, we defined matrices \mathbb{X}^+ , \mathbb{X}^- of all negative and positive samples with rows defined as

$$\begin{aligned} \mathbb{X}_{i,\bullet}^- &= \mathbf{x}_i^\top & i = 1, 2, \dots, n^-, \\ \mathbb{X}_{i,\bullet}^+ &= \mathbf{x}_i^\top & i = 1, 2, \dots, n^+. \end{aligned}$$

Moreover, for all formulations that use only negative samples to compute the threshold t , we define kernel matrix \mathbb{K}^- as

$$\mathbb{K}^- = \begin{pmatrix} \mathbb{X}^+ \\ -\mathbb{X}^- \end{pmatrix} \begin{pmatrix} \mathbb{X}^+ \\ -\mathbb{X}^- \end{pmatrix}^\top = \begin{pmatrix} \mathbb{X}^+ \mathbb{X}^{+\top} & -\mathbb{X}^+ \mathbb{X}^{-\top} \\ -\mathbb{X}^- \mathbb{X}^{+\top} & \mathbb{X}^- \mathbb{X}^{-\top} \end{pmatrix}.$$

and for all formulations that use only all samples to compute the threshold t , we define kernel matrix \mathbb{K}^\pm as

$$\mathbb{K}^\pm = \begin{pmatrix} \mathbb{X}^+ \\ -\mathbb{X} \end{pmatrix} \begin{pmatrix} \mathbb{X}^+ \\ -\mathbb{X} \end{pmatrix}^\top = \begin{pmatrix} \mathbb{X}^+ \mathbb{X}^{+\top} & -\mathbb{X}^+ \mathbb{X}^\top \\ -\mathbb{X} \mathbb{X}^{+\top} & \mathbb{X} \mathbb{X}^\top \end{pmatrix}.$$

In the rest of the text, matrix \mathbb{K} always refers to one of the kernel matrices defined above.

4.1.1 Family of *TopPushK* Formulations

In this section, we focus on the family of *TopPushK* formulations. The general optimization problem that covers all formulations from this family can be written in the following way

$$\underset{\mathbf{w}}{\text{minimize}} \quad \frac{1}{2} \|\mathbf{w}\|^2 + C \sum_{i \in \mathcal{I}_+} l(t - \mathbf{w}^\top \mathbf{x}_i) \quad (4.4a)$$

$$\text{subject to} \quad s_j = \mathbf{w}^\top \mathbf{x}_j, \quad j \in \tilde{\mathcal{I}}, \quad (4.4b)$$

$$t = \frac{1}{K} \sum_{j=1}^K s_{[j]}, \quad (4.4c)$$

where $C \in \mathbb{R}$. The set of indices $\tilde{\mathcal{I}}$ equals \mathcal{I} for *TopMeanK* and \mathcal{I}_- for other formulations. The parameter K equals 1 for *TopPush*, K for *TopPushK*, $n\tau$ for *TopMeanK*, and $n_- \tau$ for τ -FPL. Note that we use an alternative formulation with constant C , since it is more similar to the standard SVM, and we wanted to stress this similarity. For $C = 1/\lambda_{n_+}$ the new formulation is identical to the original one.

The following theorem shows the dual form of formulation (4.4). The dual formulation for *TopPush* was originally derived in [26]. We only show, that our general dual formulation also covers this special case. To keep the readability as simple as possible, we postpone all proofs to Appendix C.

Theorem 4.3: Dual formulation for *TopPushK* family

Consider Notation 4.2, surrogate function l , and formulation (4.4). Then the corresponding dual problem has the following form

$$\underset{\alpha, \beta}{\text{maximize}} \quad -\frac{1}{2} \begin{pmatrix} \alpha \\ \beta \end{pmatrix}^\top \mathbb{K} \begin{pmatrix} \alpha \\ \beta \end{pmatrix} - C \sum_{i=1}^{n_+} l^* \left(\frac{\alpha_i}{C} \right) \quad (4.5a)$$

$$\text{subject to} \quad \sum_{i=1}^{n_+} \alpha_i = \sum_{j=1}^{\tilde{n}} \beta_j, \quad (4.5b)$$

$$0 \leq \beta_j \leq \frac{1}{K} \sum_{i=1}^{n_+} \alpha_i, \quad j = 1, 2, \dots, \tilde{n}, \quad (4.5c)$$

where l^* is conjugate function of l and

	K	\mathbb{K}	\tilde{n}	$\tilde{\mathbf{x}}_j$
<i>TopPush</i>	1	\mathbb{K}^-	n_-	\mathbf{x}_j^-
<i>TopPushK</i>	K	\mathbb{K}^-	n_-	\mathbf{x}_j^-
<i>TopMeanK</i>	$n\tau$	\mathbb{K}^\pm	n	\mathbf{x}_j
τ -FPL	$n_- \tau$	\mathbb{K}^-	n_-	\mathbf{x}_j^-

If $K = 1$, the upper bound in the second constraint (4.5c) vanishes due to the first constraint. Finally, the primal variables \mathbf{w} can be computed from dual variables as follows

$$\mathbf{w} = \sum_{i=1}^{n_+} \alpha_i \mathbf{x}_i^+ - \sum_{j=1}^{\tilde{n}} \beta_j \tilde{\mathbf{x}}_j. \quad (4.6)$$

4.1.2 Family of *Pat&Mat* Formulations

In the same way, as for *TopPushK* family, we introduce a general optimization problem that covers all formulations from *Pat&Mat* family and reads

$$\begin{aligned} & \underset{\mathbf{w}}{\text{minimize}} && \frac{1}{2} \|\mathbf{w}\|^2 + C \sum_{i \in \mathcal{I}_+} l(t - \mathbf{w}^\top \mathbf{x}_i) \\ & \text{subject to} && t \text{ solves } \frac{1}{\tilde{n}} \sum_{i \in \tilde{\mathcal{I}}} l(\vartheta(\mathbf{w}^\top \mathbf{x}_j - t)) = \tau, \end{aligned} \quad (4.7)$$

where $C \in \mathbb{R}$. For *Pat&Mat* we have $\tilde{\mathcal{I}} = \mathcal{I}$ and $\tilde{n} = n$. For *Pat&Mat-NP* we have $\tilde{\mathcal{I}} = \mathcal{I}_-$ and $\tilde{n} = n_-$. Again, we use the alternative formulation with constant C . The following theorem shows the dual form of the formulation (4.7).

Theorem 4.4: Dual formulation for *Pat&Mat* family

Consider Notation 4.2, surrogate function l , and formulation (4.7). Then the corresponding dual problem has the following form

$$\underset{\alpha, \beta, \delta}{\text{maximize}} \quad -\frac{1}{2} \begin{pmatrix} \alpha \\ \beta \end{pmatrix}^\top \mathbb{K} \begin{pmatrix} \alpha \\ \beta \end{pmatrix} - C \sum_{i=1}^{n_+} l^* \left(\frac{\alpha_i}{C} \right) - \delta \sum_{j=1}^{\tilde{n}} l^* \left(\frac{\beta_j}{\delta \vartheta} \right) - \delta \tilde{n} \tau \quad (4.8a)$$

$$\text{subject to} \quad \sum_{i=1}^{n_+} \alpha_i = \sum_{j=1}^{\tilde{n}} \beta_j, \quad (4.8b)$$

$$\delta \geq 0, \quad (4.8c)$$

where l^* is conjugate function of l , $\vartheta > 0$ is a scaling parameter and

	\mathbb{K}	\tilde{n}	$\tilde{\mathbf{x}}_j$
<i>Pat&Mat</i>	\mathbb{K}^\pm	n	\mathbf{x}_j
<i>Pat&Mat-NP</i>	\mathbb{K}^-	n_-	\mathbf{x}_j^-

Finally, the primal variables \mathbf{w} can be computed from dual variables as follows

$$\mathbf{w} = \sum_{i=1}^{n_+} \alpha_i \mathbf{x}_i^+ - \sum_{j=1}^{\tilde{n}} \beta_j \tilde{\mathbf{x}}_j. \quad (4.9)$$

Note 4.5

For simplicity, the rest of the chapter covers only the *TopPushK* formulation with hinge loss. We use this formulation since it is the prototypical example for the *TopPushK* family of formulations. The results for the rest of the formulations from this family can be derived almost identically. Moreover, results for the *Pat&Mat* family of formulations can be derived similarly. Therefore, derivations for the *TopPushK* family with quadratic hinge loss and the *Pat&Mat* family with hinge and quadratic hinge loss are postponed to Appendix C.

4.2 Kernels

As we mentioned at the beginning of the chapter, our goal is to extend our framework to be usable for linearly inseparable problems. In two previous sections, we derived dual formulations for *TopPushK* and *Pat&Mat* families. In this section, we show how to employ the kernels method [40] to introduce nonlinearity into these dual formulations. For simplicity, we focus only on the *TopPushK* formulation that computes the decision threshold only from negative samples. As mentioned in Notation 4.2, *TopPushK* formulation uses kernel matrix $\mathbb{K} = \mathbb{K}^-$. The following derivation is the same for all other formulations.

To add kernels, we first realize that primal variables w can be computed from dual variables α, β using (4.6). Therefore, the classification score for any sample x can be calculated as follows

$$s = w^\top x = \sum_{i=1}^{n_+} \alpha_i x^\top x_i^+ - \sum_{i=1}^{n_-} \beta_i x^\top x_i^- \quad (4.10)$$

Importantly, all samples x_i in the previous formula occur only in the dot product with x and not separately. This property allows us to use the standard kernel trick from SVMs [25]. The kernel trick replaces the dot product of the vectors from input space using the so-called kernel function $k : \mathbb{R}^d \times \mathbb{R}^d \rightarrow \mathbb{R}$. This function represents a dot product in the space of a higher dimension

$$k(x, x') = \phi(x)^\top \phi(x'),$$

where $\phi : \mathbb{R}^d \rightarrow \mathbb{R}^D$ is a mapping function. The idea is to transform the input vectors using ϕ into some feature space in which the classification problem is easier to solve. However, getting the explicit formula for the mapping function is usually very hard. The kernel trick allows us to avoid this explicit mapping to the feature space since we can only replace the dot product in (4.10) by the kernel function k

$$s = \sum_{i=1}^{n_+} \alpha_i k(x, x_i^+) - \sum_{i=1}^{n_-} \beta_i k(x, x_i^-) \quad (4.11)$$

The downside of this approach is, that we can not compute the primal variables using (4.6) if we do not know the mapping function ϕ . We always have to calculate the scores using the formula above, which is computationally expensive.

Now we must show how to modify the original dual problem (4.5) to incorporate kernels. Recall the form of the kernel matrix \mathbb{K} for *TopPushK*

$$\mathbb{K} = \begin{pmatrix} \mathbb{X}^+ \mathbb{X}^{+\top} & -\mathbb{X}^+ \mathbb{X}^{-\top} \\ -\mathbb{X}^- \mathbb{X}^{+\top} & \mathbb{X}^- \mathbb{X}^{-\top} \end{pmatrix}.$$

Since each component of the kernel matrix \mathbb{K} is computed as a dot product of two training samples, we can replace \mathbb{K} with a matrix in the following form

$$\mathbb{K} = \begin{pmatrix} k(\mathbb{X}^+, \mathbb{X}^+) & -k(\mathbb{X}^+, \mathbb{X}^-) \\ -k(\mathbb{X}^-, \mathbb{X}^+) & k(\mathbb{X}^-, \mathbb{X}^-) \end{pmatrix} \quad (4.12)$$

The kernel function $k(\cdot, \cdot)$ is applied to all rows of both arguments. In other words, if we use the kernel trick, the original dual problem (4.5) remains almost the same. The only change is in the construction of the kernel matrix.

4.3 Coordinate Descent Algorithm

In the previous sections, we derived dual formulations for *TopPushK* and *Pat&Mat* families of formulations. Moreover, we showed how to incorporate non-linear kernels into these formulations. As a result, we can use all presented formulations even for linearly non-separable problems. However, the dimension of the dual problems is at least equal to the number of all samples n , and therefore, it is computationally expensive to use standard techniques such as gradient descent. To handle this issue, the standard coordinate descent algorithm [43, 44] has been proposed in the context of SVMs. In this section, we derive a coordinate descent algorithm suitable for our dual problems (4.5, 4.8). We also show that we can reduce the whole optimization problem to a one-dimensional quadratic optimization problem with a closed-form solution in every iteration. Therefore, every iteration of our algorithm is cheap. For a review of other approaches see [45, 46].

Recall that we perform all derivations only for *TopPushK* with hinge loss. Classification scores can be computed directly from dual variables as shown in (4.11). Using the definition (4.12) of kernel matrix \mathbb{K} , we can define a vector of scores \mathbf{s} by

$$\mathbf{s} = \mathbb{K} \begin{pmatrix} \boldsymbol{\alpha} \\ \boldsymbol{\beta} \end{pmatrix}. \quad (4.13)$$

Note that dual scores are not identical to the primal ones (4.10) (even though we use the same notation). The main difference is that dual scores use kernel function k . Therefore, they are equivalent only if the kernel function is defined as a dot product in the input space, i.e., if $k(\mathbf{x}, \mathbf{x}') = \mathbf{x}^\top \mathbf{x}'$. To simplify the indexing of the vector of scores (4.13) and kernel matrix \mathbb{K} , we introduce a new notation in Notation 4.6.

Notation 4.6

Consider any index l that satisfies $1 \leq l \leq n_+ + \tilde{n}$. Note that the length of dual variable $\boldsymbol{\alpha}$ is n_+ for both formulations (4.5) and (4.8). Therefore, we can define auxiliary index \hat{l} as

$$\hat{l} = \begin{cases} l & \text{if } l \leq n_+, \\ l - n_+ & \text{otherwise.} \end{cases}$$

Then the index l can be safely used for kernel matrix \mathbb{K} or vector of scores \mathbf{s} , while its corresponding version \hat{l} can be used for dual variables $\boldsymbol{\alpha}$ or $\boldsymbol{\beta}$.

4.3.1 Update Rules

Consider dual formulation (4.5) from Theorem 4.3 and fixed feasible dual variables $\boldsymbol{\alpha}, \boldsymbol{\beta}$. Our goal in this section is to derive an efficient iterative procedure for solving this problem. We follow the ideas presented in [43, 44] for solving SVMs using a coordinate descent algorithm. However, we must modify the approach since we have an additional constraint (4.5b). Due to this constraint, we always have to update (at least) two components of dual variables $\boldsymbol{\alpha}, \boldsymbol{\beta}$. There are only three update rules which modify two components of $\boldsymbol{\alpha}, \boldsymbol{\beta}$, and satisfy constraints (4.5b). The first one updates two components of $\boldsymbol{\alpha}$

$$\alpha_{\hat{k}} \rightarrow \alpha_{\hat{k}} + \Delta, \quad \alpha_{\hat{l}} \rightarrow \alpha_{\hat{l}} - \Delta, \quad \mathbf{s} \rightarrow \mathbf{s} + (\mathbb{K}_{\bullet, \hat{k}} - \mathbb{K}_{\bullet, \hat{l}})\Delta, \quad (4.14a)$$

where $\mathbb{K}_{\bullet, i}$ denotes i -th column of \mathbb{K} and indices \hat{k}, \hat{l} are defined in Notation 4.6. Note that the update rule for \mathbf{s} does not use matrix multiplication but only vector addition. The second rule

updates one component of α and one component of β

$$\alpha_{\hat{k}} \rightarrow \alpha_{\hat{k}} + \Delta, \quad \beta_{\hat{l}} \rightarrow \beta_{\hat{l}} + \Delta, \quad s \rightarrow s + (\mathbb{K}_{\bullet,k} + \mathbb{K}_{\bullet,l})\Delta, \quad (4.14b)$$

and the last one updates two components of β

$$\beta_{\hat{k}} \rightarrow \beta_{\hat{k}} + \Delta, \quad \beta_{\hat{l}} \rightarrow \beta_{\hat{l}} - \Delta, \quad s \rightarrow s + (\mathbb{K}_{\bullet,k} - \mathbb{K}_{\bullet,l})\Delta. \quad (4.14c)$$

Using any of the update rules above, the problem (4.5) can be written as a one-dimensional quadratic problem in the following form

$$\begin{aligned} & \underset{\Delta}{\text{maximize}} && -\frac{1}{2}a(\alpha, \beta)\Delta^2 - b(\alpha, \beta)\Delta - c(\alpha, \beta) \\ & \text{subject to} && \Delta_{lb}(\alpha, \beta) \leq \Delta \leq \Delta_{ub}(\alpha, \beta) \end{aligned}$$

where $a, b, c, \Delta_{lb}, \Delta_{ub}$ are constants with respect to Δ . The optimal solution to this problem is

$$\Delta^* = \text{clip}_{[\Delta_{lb}, \Delta_{ub}]}(\gamma), \quad (4.15)$$

where $\gamma = -\frac{b}{a}$ and $\text{clip}_{[a, b]}(x)$ amounts to clipping (projecting) x to interval $[a, b]$. Since we assume one of the update rules (4.14), the constraint (4.5b) is always satisfied after the update. Even though all three update rules hold for any surrogate, the calculation of the optimal Δ^* depends on the concrete form of surrogate function. In the following text, we show the closed-form formula for Δ^* , when the hinge loss function from Notation 2.1 is used.

Plugging the conjugate (4.2) of the hinge loss into the dual formulation (4.5) yields

$$\underset{\alpha, \beta}{\text{maximize}} \quad -\frac{1}{2} \begin{pmatrix} \alpha \\ \beta \end{pmatrix}^\top \mathbb{K} \begin{pmatrix} \alpha \\ \beta \end{pmatrix} + \sum_{i=1}^{n_+} \alpha_i \quad (4.16a)$$

$$\text{subject to} \quad \sum_{i=1}^{n_+} \alpha_i = \sum_{j=1}^{\tilde{n}} \beta_j, \quad (4.16b)$$

$$0 \leq \alpha_i \leq C, \quad i = 1, 2, \dots, n_+, \quad (4.16c)$$

$$0 \leq \beta_j \leq \frac{1}{K} \sum_{i=1}^{n_+} \alpha_i, \quad j = 1, 2, \dots, \tilde{n}. \quad (4.16d)$$

The form of \mathbb{K} and \tilde{n} depends on the used formulation as discussed in Theorem 4.3. Moreover, the upper bound in (4.16d) can be omitted for $K = 1$. Since we know the form of the optimal solution (4.15), we only need to show how to compute Δ_{lb}, Δ_{ub} and γ for all update rules (4.14). The following three propositions provide closed-form formulae for all three update rules. To keep the presentation as simple as possible, we postpone all proofs to Appendix C.2.1.

Proposition 4.7: Update rule (4.14a) for problem (4.16)

Consider problem (4.16), update rule (4.14a), indices $1 \leq k \leq n_+$ and $1 \leq l \leq n_+$ and Notation 4.6. Then the optimal solution Δ^* is given by (4.15) where

$$\begin{aligned} \Delta_{lb} &= \max\{-\alpha_{\hat{k}}, \alpha_{\hat{l}} - C\}, \\ \Delta_{ub} &= \min\{C - \alpha_{\hat{k}}, \alpha_{\hat{l}}\}, \\ \gamma &= -\frac{s_k - s_l}{\mathbb{K}_{kk} + \mathbb{K}_{ll} - \mathbb{K}_{kl} - \mathbb{K}_{lk}}. \end{aligned}$$

Proposition 4.8: Update rule (4.14b) for problem (4.16)

Consider problem (4.16), update rule (4.14b), indices $1 \leq k \leq n_+$ and $n_+ + 1 \leq l \leq \tilde{n}$ and Notation 4.6. Let us define

$$\beta_{\max} = \max_{j \in \{1, 2, \dots, \tilde{n}\} \setminus \{l\}} \beta_j.$$

Then the optimal solution Δ^* is given by (4.15) where

$$\begin{aligned} \Delta_{lb} &= \begin{cases} \max\{-\alpha_{\hat{k}}, -\beta_{\hat{l}}\} & K = 1, \\ \max\{-\alpha_{\hat{k}}, -\beta_{\hat{l}}, K\beta_{\max} - \sum_{i=1}^{n_+} \alpha_i\} & \text{otherwise,} \end{cases} \\ \Delta_{ub} &= \begin{cases} C - \alpha_{\hat{k}} & K = 1, \\ \min\{C - \alpha_{\hat{k}}, \frac{1}{K-1}(\sum_{i=1}^{n_+} \alpha_i - K\beta_{\hat{l}})\} & \text{otherwise.} \end{cases} \\ \gamma &= -\frac{s_k + s_l - 1}{\mathbb{K}_{kk} + \mathbb{K}_{ll} + \mathbb{K}_{kl} + \mathbb{K}_{lk}}. \end{aligned}$$

Proposition 4.9: Update rule (4.14c) for problem (4.16)

Consider problem (4.16), update rule (4.14c), indices $n_+ + 1 \leq k \leq \tilde{n}$ and $n_+ + 1 \leq l \leq \tilde{n}$ and Notation 4.6. Then the optimal solution Δ^* is given by (4.15) where

$$\begin{aligned} \Delta_{lb} &= \begin{cases} -\beta_{\hat{k}} & K = 1, \\ \max\{-\beta_{\hat{k}}, \beta_{\hat{l}} - \frac{1}{K} \sum_{i=1}^{n_+} \alpha_i\} & \text{otherwise,} \end{cases} \\ \Delta_{ub} &= \begin{cases} \beta_{\hat{l}} & K = 1, \\ \min\{\frac{1}{K} \sum_{i=1}^{n_+} \alpha_i - \beta_{\hat{k}}, \beta_{\hat{l}}\} & \text{otherwise.} \end{cases} \\ \gamma &= -\frac{s_k - s_l}{\mathbb{K}_{kk} + \mathbb{K}_{ll} - \mathbb{K}_{kl} - \mathbb{K}_{lk}}. \end{aligned}$$

4.3.2 Initialization

For all update rules (4.14) we assumed that the current solution α, β is feasible. So to create an iterative algorithm that solves problem (4.16) or (C.3), we need to have a way how to obtain an initial feasible solution. Such a task can be formally written as a projection of random variables α^0, β^0 to the feasible set of solutions

$$\begin{aligned} &\underset{\alpha, \beta}{\text{minimize}} \quad \frac{1}{2} \|\alpha - \alpha^0\|^2 + \frac{1}{2} \|\beta - \beta^0\|^2 \\ &\text{subject to} \quad \sum_{i=1}^{n_+} \alpha_i = \sum_{j=1}^{\tilde{n}} \beta_j, \\ &\quad 0 \leq \alpha_i \leq C, \quad i = 1, 2, \dots, n_+, \\ &\quad 0 \leq \beta_j \leq \frac{1}{K} \sum_{i=1}^{n_+} \alpha_i, \quad j = 1, 2, \dots, \tilde{n}, \end{aligned} \tag{4.17}$$

where the upper bound in the second constraint depends on the used surrogate function. To solve problem (4.17), we follow the same approach as in [47]. In the following theorem, we show that problem (4.17) can be written as a system of two equations of two variables λ and μ . Moreover, the theorem shows the concrete form of feasible solution α, β that depends only on λ and μ .

Theorem 4.10

Consider problem (4.17), some initial solution α^0, β^0 and denote the sorted version (in non-decreasing order) of β^0 as $\beta_{[\cdot]}^0$. Then if the following condition holds

$$\sum_{j=1}^K \left(\beta_{[\tilde{n}-K+j]}^0 + \max_{i=1, \dots, n_+} \alpha_i^0 \right) \leq 0, \quad (4.18)$$

the optimal solution of (4.17) amounts to $\alpha = \beta = 0$. In the opposite case, the following system of two equations

$$\sum_{i=1}^{n_+} \text{clip}_{[0, C]} \left(\alpha_i^0 - \lambda + \frac{1}{K} \sum_{j=1}^{\tilde{n}} \text{clip}_{[0, +\infty)} (\beta_j^0 + \lambda - \mu) \right) - K\mu = 0, \quad (4.19a)$$

$$\sum_{j=1}^{\tilde{n}} \text{clip}_{[0, \mu]} (\beta_j^0 + \lambda) - K\mu = 0, \quad (4.19b)$$

has a solution (λ, μ) with $\mu > 0$, and the optimal solution of (4.17) is equal to

$$\begin{aligned} \alpha_i &= \text{clip}_{[0, C]} \left(\alpha_i^0 - \lambda + \frac{1}{K} \sum_{j=1}^{\tilde{n}} \text{clip}_{[0, +\infty)} (\beta_j^0 + \lambda - \mu) \right), \\ \beta_j &= \text{clip}_{[0, \mu]} (\beta_j^0 + \lambda). \end{aligned}$$

Theorem 4.10 shows the optimal solution of (4.17) that depends only on (λ, μ) but does not provide any way to find such a solution. In the following text, we show that the number of variables in the system of equations (4.19) can be reduced to one. For any fixed μ , we denote the function on the left-hand side of (4.19b) by

$$g(\lambda; \mu) := \sum_{j=1}^{\tilde{n}} \text{clip}_{[0, \mu]} (\beta_j^0 + \lambda) - K\mu.$$

Then g is non-decreasing in λ but not necessarily strictly increasing. We denote by $\lambda(\mu)$ any such λ solving (4.19b) for a fixed μ . Denote \mathbf{z} the sorted version of $-\beta^0$. Then we have

$$g(\lambda; \mu) = \sum_{\{j \mid \lambda - z_j \in [0, \mu)\}} (\lambda - z_j) + \sum_{\{j \mid \lambda - z_j \geq \mu\}} \mu - K\mu.$$

Now we can easily compute $\lambda(\mu)$ by solving $g(\lambda(\mu); \mu) = 0$ for fixed μ . To get the solution efficiently, we derive Algorithm 3, which can be described as follows: Index i will run over \mathbf{z} while index j will run over $\mathbf{z} + \mu$. At every iteration, we know the values of $g(z_{i-1}; \mu)$ and $g(z_{j-1} + \mu; \mu)$ and we want to evaluate g at the next point. We denote the number of indices j such that $\lambda - z_j \in [0, \mu)$ by d . If $z_i \leq z_j + \mu$, then we consider $\lambda = z_i$ and since one index enters the set $\{j \mid \lambda - z_j \in [0, \mu)\}$, we increase d by one. On the other hand, if $z_i > z_j + \mu$, then we consider $\lambda = z_j + \mu$ and since one index leaves the set $\{j \mid \lambda - z_j \in [0, \mu)\}$, we decrease d by one. In both cases, g is increased by d times the difference between the new λ and old λ . Once g exceeds 0, we stop the algorithm and linearly interpolate between the last two values. To prevent an overflow, we set $z_{m+1} = +\infty$. Concerning the initial values, since $z_1 \leq z_1 + \mu$, we set $i = 2, j = 1$ and $d = 1$.

4.4 Summary

Algorithm 3 An efficient algorithm for computing $\lambda(\mu)$ from (4.17) for fixed μ .

Require: vector $-\beta^0$ sorted into z

```

1:  $i \leftarrow 2, j \leftarrow 1, d \leftarrow 1$ 
2:  $\lambda \leftarrow z_1, g \leftarrow -K\mu$ 
3: while  $g < 0$  do
4:   if  $z_i \leq z_j + \mu$  then
5:      $g \leftarrow g + d(z_i - \lambda)$ 
6:      $\lambda \leftarrow z_i, d \leftarrow d + 1, i \leftarrow i + 1$ 
7:   else
8:      $g \leftarrow g + d(z_j + \mu - \lambda)$ 
9:      $\lambda \leftarrow z_j + \mu, d \leftarrow d - 1, j \leftarrow j + 1$ 
10:  end if
11: end while
12: return linear interpolation of the last two values of  $\lambda$ 

```

Since $\lambda(\mu)$ can be computed for fixed μ using Algorithm 3, we can define auxiliary function h in the following form

$$h(\mu) = \sum_{i=1}^{n_+} \text{clip}_{[0, C]} \left(\alpha_i^0 - \lambda(\mu) + \frac{1}{K} \sum_{j=1}^{\tilde{n}} \text{clip}_{[0, +\infty)} (\beta_j^0 + \lambda(\mu) - \mu) \right) - K\mu. \quad (4.20)$$

Then the system of equations (4.19) is equivalent to $h(\mu) = 0$. The following lemma describes properties of h . Since h is decreasing in μ on $(0, \infty)$, any root-finding algorithm such as bisection can be used to find the optimal solution.

Lemma 4.11

Even though $\lambda(\mu)$ is not unique, function h from (4.20) is well-defined in the sense that it gives the same value for every choice of $\lambda(\mu)$. Moreover, h is decreasing in μ on $(0, +\infty)$.

4.4 Summary

In this chapter, we derived dual formulation for *TopPushK* and *Pat&Mat* family of formulations. Moreover, we derived simple update rules that can be used to improve the current feasible solution. We also showed that these update rules have closed-form formulae, and therefore they are simple to compute. Finally, we showed how to find an initial feasible solution. For *TopPushK* family with hinge loss, we showed the derivation in the previous section, while the derivations for *Pat&Mat* family are in Appendix C.2.2. This section combines all these intermediate results into Algorithm 4 and discusses its computational complexity.

The left column in Algorithm 4 describe the algorithm for *TopPushK* family while the right column for *Pat&Mat* family. In step 2 we initialize α , β and δ to some feasible value using Theorem 4.10 or Theorem C.17. Then, based on (4.13) we compute scores s . Each repeat loop in step 3 updates two coordinates as shown in (4.14). In step 4 we select a random index k and in the for loop in step 5 we compute the optimal (Δ_l, δ_l) for all possible combinations (k, l) as in (4.14). In step 8 we select the best pair (Δ_l, δ_l) which maximizes the corresponding objective function. Finally, based on the selected update rule we update α , β , s and δ in steps 9 and 10.

Now we derive the computational complexity of each repeat loop from step 3. The computation of (Δ_l, δ_l) amounts to solving a quadratic optimization problem in one variable. As we showed in Sections 4.3.1 and C.2.2, there is a closed-form solution and step 6 can be performed in $O(1)$. Since this is embedded in a for loop in step 5, the whole complexity of this

Algorithm 4 Coordinate descent algorithm for *TopPushK* family of formulations (**left**) and *Pat&Mat* family of formulations (**right**).

1: Set α, β using Theorem 4.10	1: Set α, β, δ using Theorem C.17
2: Set s based on (4.13)	2: Set s based on (4.13)
3: repeat	3: repeat
4: Pick random k from $\{1, \dots, n_+ + \tilde{n}\}$	4: Pick random k from $\{1, \dots, n_+ + \tilde{n}\}$
5: for $l \in \{1, \dots, n_+ + \tilde{n}\}$ do	5: for $l \in \{1, \dots, n_+ + \tilde{n}\}$ do
6: Compute Δ_l	6: Compute Δ_l and δ_l
7: end for	7: end for
8: Select the best Δ_l	8: Select the best Δ_l and δ_l
9: Update α, β, s according to (4.14)	9: Update α, β, s according to (4.14)
10:	10: set $\delta \leftarrow \delta_l$
11: until stopping criterion is satisfied	11: until stopping criterion is satisfied

loop is $O(n_+ + \tilde{n})$. Step 9 requires $O(1)$ for the update of α and β while $O(n_+ + \tilde{n})$ for the update of s . Since the other steps are $O(1)$, the total complexity of the repeat loop is $O(n_+ + \tilde{n})$. This holds only if the kernel matrix \mathbb{K} is precomputed. In the opposite case, all complexities must be multiplied by the cost of computation of components of \mathbb{K} , which is $O(d)$. This complexity analysis is summarized in Table 4.1.

Operation	\mathbb{K} precomputed	\mathbb{K} not precomputed
Evaluation of Δ_l	$O(1)$	$O(d)$
Update of α and β	$O(1)$	$O(1)$
Update of s	$O(n_+ + \tilde{n})$	$O((n_+ + \tilde{n})d)$
Total per iteration	$O(n_+ + \tilde{n})$	$O((n_+ + \tilde{n})d)$

Table 4.1: Computational complexity of one repeat loop (which updates two coordinates of α or β) from Algorithm 4.

Primal Formulation: Non-Linear Model

In Chapter 2 we introduced a general framework for binary classification at the top samples and showed multiple formulations that fall into it. All these formulations are summarized in Table 2.1. In Chapter 3, we discussed the theoretical properties of all formulations for the special case of a linear model. Since many real-world problems are not linearly separable, in Chapter 4, we derived dual forms of all formulations and employed non-linear kernels. Moreover, we derived an efficient algorithm to solve these dual formulations. However, it is still computationally expensive. Especially the evaluation of new samples is costly since the classification score for every new sample is computed from all training samples. More precisely, the classification score is calculated only from training samples whose corresponding dual variables are non-zero. Therefore, the dual formulations are unsuitable for large data. To overcome this issue, the following chapter is dedicated to our framework (2.3) with an arbitrary model f . We can mention neural networks as a prototypical example of such a model. We will not discuss *Grill* and *Grill-NP* formulations from Table 2.1, since their authors introduced in [7] an algorithm to solve this formulation that is suitable even for non-linear models. Therefore, we focus only on the remaining formulations that use surrogate false-negative rate as an objective function, i.e., we assume the following general formulation

$$\begin{aligned} \underset{\mathbf{w}}{\text{minimize}} \quad & \frac{\lambda}{2} \|\mathbf{w}\|^2 + \frac{1}{n_+} \sum_{i \in \mathcal{I}_+} l(t(\mathbf{w}) - f(\mathbf{x}_i; \mathbf{w})) \\ \text{subject to} \quad & s_i = f(\mathbf{x}_i; \mathbf{w}), \quad i \in \mathcal{I}, \\ & t = G(\mathbf{s}, \mathbf{y}), \end{aligned} \tag{5.1}$$

where f is an arbitrary model. Our goal is to show how to solve this formulation in a suitable way for large data. The standard approach is to use stochastic gradient descent. To do so, we need to know the gradient of the objective function, and therefore, we assume that the model f is differentiable. The optimization problem (5.1) depends on two decision variables \mathbf{w} and t . However, for all formulations from Table 2.1 and each \mathbf{w} , the threshold t can be computed uniquely. We stress this dependence by writing $t(\mathbf{w})$ instead of t . By doing so, we effectively remove the threshold t from the decision variables and \mathbf{w} remains the only decision variable. Denoting the objective of (5.1) by $L(\mathbf{w})$, the chain rule implies that the gradient is equal to

$$\nabla L(\mathbf{w}) = \lambda \mathbf{w} + \frac{1}{n_+} \sum_{i \in \mathcal{I}_+} l'(t(\mathbf{w}) - f(\mathbf{x}_i; \mathbf{w})) (\nabla t(\mathbf{w}) - \nabla f(\mathbf{x}_i; \mathbf{w})). \tag{5.2}$$

The only remaining part is the computation of $\nabla t(\mathbf{w})$. It is simple for most of the formulations from Table 2.1. Moreover, Theorem 3.3 shows the computation for *Pat&Mat*.

The basic idea of the stochastic gradient descent is to split the dataset into several small minibatches $\mathcal{I}_{\text{mb}}^1, \mathcal{I}_{\text{mb}}^2, \dots, \mathcal{I}_{\text{mb}}^m$ and at each iteration perform all operations only on one of them. This approach is easily applicable when for example, cross-entropy is used as an objective function since cross-entropy is additive and easily decomposable. However, in our case, the

decision threshold t depends on all scores s , and consequently, the objective function is non-additive and non-decomposable. Therefore, we cannot compute the true threshold only from one minibatch, and we need to use some approximation \hat{t} of it. The most straightforward way to approximate the true threshold is to use the same rule as for the whole dataset and compute the sampled threshold \hat{t} only on data from one minibatch. By replacing all computations on the whole dataset \mathcal{I} with their counterparts computed only on the minibatch \mathcal{I}_{mb} , we get the sampled gradient in the following form

$$\nabla \hat{L}(w) = \lambda w + \frac{1}{n_{\text{mb},+}} \sum_{i \in \mathcal{I}_{\text{mb},+}} l'(\hat{t}(w) - f(x_i; w)) (\nabla \hat{t}(w) - \nabla f(x_i; w)). \quad (5.3)$$

where $n_{\text{mb},+}$ denotes the number of positive samples in the minibatch and \hat{t} denotes the sampled version of the true threshold t . The whole procedure of stochastic gradient descent for formulations from Table 2.1 is summarized in Algorithm 5.

Algorithm 5 Stochastic gradient descent for solving problem (5.1).

Require: Dataset \mathcal{D} , minibatches $\mathcal{I}_{\text{mb}}^1, \mathcal{I}_{\text{mb}}^2, \dots, \mathcal{I}_{\text{mb}}^m$, and stepsize α^k

- 1: Initialize weights $w^0, k \leftarrow 0$
 - 2: **repeat**
 - 3: Select a minibatch $\mathcal{I}_{\text{mb}}^k$
 - 4: Compute scores s_{mb} for all $i \in \mathcal{I}_{\text{mb}}^k$ as $s_i \leftarrow f(x_i; w)$
 - 5: Compute sampled threshold $\hat{t} \leftarrow G(s_{\text{mb}}, y_{\text{mb}})$
 - 6: Compute sampled gradient $\nabla \hat{L}$ based on $\mathcal{I}_{\text{mb}}^k$ according to (5.3)
 - 7: Set $w^{k+1} \leftarrow w^k - \alpha^k \cdot \nabla \hat{L}$
 - 8: Set $k \leftarrow k + 1$
 - 9: **until** stopping criterion is satisfied
-

5.1 Bias of Sampled Gradient

In Algorithm 5, we summarized a basic form of the stochastic gradient descent algorithm that can be used for any formulation from Table 2.1 that uses surrogate false-negative rate as an objective function. The problem with this approach is that the sampled threshold \hat{t} is computed only from data from one minibatch using the same formula as for the whole dataset. However, such a choice of sampled threshold \hat{t} underestimates the true value. This issue is especially evident for *TopPush*, where the sampled maximum is always smaller or equal to the true maximum. The chances that the actual maximum is in the current minibatch are small for large data. Therefore, the sampled threshold is a biased estimate of the true threshold. Another example can be the threshold for *Pat&Mat* formulation. Consider the minibatch of size 32, a typical size used in many applications. How can we compute, for example, (0.01)-quantile from only 32 samples? Figure 5.1 illustrates the bias of sampled threshold for *Pat&Mat* with $\tau = 0.01$ and minibatches of different sizes. The bias between the true and sampled threshold is large, even for medium-sized minibatches. When the backpropagation is used, the sampling error is propagated through the whole gradient, and consequently, the sampled gradient is a biased estimate of the true gradient. This brings numerical issues as discussed in [48].

Convergence proofs of the stochastic gradient descent require that the sampled gradient is an unbiased estimate of the true gradient [48]. In other words, the bias defined as

$$\text{bias}(w) := \nabla L(w) - \mathbb{E} \nabla \hat{L}(w) \quad (5.4)$$

must equal 0 for all w . A comparison of (5.2) and (5.3) shows that a necessary condition is that the sampled threshold \hat{t} is an unbiased estimate of the true threshold t . However, as



Figure 5.1: The bias between the sampled and true thresholds computed from scores following the standard normal distribution. The threshold separates the top 1% of samples with the highest scores.

we discussed above, it is not a case for Algorithm 5. The following proposition quantifies the difference between the sampled and true threshold for methods that use quantile as the threshold.

Proposition 5.1: [49]

Consider an absolutely continuous random variable X with distribution function F . Let X_1, X_2, \dots, X_n be i.i.d. samples from X and let $\tau \in (0, 1)$. Denote the true quantile t and its sampled version as \hat{t}

$$t = F^{-1}(1 - \tau), \quad \hat{t} = F_n^{-1}(1 - \tau),$$

where F_n is the empirical distribution function. If F is differentiable with a positive gradient at t , then

$$\sqrt{n}(t - \hat{t}) \rightarrow \mathcal{N}\left(0, \frac{\tau(1 - \tau)}{F'(t)^2}\right),$$

where the convergence is in distribution and \mathcal{N} denotes the normal distribution.

This proposition states that when the minibatch size increases to infinity, the variance of the sampled threshold is approximately

$$\frac{\tau(1 - \tau)}{nF'(t)^2}.$$

Figure 5.1 shows this empirically for the case where the scores follow the standard normal distribution and $\tau = 0.01$ is the desired top fraction of all samples. The approximation is poor with both significant bias and standard deviation. The natural choice to mitigate the bias is to work with large minibatches. Even though this is not a standard way, some works suggest this route [50]. When the minibatch is large, it contains more samples, and the sampled threshold is more precise. However, such an approach is not applicable in many cases. For example, GPUs are often used to speed up the training process. But the usage of GPUs brings memory constraints, and therefore only small minibatches can be used in such a case.

5.2 DeepTopPush

In the previous sections, we derived Algorithm 5 that can be used for any formulation from Table 2.1 that uses surrogate false-negative rate as an objective function. However, this approach provides a biased sampled gradient. One way how to reduce the bias is to use large minibatches, but in many cases, this is not possible. In this section, we derive a new method *DeepTopPush*, that mitigates this bias differently.

We start with *TopPush* formulation presented in [26]. Authors of [26] proposed the *TopPush* formulation with a linear model and solved it in its dual form. In Section 2.2 we generalized this formulation for general model f , and in Chapter 3 we solved the formulation directly in its primal form for a linear model. For general model f , we stay in the primal form to be able to employ stochastic gradient descent. It means that we have the following optimization problem

$$\begin{aligned} & \underset{\mathbf{w}}{\text{minimize}} && \frac{\lambda}{2} \|\mathbf{w}\|^2 + \frac{1}{n_+} \text{fn}(\mathbf{s}, t) \\ & \text{subject to} && s_i = f(\mathbf{x}_i; \mathbf{w}), \quad i \in \mathcal{I}, \\ & && t = \max_{j \in \mathcal{I}_-} s_j. \end{aligned} \quad (5.5)$$

Since the threshold always equals one of the scores, its computation has a simple local formula. In other words, if the highest negative score corresponds to sample \mathbf{x}_{j^*} , then the gradient of the threshold equals $\nabla t = \nabla f(\mathbf{x}_{j^*}; \mathbf{w})$. Therefore, the gradient of the objective function of (5.5) reads

$$\nabla L(\mathbf{w}) = \lambda \mathbf{w} + \frac{1}{n_+} \sum_{i \in \mathcal{I}_+} l'(f(\mathbf{x}_{j^*}; \mathbf{w}) - f(\mathbf{x}_i; \mathbf{w})) (\nabla f(\mathbf{x}_{j^*}; \mathbf{w}) - \nabla f(\mathbf{x}_i; \mathbf{w})). \quad (5.6)$$

Using the same transition to the minibatches as in previous sections, we get the following formula for sampled gradient

$$\nabla \hat{L}(\mathbf{w}) = \lambda \mathbf{w} + \frac{1}{n_{\text{mb},+}} \sum_{i \in \mathcal{I}_{\text{mb},+}} l'(f(\mathbf{x}_{j_{\text{mb}}^*}; \mathbf{w}) - f(\mathbf{x}_i; \mathbf{w})) (\nabla f(\mathbf{x}_{j_{\text{mb}}^*}; \mathbf{w}) - \nabla f(\mathbf{x}_i; \mathbf{w})), \quad (5.7)$$

where j_{mb}^* represents the index of the negative sample with the highest score from the current minibatch. As discussed in the previous section, such a choice of the decision threshold provides a lower estimate of the true threshold. To improve this approximation, we modify the idea presented in [39]. The authors of [39] suggest using delayed classification scores to compute the threshold. We used this approach in Section 3.4 to prove the convergence of stochastic gradient descent for *Pat&Mat* and *Pat&Mat-NP* formulation with a linear model. However, even in such a case, the resulting sampled gradient \hat{t} is just an approximation of the true gradient t . To improve this approach, we use the fact that the threshold for *TopPush* is always equal to the negative sample with the highest score. When the weights \mathbf{w} of model f are updated using stochastic gradient descent, the scores \mathbf{s} usually do not change much. It is true especially for small learning rates. Therefore, if some negative sample has the highest score, it will likely have the highest score even after the gradient step. Since we can easily track to which negative sample this highest score corresponds, we can enhance the next minibatch by this sample. This approach significantly increases the chance that the minibatch contains the negative sample with the highest score. In such a case, the sampled threshold \hat{t} is not just an approximation but equals the true threshold t . The whole procedure is summarized in Algorithm 6.

Algorithm 6 *DeepTopPush* as an efficient method for maximizing accuracy at the top.

Require: Dataset \mathcal{D} , minibatches $\mathcal{I}_{\text{mb}}^1, \mathcal{I}_{\text{mb}}^2, \dots, \mathcal{I}_{\text{mb}}^m$, and stepsize α^k

- 1: Initialize weights \mathbf{w}^0 , $k \leftarrow 0$, and random index j_{mb}^*
- 2: **repeat**
- 3: Select a minibatch $\mathcal{I}_{\text{mb}}^k$
- 4: Enhance minibatch $\mathcal{I}_{\text{mb}}^{\text{enh}} = \mathcal{I}_{\text{mb}}^k \cup \{j_{\text{mb}}^*\}$
- 5: Compute scores $s_i \leftarrow f(\mathbf{x}_i; \mathbf{w})$ for all $i \in \mathcal{I}_{\text{mb}}^{\text{enh}}$
- 6: Find index of sampled threshold $j_{\text{mb}}^* \leftarrow \arg \max \{s_j \mid j \in \mathcal{I}_{\text{mb}}^{\text{enh}} \cap \mathcal{I}_-\}$
- 7: Compute sampled gradient $\nabla \hat{L}$ based on $\mathcal{I}_{\text{mb}}^{\text{enh}}$ according to (5.7)
- 8: Set $\mathbf{w}^{k+1} \leftarrow \mathbf{w}^k - \alpha^k \cdot \nabla \hat{L}$
- 9: Set $k \leftarrow k + 1$
- 10: **until** stopping criterion is satisfied

Note 5.2: Other formulations

Algorithm 6 is applicable only on the *TopPush* formulation since all other formulations use more samples to compute the threshold. However, we can modify the algorithm to be usable, for example, with *TopPushK* formulation. Since *TopPushK* uses the mean of K highest negative scores as a threshold, we need to enhance the current minibatch by K indices corresponding to the K highest negative scores. However, since our goal was to use small minibatches, such an approach makes sense only for small K .

5.3 Theoretical Justification

In the previous section, we derived *DeepTopPush* method for solving the *TopPush* formulation. In Section 5.1, we discussed that the convergence proof of stochastic gradient descent requires that the sampled gradient is an unbiased estimate of the true gradient. Therefore, we are ultimately interested in the bias of the sampled gradient $\nabla \hat{L}(\mathbf{w})$ defined in (5.4). Recall that j^* is the index of true threshold on the whole dataset, while j_{mb}^* is the index of sampled threshold on the minibatch. We split the computation based on whether these two indices are identical or not.

Lemma 5.3

Let j^* be unique. Assume that the selection of positive and negative samples into the minibatch is independent and that the threshold is computed from negative samples while the objective is computed from positive samples. Then the conditional expectation of the sampled gradient satisfies

$$\mathbb{E}[\nabla \hat{L}(\mathbf{w}) | j_{\text{mb}}^* = j^*] = \nabla L(\mathbf{w}).$$

Theorem 5.4

Under the assumptions of Lemma 5.3, the bias of the sampled gradient from (5.4) satisfies

$$\text{bias}(\mathbf{w}) = \mathbb{P}[j_{\text{mb}}^* \neq j^*] \left(\nabla L(\mathbf{w}) - \mathbb{E}[\nabla \hat{L}(\mathbf{w}) | j_{\text{mb}}^* \neq j^*] \right). \quad (5.8)$$

The assumptions of Theorem 5.4 hold only for *TopPush* formulation. The bias (5.8) consists of a multiplication of two terms. As we discussed in the previous sections, there are two strategies to reduce the bias:



Figure 5.2: The **top** figure shows the comparison of the true threshold (red dashed line) and sampled threshold for *TopPush* (gray dotted line) and *DeepTopPush* (blue line). The **bottom** figure shows the angle between true and sampled gradients for *TopPush* (gray dotted line) and *DeepTopPush* (blue line). In this case, the red dashed lines represent 0 and 90 degrees angles. The experiment was performed on the CIFAR10 dataset with a minibatch of size 32 and 10 training epochs.

1. **Large minibatches:** When the minibatch is large, it contains more samples, and the chance that j_{mb}^* differs from j^* decreases. This reduces the first term in (5.8). Moreover, Proposition 5.1 ensures that the difference between the sampled threshold \hat{t} and the true threshold t is small. Then the difference between the true gradient (5.6) and the sampled gradient (5.7) decreases as well. This reduces the second term in (5.8).
2. **Enhanced minibatch:** The enhanced minibatch increases the chance that j_{mb}^* equals j^* . This reduces the first term in (5.8).

The former strategy uses Algorithm 5 while the latter is described only for formulation (5.5) in Algorithm 6. For clarity, we use the name *DeepTopPush* for Algorithm 6 that solves formulation (5.5). Similarly, we use the name *TopPush* if Algorithm 5 is used to solve formulation (5.5).

Figure 5.2 shows the effect of the enhanced minibatch on the training. The top part of the figure compares the value of the true threshold t and its sampled version \hat{t} during training. The red dashed line represents true threshold t . The full blue line shows the sampled threshold obtained by *DeepTopPush* (enhanced minibatch), while the dotted grey line the same for *TopPush*. While the sampled threshold for *TopPush* jumps wildly, for *DeepTopPush* is smooth and often equal to the true threshold. It shows the importance of the enhanced minibatch. Moreover, Theorem 5.4 implies that for *DeepTopPush* the sampled gradient is an unbiased estimate of the true gradient. It is even more pronounced in the bottom part of Figure 5.2, which shows the angle between the true gradient ∇L and the sampled gradient $\nabla \hat{L}$. This angle is essential because [51] showed that if this angle is in the interval $[0, 90)$, then gradient descent schemes converge. Which is precisely what happened for *DeepTopPush*. When the threshold is correct, the true and sampled gradients are parallel to each other, and the gradient descent moves in the correct direction.

Numerical Experiments

In previous sections, we derived a general framework for classification at the top and showed that multiple well-known formulations fall into it. The summary of all formulations presented in this work is available in Table 2.1. The goal of this chapter is to verify the properties of these formulations experimentally.

6.1 Settings

In this section, we describe in detail all settings used for the experiments. The section consists of five subsections. The first one discusses which formulations from Table 2.1 we use for the experimental evaluation. In this subsection, we also introduce baseline formulations used for the comparison. In the second one, we introduce datasets used in the experiments and describe their structure. A detailed description of the datasets is then provided in separate sections with their corresponding experiment results. The third and fourth subsections contain a detailed description of performance metrics. The last subsection contains a description of tools used for implementation. All codes used for the experiments, as well as all experiment configurations, are publicly available on GitHub:

<https://github.com/VaclavMacha/ClassificationAtTopExperiments.jl>

6.1.1 Formulations

Formulations from Table 2.1 can be divided into three categories:

- The first category contains *TopPush* and *TopPushK* formulations. These formulations minimize the surrogate approximation of the false-negative rate and use the mean of a small fraction of the negative samples with the highest scores as a threshold.
- The second category consists of *Grill*, *TopMeanK*, and *Pat&Mat* formulations. Similarly to *TopPush* and *TopPushK*, these formulations use the surrogate approximation of the false-negative rate as an objective function. The *Grill* formulation also adds the surrogate approximation of the false-positive rate into the objective function. All three formulations use some approximation of the top τ -quantile of all scores as a threshold.
- The last category consists of *Grill-NP*, τ -FPL, and *Pat&Mat-NP*. These formulations use the same objectives as their corresponding formulations from the second category. However, they differ in the definition of the decision threshold. All three formulations use some kind of approximation of the top τ -quantile of negative scores as a threshold.

To simplify the setup of all experiments, we decided to focus on formulations that only use negative samples for the threshold computation, i.e., formulations from the first and third

categories. Moreover, we decided to omit the *Grill-NP* formulation in the final experiments because of its poor results in preliminary experiments. The performance of selected formulations can be compared by basic performance metrics, as shown later in Section 6.1.4.

In total, we use four different formulations from Table 2.1, namely *TopPush*, *TopPushK*, τ -*FPL*, and *Pat&Mat-NP*. Moreover, for *TopPushK*, we use two different values of $K = \{5, 10\}$ and consider the resulting formulations as separate formulations, i.e., we have *TopPushK* (5) and *TopPushK* (10). Similarly, for τ -*FPL* and *Pat&Mat* we use two different values of $\tau = \{0.01, 0.05\}$. For all formulations, we use the hinge loss defined in Notation 2.1 as a surrogate function.

The final number of unique formulations is seven. To show that they bring advantages, we must compare them to standard methods. In previous chapters, we showed how to solve presented formulations in their primal (Chapters 3 and 5) and dual form (Chapter 4). Whenever we use the primal form in the experiments, we use binary cross-entropy defined in the following way as a baseline formulation

$$\begin{aligned} & \underset{\mathbf{w}}{\text{minimize}} && \frac{1}{n} \sum_{i \in \mathcal{I}} (-y_i \log(s_i) - (1 - y_i) \log(1 - s_i)) \\ & \text{subject to} && s_i = f(\mathbf{x}_i; \mathbf{w}), \quad i \in \mathcal{I}. \end{aligned} \tag{6.1}$$

We decided to use binary cross-entropy since it is one of the most used objective functions for binary classification in machine learning applications. We will denote binary cross-entropy in the following text as *BinCross*. In experiments with dual forms of our formulations, we use C-SVC variant of SVM [52, 25, 53] defined by

$$\begin{aligned} & \underset{\mathbf{w}, b, \xi}{\text{minimize}} && \frac{1}{2} \|\mathbf{w}\|^2 + C \sum_{i \in \mathcal{I}} \xi_i \\ & \text{subject to} && y_i (\mathbf{w}^\top \phi(\mathbf{x}_i) + b) \geq 1 - \xi_i, \quad i \in \mathcal{I}, \\ & && \xi_i \geq 0, \quad i \in \mathcal{I}, \end{aligned} \tag{6.2}$$

where $y_i \in \{-1, 1\}$ for all $i \in \mathcal{I}$ and $\phi(\mathbf{x}_i)$ maps \mathbf{x}_i into a higher-dimensional space (see Section 4.2). The corresponding dual form is as follows

$$\begin{aligned} & \underset{\boldsymbol{\alpha}}{\text{maximize}} && -\frac{1}{2} \boldsymbol{\alpha}^\top \mathbb{K} \boldsymbol{\alpha} - \sum_{i=1}^n \alpha_i \\ & \text{subject to} && \sum_{i=1}^n y_i \alpha_i = 0, \\ & && 0 \leq \alpha_i \leq C, \quad i = 1, 2, \dots, n, \end{aligned} \tag{6.3}$$

where the kernel matrix \mathbb{K} is defined for all $i, j = 1, 2, \dots, n$ as

$$\mathbb{K}_{i,j} = y_i y_j k(\mathbf{x}_i, \mathbf{x}_j) = \phi(\mathbf{x}_i)^\top \phi(\mathbf{x}_j).$$

Note that the dual form of C-SVC is very similar to the dual forms of our formulations derived in Chapter 4. We will denote C-SVC as SVM.

In total, we have nine different formulations for experiments, as seen in Table 6.1. *BinCross* formulation is used only for experiments with primal forms of our formulations, while *SVM* is used only when dual forms are used. The following section discusses which hyper-parameters are used for each formulation. Since we used a slightly different primal form (standard formulation for SVM) for the derivation of dual forms, we also show how to convert used parameters to the resulting dual forms and get identical experiment settings.

6.1.2 Hyper-parameters

The selected formulations differ in the number of available hyper-parameters. Therefore, we decided to use a fixed value for all but one of the hyper-parameters for each formulation. For most of the considered formulations, the only hyper-parameter is the regularization constant λ . In our experiments, we used the following six values of this hyper-parameter

$$\lambda \in \{0, 10^{-5}, 10^{-4}, 10^{-3}, 10^{-2}, 10^{-1}\}.$$

The only exceptions are the formulations derived from *Pat&Mat-NP* since they also have the scaling parameter ϑ . Since the parameter is essential for the approximation quality of the threshold, we decided to fine-tune this hyper-parameter instead of the regularization constant λ . Therefore, we fixed λ to 10^{-3} for *Pat&Mat-NP* formulations and used the following six different values of the scaling parameter

$$\vartheta \in \{10^{-5}, 10^{-4}, 10^{-3}, 10^{-2}, 10^{-1}, 1\}.$$

Since we used a slightly different (but equivalent) primal formulation for the derivation of the dual forms, we use λ to compute the hyper-parameter C used in these dual forms

$$C = \frac{1}{\lambda \tilde{n}},$$

where $\tilde{n} = n$ for *SVM* and $\tilde{n} = n_+$ otherwise. In all experiments, the best hyperparameter is selected based on the validation data and the appropriate performance metric. A summary of all used formulations and their hyper-parameters is in Table 6.1.

Formulation	Fixed parameters	Hyper-parameter	Primal Form	Dual Form
<i>BinCross</i>	—	λ	✓	✗
<i>SVM</i>	—	λ	✗	✓
<i>TopPush</i>	—	λ	✓	✓
<i>TopPushK</i> (5)	$K = 5$	λ	✓	✓
<i>TopPushK</i> (10)	$K = 10$	λ	✓	✓
τ -FPL (0.01)	$\tau = 0.01$	λ	✓	✓
τ -FPL (0.05)	$\tau = 0.05$	λ	✓	✓
<i>Pat&Mat-NP</i> (0.01)	$\tau = 0.01$	ϑ	✓	✓
<i>Pat&Mat-NP</i> (0.05)	$\tau = 0.05$	ϑ	✓	✓

Table 6.1: Summary of all formulations used for experiments. The first column shows the aliases used for the formulations when describing the experiment results. The second column shows fixed parameters used for each formulation, while the third column shows which hyper-parameters are tuned using the validation set. The last two columns indicate whether the formulation is used in the experiments with primal forms, dual forms, or both.

6.1.3 Datasets

We consider various datasets summarized in Table 6.2 for the numerical experiments. All these datasets can be divided into three categories:

1. **Image Recognition:** In this category, we test formulations from Table 6.1 on datasets from the domain of image recognition. We use this domain since it is one of the most popular with plenty of publicly available datasets.
2. **Steganalysis:** In this category, we use selected formulations in the domain of steganalysis. In this domain, the problem of maximizing the true-positive rate at the specific level of the false-positive rate is well-known and essential, as we show at the beginning of Section 6.3.
3. **Malware Detection:** In this category, we use selected formulations for malware detection. Like in steganalysis, maximizing the true-positive rate at the specific level of the false-positive rate is crucial for malware detection, as discussed at the beginning of Section 6.4.

Each category has a separate section later in the text. It is worth mentioning that not all datasets used in the experiments are primarily designed for the classification at the top. For example, all datasets from the first category are general-purpose image classification datasets. We use these datasets since they are publicly available and well-known. Since all these datasets are multiclass, we need to adjust the labels to get a binary classification problem. Therefore, for each data set, we select one class as the positive class and consider the rest as the negative class. It is also worth noting that the Malware Detection dataset does not include a validation set. The computational demands of training on this dataset were so large that we were only able to train four formulations without any hyperparameter tuning. Therefore, there was no need for a validation set.

Dataset	y^+	d	Train		Validation		Test	
			n	$\frac{n_+}{n}$	n	$\frac{n_+}{n}$	n	$\frac{n_+}{n}$
MNIST	1	$28 \times 28 \times 1$	45 000	11.3%	15 000	11.2%	10 000	11.4%
FashionMNIST	1	$28 \times 28 \times 1$	45 000	10.0%	15 000	9.9%	10 000	10.0%
CIFAR10	1	$32 \times 32 \times 3$	37 500	10.0%	12 500	9.9%	10 000	10.0%
CIFAR20	1	$32 \times 32 \times 3$	37 500	5.0%	12 500	5.1%	10 000	5.0%
CIFAR100	1	$32 \times 32 \times 3$	37 500	1.0%	12 500	1.0%	10 000	1.0%
SVHN2	1	$32 \times 32 \times 3$	54 944	18.9%	18 313	18.9%	26 032	19.6%
SVHN2-Extra	1	$32 \times 32 \times 3$	453 291	17.3%	151 097	17.1%	26 032	19.6%
Nsf5	—	22510×1	186 583	9.1%	62 194	9.1%	248 776	9.1%
JMiPOD	—	$256 \times 256 \times 3$	186 515	9.1%	62 172	9.1%	248 686	9.1%
Malware	—	variable	6 580 166	87.22%	—	—	800 346	91.8%

Table 6.2: Structure of datasets: The training, validation and testing sets show the positive label y^+ , the number of features d , samples n and the fraction of positive samples $\frac{n_+}{n}$. Datasets depicted in red are not publicly available.

6.1.4 Performance Criteria

In this section, we describe which performance criteria are used for evaluation and how these criteria are related to the tested formulations.

As we discussed at the beginning of Section 6.1, we decided to only test formulations that minimize the false-negative rate (or a combination of false-negative and false-positive rate) and use only negative samples for the threshold computation. This choice allows us to use simple metrics to compare the formulations. The first metric that we use in the experiments is $\text{TPR@}K$ defined as follows

$$\text{TPR@}K = \frac{1}{n_+} \sum_{i \in \mathcal{I}_+} \mathbb{1}_{[s_i \geq t]} \quad \text{where} \quad t = \frac{1}{K} \sum_{j=1}^K s_{[j]}^-.$$

This metric computes the true-positive rate at a threshold t defined as the mean of K -largest negative scores. For $K = 1$, the threshold corresponds to the threshold used by *TopPush* formulation. Otherwise, threshold t corresponds to the threshold used by *TopPushK*. Moreover, since minimizing the false-negative rate is equivalent to maximizing the true-positive rate, both *TopPush* and *TopPushK* should optimize the $\text{TPR@}K$ metric. In the upcoming experiments, we use this metric with three different values of $K \in \{1, 5, 10\}$.

The second metric is defined in a similar way

$$\text{TPR@}\tau = \frac{1}{n_+} \sum_{i \in \mathcal{I}_+} \mathbb{1}_{[s_i \geq t]} \quad \text{where} \quad t = \max \left\{ t \left| \frac{1}{n_-} \sum_{i \in \mathcal{I}_-} \mathbb{1}_{[s_i \geq t]} \geq \tau \right. \right\}.$$

This metric computes the true-positive rate at a specific top τ -quantile of negative scores. This metric is ideal for testing the performance of τ -FPL and *Pat&Mat-NP* formulations since both maximize the true-positive rate and use some approximation of the true top τ -quantile of negative scores as a threshold. In our experiments, we use this metric with two different values of $\tau \in \{0.01, 0.05\}$.

The two previous metrics are specific to the formulations from our framework. However, we should also test if the baseline formulations work correctly. Since the baseline methods are designed to optimize overall performance, we use the area under the ROC curve to measure the overall performance. The summary of all used metrics is in Table 6.3.

Formulation	AUC	TPR@K			TPR@ τ	
		1	5	10	0.01	0.05
<i>BinCross</i>	✓	—	—	—	—	—
<i>SVM</i>	✓	—	—	—	—	—
<i>TopPush</i>	—	✓	—	—	—	—
<i>TopPushK</i> (5)	—	—	✓	—	—	—
<i>TopPushK</i> (10)	—	—	—	✓	—	—
τ -FPL (0.01) and <i>Pat&Mat-NP</i> (0.01)	—	—	—	—	✓	—
τ -FPL (0.05) and <i>Pat&Mat-NP</i> (0.05)	—	—	—	—	—	✓

Table 6.3: The summary of all used performance metrics used for evaluation. In total, we use six different metrics and nine different formulations. For each formulation ✓ denotes the metric in which the formulation should be the best.

6.1.5 Critical Difference Diagrams

All metrics from Section 6.1.4 can be used to compare different formulations on a single dataset. However, these metrics are unsuitable for comparing multiple formulations on multiple datasets. To address this issue, we use the Friedman test [54] as suggested in [55].

Consider that we have m datasets, and k formulations. Then for each dataset i , each formulation j is ranked by rank r_j^i according to some performance criterium. Any performance metric from the previous section can be used. The formulation that provides the best result gets ranked 1; the second best gets ranked 2, and so on. If two formulations provide the same results, the average ranks are assigned. The average rank overall dataset for formulation j is computed as

$$R_j = \frac{1}{m} \sum_{i=1}^m r_j^i.$$

The Friedman test compares the average ranks of formulations under the null hypothesis, which states that all formulations are equivalent. Therefore, their average ranks should be equal. If the null hypothesis is rejected, we proceed with the post hoc Nemenyi test [56] that compares all formulations to each other. The performance of the two formulations is significantly different if the corresponding average ranks differ by at least the critical difference

$$CD = q_\alpha \sqrt{\frac{k(k+1)}{6m}},$$

where critical values q_α are based on the Studentized range statistic divided by $\sqrt{2}$, see Table 5(a) in [55]. The results of this post hoc test can be easily visualized using critical difference diagrams proposed in [55]. The x -axis of such a diagram shows the average rank over all datasets for each formulation. Formulations that are not significantly different according to the Nemenyi test are connected using a green horizontal line. As an example, see Figure 6.1.

6.1.6 Implementation

For the implementation of all experiments, we use the Julia programming language [57]. The dual formulations are implemented from scratch, while the primal formulations are implemented using Flux.jl [58, 59] library. This library provides all the necessary tools for building neural networks. Moreover, the library allows the implementation of a custom gradient for any function, which allows us to implement all formulations from Table 2.1. For experiments with SVM, we use the Julia wrapper for the LIBSVM library [53].

6.2 Image Recognition

In this section, we present experiments with six well-known image recognition datasets. All these datasets are publicly available. MNIST [60] and FashionMNIST [61] are grayscale datasets of digits and fashion items, respectively. CIFAR100 [62] is a dataset of colored images of different items grouped into 100 classes. CIFAR10 and CIFAR20 merge these classes into 10 and 20 superclasses, respectively. Finally, SVHN2 [63] contains colored images of house numbers. All these datasets are originally divided only into training and test sets. We select 25% samples from the training set to obtain the validation set. For a more detailed description of the structure of datasets, see Table 6.2.

None of these datasets are primarily designed for the problem of classification at the top. We presented these datasets to show that introduced formulations can be helpful even for general-purpose datasets and may improve performance on specific metrics. However, there are some drawbacks to using these datasets. For example, many state-of-the-art neural network

architectures achieve almost the perfect classification on some of these datasets. Therefore, there is no room for improvement, and we have to use much simpler architectures to show the behavior of formulations presented in this work (Section 6.2.3).

For comparison we use critical difference diagrams introduced in Section 6.1.5. One of the basic assumptions of the critical difference diagrams to work appropriately is a large number of used datasets. Since we performed all experiments for each formulation and each dataset ten times with different random seeds for train/valid/test split, we decided to consider each of these runs as a separate dataset. It is important to say that we use this setting only for the critical difference diagrams. Since the critical diagrams show the relative performance of the formulations against each other, we can easily see if any formulation is significantly worse or better. However, the critical diagrams do not provide any information on the actual performance of the formulations. Therefore, even if one formulation outperforms other tested formulations, it does not mean that its performance is good.

To address the issue above, we also compare concrete performance metrics on each dataset separately. Since we have six hyper-parameters for each formulation, we always select the best result for each formulation on the validation set based on the criterion for which the specific formulation is optimized. Then for each formulation, we select the median of the best results from ten independent runs. Moreover, the best result for each dataset is highlighted in green, while the worst result is highlighted in red.

6.2.1 Primal Formulation: Linear Model

In this section, we present results for a primal form of formulations from Table 6.1 with a linear model. For training, we use stochastic gradient descent with balanced mini-batches of size 512. As an optimizer, we use the ADAM [64] with default settings and initial step length $\alpha = 0.01$, which we discount every five epochs by the factor of 0.8 using an exponential decay scheme. We also fix the number of epochs to 100, and repeat each experiment ten times with different random seeds.

As mentioned earlier, we use critical difference diagrams (Figure 6.1) and medians of ten independent runs (Table 6.4) for comparison. We make several observations:

- *TopPushK* formulations provide a slight (not statistically significant) improvement over *TopPush* in most of the experiments, as shown in Figure 6.1, where a green line connects all three formulations for almost all metrics. The only exception is the $\text{TPR@}\tau = 0.01$ metric, for which *TopPush* is significantly worse than other formulations.
- *BinCross* formulation works best for AUC metric and is not suitable for any other metric; see Figure 6.1 or Table 6.4. *BinCross* consistently provides the best results for AUC for all datasets. On the other hand, *BinCross* works poorly for metrics that operate at the absolute top, such as $\text{TPR@}K = 1$, $\text{TPR@}K = 5$, or $\text{TPR@}K = 10$.
- *Pat&Mat-NP* formulations provide very good results for all metrics. Moreover, *Pat&Mat-NP* (0.01) is the best formulation for $\text{TPR@}\tau = 0.01$, and *Pat&Mat-NP* (0.05) for $\text{TPR@}\tau = 0.05$. It means that both methods are the best for the criterion for which they are optimized. The same behavior can also be seen in Table 6.4, where *Pat&Mat-NP* (0.05) is the best formulation for $\text{TPR@}\tau = 0.01$ almost for all datasets.
- τ -FPL (0.05) works very well for both $\text{TPR@}\tau = 0.01$ and $\text{TPR@}\tau = 0.05$. The formulation achieves almost as good results for both metrics as *Pat&Mat-NP* formulations.
- All formulations provide very poor results for CIFAR and SVHN2 datasets, as shown in Table 6.4. The use of a simple linear model causes this. However, the obtained results are still relevant since we compare the relative performance of the formulations to each other and not the absolute performance.



Figure 6.1: **Primal formulation with a linear model:** Critical difference diagrams (level of importance 0.05) of the Nemenyi post hoc test for the Friedman test. Each diagram shows the mean rank of each method, with rank one being the best. The green horizontal lines group methods with mean ranks that are not significantly different. The critical difference diagrams were computed for mean rank averages over all datasets.

TPR@K = 10

Formulation	MNIST	FashionMNIST	CIFAR10	CIFAR20	CIFAR100	SVHN2	SVHN2Extra
<i>BinCross</i>	68.54	85.65	1.25	1.40	2.00	0.04	0.02
<i>TopPush</i>	89.38	93.70	2.25	0.40	4.00	0.02	0.02
<i>TopPushK</i> (5)	89.60	93.30	3.30	1.10	3.00	0.04	0.06
<i>TopPushK</i> (10)	89.64	92.75	3.90	0.70	4.50	0.04	0.09
τ -FPL (0.01)	83.35	92.40	2.90	0.80	2.50	0.03	0.02
τ -FPL (0.05)	40.26	79.65	3.60	1.00	5.50	0.04	0.09
<i>Pat&Mat-NP</i> (0.01)	87.88	92.75	5.00	1.10	4.00	0.12	0.09
<i>Pat&Mat-NP</i> (0.05)	51.72	81.60	3.80	1.20	3.00	0.14	0.06

TPR@ τ = 0.05

Formulation	MNIST	FashionMNIST	CIFAR10	CIFAR20	CIFAR100	SVHN2	SVHN2Extra
<i>BinCross</i>	99.65	99.30	43.40	32.90	54.50	5.53	5.91
<i>TopPush</i>	99.12	98.30	31.10	16.30	43.50	5.22	6.40
<i>TopPushK</i> (5)	99.21	98.30	35.50	20.20	42.50	6.78	7.42
<i>TopPushK</i> (10)	99.30	98.30	37.90	20.80	46.50	6.15	8.07
τ -FPL (0.01)	99.47	98.75	35.85	24.00	44.00	6.90	7.76
τ -FPL (0.05)	99.56	99.20	39.50	25.70	50.50	8.16	9.69
<i>Pat&Mat-NP</i> (0.01)	99.52	98.85	45.35	33.70	56.00	9.28	12.47
<i>Pat&Mat-NP</i> (0.05)	99.65	99.40	46.80	34.80	58.50	9.34	12.25

AUC

Formulation	MNIST	FashionMNIST	CIFAR10	CIFAR20	CIFAR100	SVHN2	SVHN2Extra
<i>BinCross</i>	99.86	99.83	84.00	76.26	88.48	57.82	56.10
<i>TopPush</i>	99.78	99.42	73.84	65.76	82.10	51.08	51.30
<i>TopPushK</i> (5)	99.80	99.42	76.67	65.70	81.52	50.98	50.69
<i>TopPushK</i> (10)	99.82	99.48	77.74	66.87	81.91	51.90	50.58
τ -FPL (0.01)	99.84	99.72	77.34	69.24	82.96	51.04	50.62
τ -FPL (0.05)	99.81	99.80	79.41	70.86	84.56	51.78	50.76
<i>Pat&Mat-NP</i> (0.01)	99.85	99.68	82.34	74.56	86.13	56.38	51.93
<i>Pat&Mat-NP</i> (0.05)	99.84	99.81	83.35	75.44	87.22	56.40	52.50

Table 6.4: **Primal formulation with a linear model:** Each table corresponds to one performance metric, and all presented results are medians of ten independent runs for each dataset and formulation pair. The best result for each dataset is highlighted in green, while the worst result is highlighted in red. For better readability, we have reduced the number of discussed metrics compared to Figure 6.1.

6.2.2 Dual Formulation: Linear Model

In this section, we present results for a dual form of formulations from Table 6.1 with a Gaussian kernel model. For training, we use the coordinate descent algorithm introduced in Section 4.3. We set a number of steps to 20 epochs. For all experiments, we use precomputed kernel matrix with a Gaussian kernel function defined as

$$k(\mathbf{x}_i, \mathbf{x}_j) = \exp\left\{-\frac{\|\mathbf{x}_i - \mathbf{x}_j\|^2}{d}\right\},$$

where d is the dimension of the primal problem. We used this value of d since it is the default setting for the Gaussian kernel function in LIBSVM [53]. We only use one kernel function for computational reasons. In addition, we are more interested in the comparison of methods between each other than in obtaining the best results possible.

In Figure 6.2, we investigate the convergence of the coordinate descent algorithm introduced in Section 4.3 for three formulations, namely *TopPush*, *TopPushK*, and *Pat&Mat-NP*. In each column, we show the primal and dual objective function convergence for one formulation. To solve the primal problem, we used full gradient descent. Computation of the full gradient is computationally intensive, even for relatively small datasets such as MNIST. Therefore, for this experiment (and only for this experiment) we use the Ionosphere dataset [65], which is small. We can see that *TopPush* and *TopPushK* converge to the same objective for primal and dual problems. It means that both problems were solved to optimality. However, there is a little gap between the optimal primal and dual form solution for *Pat&Mat-NP*. In other words, *Pat&Mat-NP* may suffer from convergence issues when solving the proposed coordinate descent algorithm.

For comparison of all formulations, we use the same two approaches as in Section 6.2.1. From Figure 6.3 and Table 6.5, we make several observations:

- We observe that some formulations have problems with convergence and, in some cases, even diverge for some datasets. The improper choice of the kernel function parameters can be the cause. As a result, CD diagrams may provide unreliable results. If the formulation diverges in some experiments, it immediately obtains very high ranks for these experiments that skew the final diagram. It is especially evident for *Pat&Mat-NP* and SVM formulations.
- Figure 6.3 shows that *Pat&Mat-NP* formulations provide the worst results for all metrics. It can be caused by the bad convergence of the coordinate descent algorithm, as shown in Figure 6.2. However, it is important to say that Figure 6.3 shows only relative results. From Table 6.5 is clear that even though *Pat&Mat-NP* usually provides worse results than other formulations, the results are, in many cases, only slightly worse.
- Similarly to *Pat&Mat-NP*, the SVM formulation does not perform well for most metrics. However, as shown in Table 6.5, the results are usually only slightly worse than those of other formulations.
- Most formulations perform well on the criteria for which they are optimized. The only exceptions are SVM and *Pat&Mat* formulations.
- Most formulations provide an AUC greater than 99% on the MNIST and FashionMNIST datasets. These two datasets are very easy when a non-linear model is used.
- τ -FPL formulations work very well for $\text{TPR}@ \tau = 0.01$, $\text{TPR}@ \tau = 0.05$ and AUC metric.
- *TopPush*, *TopPushK* (5) and *TopPushK* (10) provides very good results for $\text{TPR}@K = 1$, $\text{TPR}@K = 5$ and $\text{TPR}@K = 10$.



Figure 6.2: Convergence of the objectives for the primal (red line) and dual (blue dashed line) forms with linear kernel.

6.2.3 Primal Formulation: Non-Linear Model

In this section, we present results for a primal form of formulations from Table 6.1 with a non-linear model. For training, we use the same setting as in Section 6.2.1. For MNIST and FashionMNIST datasets, we use a neural network consisting of two convolution layers, followed by a max pooling layer and one fully connected layer of the proper size for binary classification. The rest of the datasets use a similar architecture but with three convolutional layers instead of two. We purposely do not use state-of-the-art architectures since they often lead to a perfect separation of used datasets. Our goal is to show that formulations from Table 6.1 can improve specific metrics such as $\text{TPR@}\tau = 0.05$ (when compared to *BinCross*) even with these subpar architectures.

For comparison of all formulations, we use the same two approaches as in Section 6.2.1. From Figure 6.4 and Table 6.6, we make several observations:

- Most formulations perform well on the criteria for which they are optimized and provide almost perfect separation on MNIST dataset and FashionMNIST dataset.
- *DeepTopPush* does not provide good results. In fact, the formulation is the worst in five out of six metrics in Figure 6.4. However, it can be caused by using relatively large mini-batches concerning the size of the datasets. The true power of the *DeepTopPush* is shown in Section 6.3 and 6.4.
- *BinCross* formulation performs consistently very well for all metrics. Nevertheless, *BinCross* is the best for neither of the metrics.
- *TopPushK* (10) fails many times. It is especially evident from Table 6.6. *TopPushK* (10) achieves 100% for $\text{TPR@}K = 10$ metric for most datasets, which seems as a very good result. However, if we take a look at the AUC, we can see that the formulation achieves 0% for the same datasets. The reason for that is simple, *TopPushK* (10) assigns the same score to all samples and therefore achieves 100% true-positive rate but also 100% false-positive rate.
- *Pat&Mat-NP* formulations provide very good results for all metrics. Moreover, *Pat&Mat-NP* (0.01) is the best formulation for $\text{TPR@}\tau = 0.01$, and *Pat&Mat-NP* (0.05) for $\text{TPR@}\tau = 0.05$. It means that both methods are the best for the criterion for which they are optimized. This behavior can also be seen in Table 6.4, where *Pat&Mat-NP* (0.05) is the best formulation for $\text{TPR@}\tau = 0.01$ for all datasets.
- τ -FPL formulations work well on MNIST and FashionMNIST datasets, but are subpar on the rest.

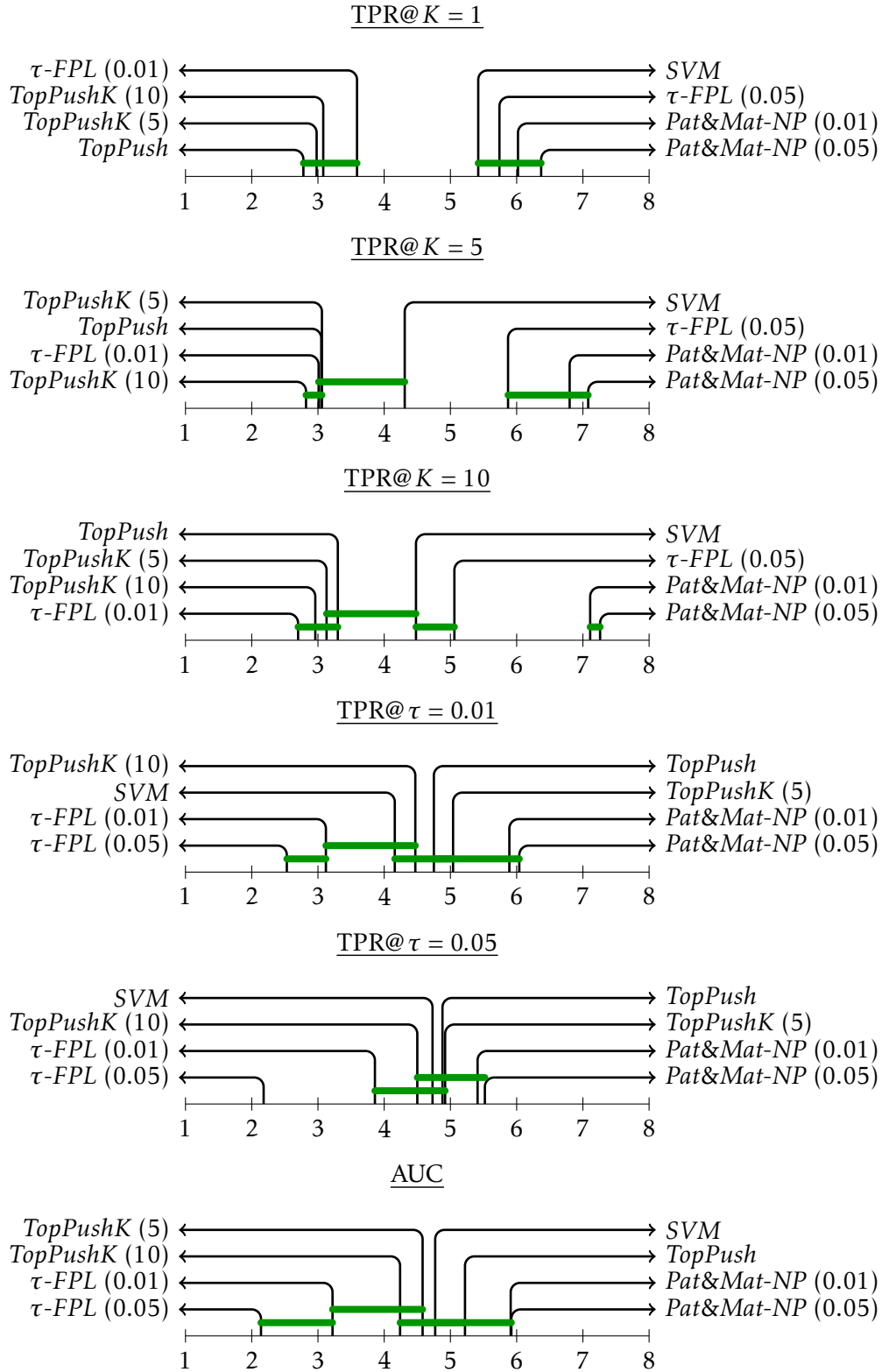


Figure 6.3: **Dual formulations with a gaussian kernel:** Critical difference diagrams (level of importance 0.05) of the Nemenyi post hoc test for the Friedman test. Each diagram shows the mean rank of each method, with rank one being the best. The green horizontal lines group methods with mean ranks that are not significantly different. The critical difference diagrams were computed for mean rank averages over all datasets.

TPR@K = 10

Formulation	MNIST	FashionMNIST	CIFAR10	CIFAR20	CIFAR100	SVHN2
SVM	97.89	95.40	9.10	4.90	11.50	4.52
<i>TopPush</i>	97.62	94.80	10.45	6.10	11.00	5.23
<i>TopPushK</i> (5)	97.97	94.90	10.05	6.00	11.0	5.07
<i>TopPushK</i> (10)	97.97	94.90	9.85	6.10	11.00	5.18
τ -FPL (0.01)	98.02	95.05	10.70	5.90	10.5	5.25
τ -FPL (0.05)	92.56	92.20	10.15	5.10	10.0	5.24
<i>Pat&Mat-NP</i> (0.01)	88.37	92.50	7.45	1.40	5.00	4.02
<i>Pat&Mat-NP</i> (0.05)	52.60	92.50	7.45	1.30	5.00	4.05

TPR@ τ = 0.05

Formulation	MNIST	FashionMNIST	CIFAR10	CIFAR20	CIFAR100	SVHN2
SVM	99.74	98.90	60.00	44.80	59.00	59.72
<i>TopPush</i>	99.74	98.80	57.10	37.70	59.50	72.54
<i>TopPushK</i> (5)	99.82	98.90	56.25	38.80	57.50	71.40
<i>TopPushK</i> (10)	99.82	98.90	56.90	38.70	58.00	71.61
τ -FPL (0.01)	99.82	98.90	58.10	39.10	59.00	73.52
τ -FPL (0.05)	99.74	99.10	60.80	44.40	61.00	74.26
<i>Pat&Mat-NP</i> (0.01)	99.30	98.10	54.70	44.60	62.50	63.47
<i>Pat&Mat-NP</i> (0.05)	99.38	98.10	54.70	44.50	63.50	63.48

AUC

Formulation	MNIST	FashionMNIST	CIFAR10	CIFAR20	CIFAR100	SVHN2
SVM	99.94	99.66	90.02	79.75	87.80	90.14
<i>TopPush</i>	99.94	99.56	89.35	79.06	87.03	92.77
<i>TopPushK</i> (5)	99.95	99.64	89.05	79.13	87.21	92.60
<i>TopPushK</i> (10)	99.95	99.67	89.16	79.27	87.78	92.67
τ -FPL (0.01)	99.97	99.68	89.83	79.07	87.64	92.98
τ -FPL (0.05)	99.93	99.80	90.34	80.17	88.56	93.16
<i>Pat&Mat-NP</i> (0.01)	99.78	99.40	87.62	78.82	89.78	90.80
<i>Pat&Mat-NP</i> (0.05)	99.78	99.40	87.61	78.76	89.52	90.82

Table 6.5: **Dual formulations with a gaussian kernel:** Each table corresponds to one performance metric, and all presented results are medians of ten independent runs for each dataset and formulation pair. The best result for each dataset is highlighted in green, while the worst result is highlighted in red. For better readability, we have reduced the number of discussed metrics compared to Figure 6.3.



Figure 6.4: **Primal formulations with a non-linear model:** Critical difference diagrams (level of importance 0.05) of the Nemenyi post hoc test for the Friedman test. Each diagram shows the mean rank of each method, with rank one being the best. The green horizontal lines group methods with mean ranks that are not significantly different. The critical difference diagrams were computed for mean rank averages over all datasets.

TPR@K = 10

Formulation	MNIST	FashionMNIST	CIFAR10	CIFAR20	CIFAR100	SVHN2	SVHN2Extra
<i>BinCross</i>	99.26	98.10	11.40	3.50	5.00	11.34	15.95
<i>DeepTopPush</i>	98.42	97.60	0.20	0.20	0.00	0.17	0.00
<i>TopPushK</i> (5)	98.54	97.50	2.00	0.00	8.50	10.58	16.12
<i>TopPushK</i> (10)	98.24	96.90	12.55	100.00	100.00	100.00	100.00
τ -FPL (0.01)	98.72	97.50	1.00	0.20	9.00	9.52	0.00
τ -FPL (0.05)	96.78	96.50	14.80	0.30	8.50	13.05	12.48
<i>Pat&Mat-NP</i> (0.01)	98.54	97.45	32.45	4.80	20.00	13.92	19.33
<i>Pat&Mat-NP</i> (0.05)	82.86	94.30	26.55	5.90	11.50	11.36	15.98

TPR@ τ = 0.05

Formulation	MNIST	FashionMNIST	CIFAR10	CIFAR20	CIFAR100	SVHN2	SVHN2Extra
<i>BinCross</i>	100.00	99.90	83.35	48.00	82.00	94.66	97.71
<i>DeepTopPush</i>	99.82	99.70	5.85	8.90	9.00	40.14	0.00
<i>TopPushK</i> (5)	100.00	99.85	34.30	7.70	53.50	86.54	93.96
<i>TopPushK</i> (10)	100.00	99.90	27.95	0.00	0.00	0.00	0.00
τ -FPL (0.01)	100.00	99.90	24.40	11.50	65.50	87.60	0.00
τ -FPL (0.05)	100.00	99.90	82.75	18.00	66.50	94.51	97.52
<i>Pat&Mat-NP</i> (0.01)	100.00	99.90	91.55	52.20	79.00	95.49	98.43
<i>Pat&Mat-NP</i> (0.05)	100.00	99.90	91.75	57.70	85.00	95.53	98.50

AUC

Formulation	MNIST	FashionMNIST	CIFAR10	CIFAR20	CIFAR100	SVHN2	SVHN2Extra
<i>BinCross</i>	100.00	99.98	96.85	84.67	95.94	98.54	99.20
<i>DeepTopPush</i>	99.98	99.95	49.51	59.40	56.68	83.12	1.61
<i>TopPushK</i> (5)	100.0	99.97	77.10	55.50	84.24	96.57	98.32
<i>TopPushK</i> (10)	100.00	99.98	74.26	0.00	0.00	0.00	0.00
τ -FPL (0.01)	100.0	99.98	70.96	60.03	90.16	96.68	25.84
τ -FPL (0.05)	99.99	99.97	95.86	68.18	90.76	98.50	99.12
<i>Pat&Mat-NP</i> (0.01)	99.99	99.98	97.90	84.38	93.84	98.74	99.38
<i>Pat&Mat-NP</i> (0.05)	99.96	99.96	98.24	88.39	96.56	98.76	99.32

Table 6.6: **Primal formulations with a non-linear model:** Each table corresponds to one performance metric, and all presented results are medians of ten independent runs for each dataset and formulation pair. The best result for each dataset is highlighted in green, while the worst result is highlighted in red. For better readability, we have reduced the number of discussed metrics compared to Figure 6.4.

6.3 Steganalysis

In the previous section, we presented results on standard image recognition datasets. Even though the results are quite good, they did not fully show the importance of the problem of classification at the top. To show the importance of this problem properly, we need to find the field where the maximizing true-positive rate at the low false-positive rate is an important task. Such a field can be, for example, steganalysis.

The standard way to share secret information these days is through encryption. However, in such a case, the presence of a secret message (even though encrypted) is obvious. Steganography aims to hide the fact that communication is taking place by hiding the secret message within an ordinary file (usually called a cover file) to avoid detection. The secret message is then extracted at its destination. The secret data can be hidden in almost any type of digital content. However, the most popular are images. There are two reasons for this. The first of them is the ubiquity of images on the Internet and, therefore, the ease of using them as cover files for secret messages. The second reason is their large potential payload, i.e., it is possible to hide a lot of information in high-resolution images. With an appropriate cover image and steganography tools, it is possible to create a stego-image (image with a hidden message) that can not be recognized from the cover image by human perception. However, each tool leaves a fingerprint or signature in the image that can be used to detect stego images. The field that tries to detect stego images and possibly decrypt messages from them is called steganalysis. In steganalysis, the goal is to achieve the best true-positive rate with the lowest possible false-positive rate. Therefore steganalysis is the domain suitable for the problem of classification at the top. [66, 67]

For the experiments, we use two private steganography datasets. Both these datasets are created from the same database of cover images comprising approximately 450 000 images from Flickr. All these images are in JPEG format with a quality factor of 80. The datasets used for the experiments differ in the algorithm that was used to generate the stego images. The stego images for the first dataset were generated using the **Nsf5** algorithm [68], while the stego images for the second dataset were generated using the **JMiPOD** algorithm [69]. For simplicity, we have named the datasets according to the stego algorithms used.

6.3.1 Nsf5

As we mentioned before, the stego images in the first dataset were generated using the **Nsf5** algorithm [68] using the payload 0.2. Since generating stego images is expensive, only 10% of all cover images are used to generate their stego counterparts. Moreover, the dataset does not contain images but 22 500 features extracted using the CC-JRM algorithm [70]. Finally, the whole dataset is divided into train/validation/test sets in the 0.45/0.05/0.5 ratio. The resulting sizes of the splits, as well as the number of stego samples in them, are summarized in Table 6.2.

Since the resulting classification task is relatively easy to solve, we decided to use a simple linear model. The number of training samples and their size is not too large. Therefore we can load the whole dataset into memory. It allows us to use full gradient descent instead of its stochastic version. As an optimizer, we use the ADAM [64] with default settings and fixed step length $\alpha = 0.01$. We also fix the number of epochs to 1000 for all formulations. Finally, we repeat each experiment ten times with ten different random seeds.

Figure 6.5 shows ROC curves for the test set of **Nsf5** dataset. For simplicity, we show ROC curves only for one experiment run. Moreover, Table 6.7 shows seven different performance metrics computed for each formulation. Each shown result in this table is a median of ten independent runs. *BinCross* provides inferior results for all metrics. The best and worst results are highlighted in green and red. Surprisingly, *BinCross* performs the worst even for the AUC. On the other hand, *DeepTopPush* excels at very low false-positive rates, as seen from the table and the figure. In fact, *DeepTopPush* provides the best results for four out of seven performance

Figure 6.5: **Nsf5 dataset**: ROC curves with logarithmic x -axis.

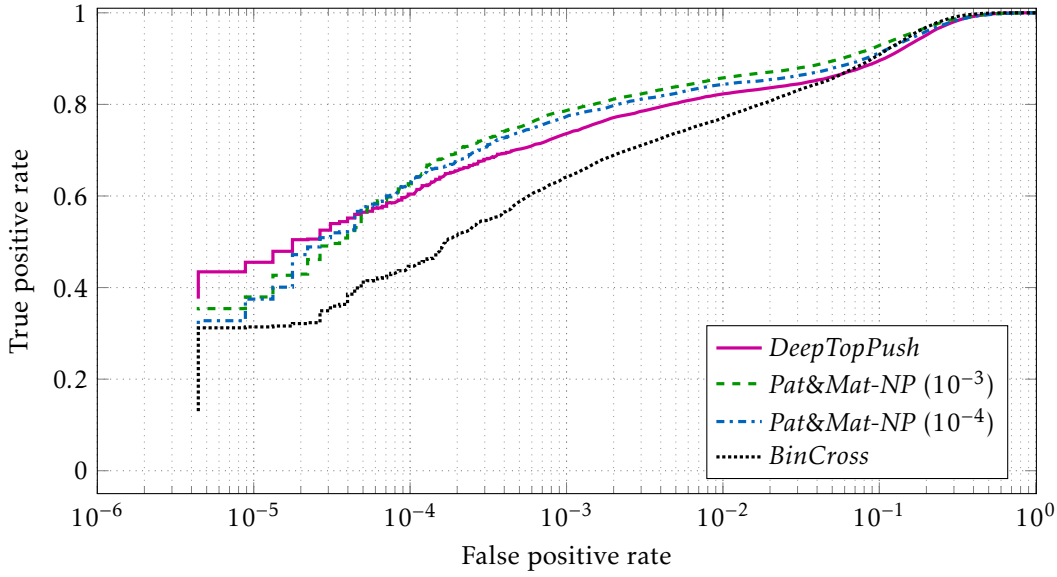
Formulation	AUC	TPR@K			TPR@ τ		
		1	10	5	10^{-5}	10^{-4}	10^{-3}
<i>BinCross</i>	95.84	0.0	0.0	0.0	0.0	0.02	0.7
<i>DeepTopPush</i>	98.29	5.07	35.48	57.66	48.65	89.56	93.67
<i>Pat&Mat-NP</i> (10^{-5})	98.81	2.55	23.02	47.24	35.28	91.9	95.84
<i>Pat&Mat-NP</i> (10^{-4})	98.98	0.0	0.05	4.34	1.78	79.76	96.18
<i>Pat&Mat-NP</i> (10^{-3})	99.26	0.0	0.0	0.01	0.0	0.29	91.98

Table 6.7: **NSF5 dataset**: All presented results are medians of ten independent runs with different random seeds. Each column of the table corresponds to one performance metric, and every row to one formulation. The best result for each metric is highlighted in green, while the worst is highlighted in red.

metrics. Note that all these four metrics operate at extremely low false-positive rates. We can also see that *Pat&Mat-NP* (10^{-5}) is the best at false-positive rate 10^{-4} . This is probably caused by the approximation of the true top τ -quantile of all scores of negative samples used in *Pat&Mat-NP* formulation. Therefore, *Pat&Mat-NP* (10^{-5}) is optimized for a false-positive rate slightly higher than 10^{-5} and as a consequence outperforms *Pat&Mat-NP* (10^{-4}) at false-positive rate 10^{-4} . Similar behavior can be seen for *Pat&Mat-NP* (10^{-4}) and *Pat&Mat-NP* (10^{-3}) at false-positive rate 10^{-3} .

6.3.2 JMiPOD

The second dataset was created in a different way. Firstly only images that can be cropped to size 256×256 were used. All such images were cropped losslessly using *jpegtran* library [71] and the stego images were generated using the JMiPOD algorithm [69] using payload 0.1. As in the case of Nsf5 dataset, only 10% of all cover images are used to generate their stego counterparts. Unlike the Nsf5 dataset, **JMiPOD** dataset contains images and not features extracted from

Figure 6.6: **JMiPOD dataset**: ROC curves with logarithmic x -axis.

Formulation	AUC	TPR@ K			TPR@ τ		
		1	10	5	10^{-5}	10^{-4}	10^{-3}
<i>BinCross</i>	97.5	13.52	24.65	29.54	27.28	44.58	63.84
<i>DeepTopPush</i>	97.26	34.25	42.57	47.3	43.59	60.42	73.67
<i>Pat&Mat-NP</i> (10^{-4})	97.49	25.66	36.76	45.19	38.28	63.49	77.43
<i>Pat&Mat-NP</i> (10^{-3})	98.0	26.99	38.76	44.83	42.17	64.5	78.11

Table 6.8: **JMiPOD dataset**: All presented results are medians of ten independent runs with different random seeds. Each column of the table corresponds to one performance metric, and every row to one formulation. The best result for each metric is highlighted in green, while the worst is highlighted in red.

them. The entire dataset is divided into train/validation/test sets in the 0.375/0.125/0.5 ratio. The resulting sizes of the splits and the number of stego images in them are summarized in Table 6.2.

In this case, the resulting classification task is quite complicated. Therefore we decided to use pre-trained EfficientNet-B0 [72] as the model. Originally the model was trained for 1000 classes. Therefore, we removed the last fully-connected layer and replaced it with a randomly initialized fully-connected layer of appropriate size for binary classification. The resulting model is large, and it is not possible to use a full gradient. For this reason, we use stochastic gradient descent with balanced mini-batches of size 256. As an optimizer, we use the ADAM [64] with default settings and fixed step length $\alpha = 0.01$. Finally, we fix the number of epochs to 30 for all formulations, and we repeat each experiment ten times with different random seeds.

Figure 6.6 shows ROC curves for the test set of **JMiPOD** dataset. Moreover, Table 6.8 shows seven performance metrics. Each shown result in this table is a median of ten independent runs. The best and worst results are highlighted in green and red. Since trained models use stochastic gradient descent, the results are not as evident as for the Nsf5 dataset. *BinCross* still

provides the worst results for most metrics, but the differences are much smaller than for the Nsf5 dataset. We can see that *DeepTopPush* again provides the best performance for four of the seven metrics. It shows that the enhanced minibatch used in *DeepTopPush* Algorithm 6 improves the approximation quality of the true threshold and reduces the bias of the sampled gradient (as we already showed in Figure 5.2). Even though *Pat&Mat-NP* (10^{-3}) and *Pat&Mat-NP* (10^{-4}) were trained for different levels of false-positive rate, they both perform similarly. As we said before, the decision threshold t of *Pat&Mat-NP* model approximates the true top τ -quantile of all scores of negative samples. Since we use mini-batches with 128 negative samples, the smallest quantile that can be found on this minibatch is $\tau = \frac{1}{128} \approx 0.0078$. If we try to approximate smaller quantiles, we always get the same results. Therefore, *Pat&Mat-NP* (10^{-3}) and *Pat&Mat-NP* (10^{-4}) should work almost identically, and we can see from both the figure and the table, that these two formulations provide similar results. For this reason we omit *Pat&Mat-NP* (10^{-5}) in this experiment.

6.4 Malware Detection

In the previous section, we presented results from the domain of steganalysis. Another domain in which formulations from the presented framework can be very useful is the domain of malware detection. As an example, consider standard antivirus software on a personal computer. Every user wants to be protected, so the goal of antivirus software is to detect as much malware as possible. However, if the antivirus is too restrictive, it can easily happen that clean software is marked as malware, i.e., the antivirus can easily produce false alarms. If the antivirus produces false alarms too often, it can negatively affect the user experience and may lead to uninstalling the antivirus completely. Therefore, the goal of every antivirus is to maximize a true-positive rate at a very low false-positive rate, which is precisely what the formulations from the framework do.

In this section, we present results on a real-world dataset provided by a renowned cybersecurity company. The dataset consists of malware analysis reports of executable files. The dataset is extremely tough as individual samples are JSON files whose size ranges from 1kB to 2.5MB. The sample structure is highly complicated because each sample has a different number of features, and features may have a complicated structure, such as a list of ports to which the file connects. This contrasts sharply with standard datasets, where each sample has the same number of features, and each feature is a real number. The usual approach to processing such complicated data is to manually create feature vectors and use them for training instead of the original data. However, such an approach is extremely time-demanding and requires expert knowledge of the original data. For this reason, we decided to use a different approach called Hierarchical Multiple Instance Learning (HMIL) [73]. For the training, we use a publicly available implementation of HMIL [74], which allows training models directly from JSON files without requiring complicated feature extraction.

Due to the immense dataset size (see Table 6.2), we train each formulation only once. Moreover, we use only the formulations that worked the best in the previous experiments, i.e., we use only the *BinCross*, *Pat&Mat-NP* (10^{-2}), *Pat&Mat-NP* (10^{-3}) and *DeepTopPush*. As an optimizer, we use the ADAM [64] with default settings and fixed step length $\alpha = 0.01$. We also use balanced mini-batches of size 2000, which allows us to obtain a very good estimate of the true thresholds as discussed in Section 5.3. Finally, we fix the number of epochs to 100.

Figure 6.7 shows the ROC curves for all formulations. It is clear that *DeepTopPush* is the best at low false-positive rates. Even at the extremely low false positive rate $\tau = 10^{-5}$, *DeepTopPush* correctly identified 46% of malware. We can also see that *Pat&Mat-NP* (10^{-3}) is the best at false-positive rate 10^{-3} , which is exactly the point for which the formulation should be optimized. However, at this false-positive rate, *DeepTopPush* performs almost as well as *Pat&Mat-NP* (10^{-3}). Finally, all formulations perform equally well at the false-positive rate 10^{-2} .



Figure 6.7: **Malware detection:** ROC curves with logarithmic x -axis.

Conclusion

Binary classification is focused on classification performance on all samples. In Chapter 1, we discussed many problems in which the performance on all samples is not desired and only performance on a small amount of samples is important. In this work, we studied the problem of classification at the top, which focuses on these specific problems. In the following list, we provide the main contributions of this work:

- **Introduction of a unified framework for classification at the top:** In Chapter 1 we showed that many well-known categories of problems, such as ranking, accuracy at the top, or hypothesis testing, are closely related to classification at the top. This leads us to introduce a unified framework for classification at the top in Chapter 2. We showed that several known formulations (*TopPush*, *Grill*, τ -FPL) fall into our framework and derived some completely new formulations (*Pat&Mat*, *Pat&Mat-NP*). The summary of all presented formulations can be found in Table 2.1.
- **Introduction of *Pat&Mat* and *Pat&Mat-NP* formulations:** In Chapter 2, we introduced the *Pat&Mat* formulation as an alternative to the *TopMeanK* formulation. These two formulations differ only in the decision threshold approximation. *Pat&Mat* formulation uses surrogate approximation of the true quantile while *TopMeanK* approximates the true quantile using mean. We showed, that the threshold used in *Pat&Mat* provides worse approximation of the true threshold, but has better theoretical properties. Similarly, we introduced the *Pat&Mat-NP* formulation as an alternative to the τ -FPL formulation.
- **Derivation of theoretical properties for a linear classifier:** In Chapter 3, we performed a theoretical analysis of the presented formulations when the linear model is used. We showed that known formulations suffer from certain disadvantages. *TopPush* and τ -FPL are sensitive to outliers and *Grill* is non-convex. On the other hand, we showed that newly introduced *Pat&Mat* and *Pat&Mat-NP* formulations are both robust and convex. We also proved the global convergence of the stochastic gradient descent for *Pat&Mat* and *Pat&Mat-NP*.
- **Derivation of dual forms and use of non-linear kernels:** In Chapter 4, we showed that all presented formulations (except for *Grill* and *Grill-NP*) can be divided into two families based on the form of the constraints, namely *TopPushK* and *Pat&Mat* family of formulations. We derived dual forms for *TopPushK* and *Pat&Mat* family of formulations. Moreover, for both these formulations we show how to incorporate non-linear kernels.
- **Derivation of an efficient algorithm for solving dual forms:** In Chapter 4, we proposed a new coordinate descent algorithm for solving dual forms of *TopPushK* and *Pat&Mat* family of formulations. The resulting algorithm depends on the used surrogate function. Therefore, we derived the closed-form formulae for selected surrogate functions. Since the algorithm needs a feasible solution for initialization, we also showed how to find such a solution.
- **Introduction of a modified stochastic gradient descent:** In Chapter 5, we study the primal formulations with non-linear models. More precisely, we used neural networks.

We showed that when we use a non-linear model, the resulting formulations are non-decomposable. This property is caused by the special threshold constraint in (2.3) and prevents us from using stochastic gradient descent in a standard way. We introduced modified stochastic gradient descent for our formulations. Unfortunately, we showed that modified stochastic gradient descent leads to a biased estimate of the true gradient.

- **Introduction of *DeepTopPush* formulation:** As mentioned above, the proposed modified stochastic gradient descent leads to a biased estimate of the true gradient. In Chapter 5, we suggested that this can be mitigated by using a large minibatch. However, such an approach is often not possible. For such cases, we proposed *DeepTopPush* as an efficient alternative to *TopPush* formulation that does not suffer from this issue. For *DeepTopPush*, we implicitly removed some optimization variables, created an unconstrained end-to-end network, and used the stochastic gradient descent to train it. We modified the minibatch so that the sampled threshold (computed on a minibatch) is a good estimate of the true threshold (computed on all samples). We showed both theoretically and numerically that this procedure reduces the bias of the sampled gradient.
- **Numerical comparison:** In Chapter 6, we performed a numerical comparison of all presented formulations. We showed a good performance of our newly introduced formulation *Pat&Mat-NP*, when used in its primal form. We also showed that *DeepTopPush* formulation could be beneficial, especially for very large real-world datasets. Lastly, we demonstrated that standard formulations provide poor results at very low false-positive rates on steganalysis datasets and malware detection datasets, while the formulations proposed in this work outperform them.

Future Work

The problem of classification at the top is well-defined for binary classification problems. However, there is no straightforward extension of classification at the top for multiclass problems. For instance, consider the problem of malware detection. In Chapter 6, we introduced malware detection as a problem in which we only want to decide whether some binary file is malware. However, there are plenty of different types of malware families. Therefore it would be better to formulate the problem as a multiclass classification problem, i.e., one class for clean software and one class for each malware family. Any standard multiclass classifier could solve this problem. However, these do not provide the option to maximize the number of correctly classified samples with a prescribed level of false alarms. The most straightforward approach would be to create a two-stage classification. In the first stage, we could use classification at the top to detect malware with the desired level of false-positive rate (false alarms). Then, in the second stage, we could use a standard multiclass classifier to find the family to which the detected malware belongs. The drawback of this approach is that we can only set a global level of false alarms instead of specific levels for each class. The logic is similar to the problem of accuracy at the top. However, further research would be needed since there is no straightforward way to extend accuracy at the top for the multiclass problem.

Apendices

Appendix for Chapter 2

Lemma 2.7

Consider *Grill*, *Grill-NP*, *TopMeanK* and τ -FPL formulations and Notation 2.2. If the following inequality holds

$$s_{[n_+\tau]}^+ > s_{[n_-\tau]}^-,$$

then *Grill* has larger threshold than *Grill-NP*. In the same way, if the following inequality holds

$$\frac{1}{n_+\tau} \sum_{i=1}^{n_+\tau} s_{[i]}^+ > \frac{1}{n_-\tau} \sum_{i=1}^{n_-\tau} s_{[i]}^-$$

then *TopMeanK* has larger threshold than τ -FPL.

Proof:

Since s^+ and s^- are computed on disjunctive indices, we have

$$s_{[n\tau]} \geq \min\{s_{[n_+\tau]}^+, s_{[n_-\tau]}^-\}.$$

Since $s_{[n\tau]}$ is the threshold for *Grill* and $s_{[n_-\tau]}^-$ is the threshold for *Grill-NP*, the first statement follows. The second part can be shown in a similar way. ■

Lemma 2.5

Consider vector of scores s and its sorted version $s_{[\cdot]}$ with non-increasing elements as defined in Notation 2.2, and threshold for *Pat&Mat* formulation

$$h(t) = \sum_{i \in \mathcal{I}} l(\vartheta(s_i - t)) - n\tau, \quad (2.14)$$

where $\vartheta > 0$ and l is the hinge loss from Notation 2.1. For all $i \in \mathcal{I}$ define $t_i = s_{[i]} + \frac{1}{\vartheta}$. Then for all $i = 2, 3, \dots, n$ we have

$$h(t_i) = h(t_{i-1}) + (i-1)\vartheta(t_{i-1} - t_i), \quad (2.15)$$

with the initial condition $h(t_1) = -n\tau$.

Proof:

Observe that

$$\begin{aligned}
 h(t_j) &= h\left(s_{[j]} + \frac{1}{\vartheta}\right) = \sum_{i \in \mathcal{I}} l\left(\vartheta\left(s_i - \left(s_{[j]} + \frac{1}{\vartheta}\right)\right)\right) - n\tau \\
 &= \sum_{i \in \mathcal{I}} \max\left\{0, 1 + \vartheta\left(s_i - s_{[j]} - \frac{1}{\vartheta}\right)\right\} - n\tau \\
 &= \sum_{i \in \mathcal{I}} \max\{0, \vartheta(s_i - s_{[j]})\} - n\tau \\
 &= \sum_{i=1}^{j-1} \vartheta(s_{[i]} - s_{[j]}) - n\tau,
 \end{aligned}$$

where the last equality holds since $\vartheta > 0$ and $s_{[i]} - s_{[j]} \leq 0$ for all $i \geq j$. From here, we obtain $h(t_1) = -n\tau$. Moreover, we have

$$\begin{aligned}
 h(t_j) &= \sum_{i=1}^{j-1} \vartheta(s_{[i]} - s_{[j]}) - n\tau \\
 &= \sum_{i=1}^{j-2} \vartheta(s_{[i]} - s_{[j]}) + \vartheta(s_{[j-1]} - s_{[j]}) - n\tau \\
 &= \sum_{i=1}^{j-2} \vartheta(s_{[i]} - s_{[j]} + s_{[j-1]} - s_{[j-1]}) + \vartheta(s_{[j-1]} - s_{[j]}) - n\tau \\
 &= \sum_{i=1}^{j-2} \vartheta(s_{[i]} - s_{[j-1]}) + \sum_{i=1}^{j-2} \vartheta(s_{[j-1]} - s_{[j]}) + \vartheta(s_{[j-1]} - s_{[j]}) - n\tau \\
 &= h(t_{j-1}) + (j-1)\vartheta(s_{[j-1]} - s_{[j]}) \\
 &= h(t_{j-1}) + (j-1)\vartheta(t_{j-1} - t_j),
 \end{aligned}$$

which finishes the proof. ■

Appendix for Chapter 3

B.1 Convexity

Proposition 3.1

Consider fixed vector of scores \mathbf{s} with elements defined as $s_i = \mathbf{w}^\top \mathbf{x}_i$ for all $i \in \mathcal{I}$. Moreover, consider thresholds for *TopPush*, *Grill*, *TopMeanK* and *Pat&Mat* from Section 2.2 and 2.3 defined as

$$\begin{aligned} t_0(\mathbf{w}) &= s_{[1]}^-, & t_1(\mathbf{w}) &= \max \left\{ t \mid \frac{1}{n} \sum_{i \in \mathcal{I}} \mathbb{1}_{[s_i \geq t]} \geq \tau \right\}, \\ t_2(\mathbf{w}) &= \frac{1}{K} \sum_{i=1}^K s_{[i]}, & t_3(\mathbf{w}) &\text{ solves } \frac{1}{n} \sum_{i \in \mathcal{I}} l(\vartheta(s_i - t)) = \tau, \end{aligned}$$

Then thresholds t_0 , t_2 and t_3 are convex functions of weights \mathbf{w} , while the threshold t_1 is non-convex.

Proof of Proposition 3.1 on page 28:

From Notation 2.2, threshold t_0 is just a maximum from vector \mathbf{s}^- of scores of all negative samples. Since maximum is a convex function, threshold t is a convex function of weights \mathbf{w} . Moreover, it is easy to show that the quantile t_1 is not convex. Due to [32], the mean of the K highest values of a vector is a convex function. Therefore, threshold t_2 is a convex function of weights \mathbf{w} . It remains to analyze threshold t_3 . Let us define function g as follows

$$g(\mathbf{w}, t) := \frac{1}{n} \sum_{i \in \mathcal{I}} l(\mathbf{w}^\top \mathbf{x}_i - t) - \tau.$$

where we set $\vartheta = 1$ for simplicity. Then t_3 is defined via an implicit equation $g(\mathbf{w}, t) = 0$. Since l is convex, we immediately obtain that g is jointly convex in both variables.

To show the convexity, consider $\mathbf{w}, \tilde{\mathbf{w}} \in \mathbb{R}^d$ and the corresponding thresholds $t = t_3(\mathbf{w})$, $\tilde{t} = t_3(\tilde{\mathbf{w}})$. Then for any $\lambda \in [0, 1]$, we have

$$g(\lambda \mathbf{w} + (1 - \lambda) \tilde{\mathbf{w}}, \lambda t + (1 - \lambda) \tilde{t}) \leq \lambda g(\mathbf{w}, t) + (1 - \lambda) g(\tilde{\mathbf{w}}, \tilde{t}) = 0. \quad (\text{B.1})$$

The inequality follows from the convexity of g and the equality from $g(\mathbf{w}, t) = g(\tilde{\mathbf{w}}, \tilde{t}) = 0$, which holds due to the definition of t_3 . From the definition of t_3 , we also have

$$g(\lambda \mathbf{w} + (1 - \lambda) \tilde{\mathbf{w}}, t_3(\lambda \mathbf{w} + (1 - \lambda) \tilde{\mathbf{w}})) = 0. \quad (\text{B.2})$$

Since g is non-increasing in the second variable, from (B.1) and (B.2) we deduce

$$t_3(\lambda w + (1 - \lambda)\tilde{w}) \leq \lambda t + (1 - \lambda)\tilde{t} = \lambda t_3(w) + (1 - \lambda)t_3(\tilde{w}),$$

which implies that function $w \mapsto t_3(w)$ is convex. ■

Theorem 3.2

If the threshold $t = t(w)$ is a convex function of weights w , then function

$$L(w) = \overline{\text{fn}}(s, t) = \sum_{i \in \mathcal{I}_+} l(t - w^\top x_i)$$

is convex.

Proof of Theorem 3.2 on page 28:

Due to the definition (2.2), the objective function L equals to

$$L(w) = \overline{\text{fn}}(s, t(w)) = \sum_{i \in \mathcal{I}_+} l(t(w) - w^\top x_i).$$

Here we write $t(w)$ to stress the dependence of t on w . Since $w \mapsto t(w)$ is a convex function, we also have that $w \mapsto t(w) - w^\top x$ is a convex function. From its definition, the surrogate function l is convex and non-decreasing. Since the composition of a convex function with a non-decreasing convex function is a convex function, this finishes the proof. ■

B.2 Differentiability

Theorem 3.3

Consider thresholds from Proposition 3.1. Threshold t_0 , t_1 and t_2 are non-differentiable functions of weights w . Moreover, if the surrogate function l is differentiable, threshold t_3 is a differentiable function of weights w , and its derivative equals

$$\nabla t_3(w) = \frac{\sum_{i \in \mathcal{I}} l'(\vartheta(w^\top x_i - t_3(w))) x_i}{\sum_{j \in \mathcal{I}} l'(\vartheta(w^\top x_j - t_3(w)))}.$$

Proof of Theorem 3.3 on page 28:

The non-differentiability of t_0 , t_1 and t_2 happens whenever the threshold value is achieved at two different scores. The result for t_3 follows directly from the implicit function theorem. ■

B.3 Stability

Example 3.4: Degenerate Behaviour

Consider n negative samples uniformly distributed in $[-1, 0] \times [-1, 1]$, n positive samples uniformly distributed in $[0, 1] \times [-1, 1]$ and one negative sample at $(2, 0)$. An illustration of such settings is provided in Figure 3.1 (left). If n is large enough, the point at $(2, 0)$ is an outlier and the problem is (almost) perfectly separable using the separating hyperplane with normal vector $w_1 = (1, 0)$.

Additionally to the assumptions from Example 3.4, we consider the hinge loss function and no regularization for all formulations from Table 2.1. We also assume that n is large, and the outlier may be ignored for the computation of thresholds that require a large number of points.

TopPush formulation (2.5):

- For $w_0 = (0, 0)^\top$, all scores are equal to 0. Since the threshold t is the largest negative score, it also equals 0. Consequently, the value of the objective function is

$$L(w_0) = \frac{1}{n_+} \sum_{i \in \mathcal{I}_+} \max\{0, 1 + (0 - 0)\} = 1.$$

- For $w_1 = (1, 0)^\top$, the largest negative score equals 2; therefore $t = 2$. Then, the value of the objective function is

$$L(w_1) \approx \int_0^1 \max\{0, 1 + (2 - s_i)\} = \int_0^1 (3 - s) ds = \frac{5}{2},$$

where we can remove the max operator since all positive samples are uniformly distributed in $[0, 1] \times [-1, 1]$, and their scores are uniformly distributed in $[0, 1]$.

TopPushK formulation (2.6):

- For $w_0 = (0, 0)^\top$, the threshold and the objective function is the same as for *TopPush*.
- For $w_1 = (1, 0)^\top$, the threshold is the mean of K largest negative scores. The largest negative score equals 2 and for sufficiently large n , the rest of K largest negative scores equal 0. Therefore, the threshold is $t = \frac{2}{K}$. Then, the value of the objective function is

$$L(w_1) \approx \int_0^1 \max\left\{0, 1 + \left(\frac{2}{K} - s\right)\right\} ds = \int_0^1 \left(1 + \frac{2}{K} - s\right) ds = \frac{1}{2} + \frac{2}{K},$$

where we can remove the max operator since all positive scores are uniformly distributed in $[0, 1]$.

Grill formulation (2.9):

- For $w_0 = (0, 0)^\top$, all scores equal 0 and the threshold (top τ -quantile) is also 0. The objective reads

$$L(w_0) = \frac{1}{n_+} \sum_{i \in \mathcal{I}_+} \max\{0, 1 + (0 - 0)\} + \frac{1}{n_-} \sum_{i \in \mathcal{I}_-} \max\{0, 1 + (0 - 0)\} = 1 + 1 = 2.$$

- For $w_1 = (1, 0)^\top$, all scores are uniformly distributed in $[-1, 1]$ and the top τ -quantile of all score equals $t = 1 - 2\tau$. Then for $\tau \leq \frac{1}{2}$, the value of the objective function is

$$\begin{aligned} L(w_1) &\approx \int_0^1 \max\{0, 1 + (1 - 2\tau - s)\} ds + \int_{-1}^0 \max\{0, 1 + (s - 1 + 2\tau)\} ds \\ &= \int_0^1 \max\{0, 2(1 - \tau) - s\} ds + \int_{-1}^0 \max\{0, s + 2\tau\} ds \\ &= \int_0^1 (2(1 - \tau) - s) ds + \int_{-2\tau}^0 (s + 2\tau) ds \\ &= \frac{3}{2} - 2\tau(1 - \tau) \end{aligned}$$

TopMeanK formulation (2.11):

- For $w_0 = (0, 0)^\top$, the threshold and objective function is the same as for *TopPushK*.
- For $w_1 = (1, 0)^\top$, the threshold is the mean of $K = n\tau$ largest scores. Since all scores are uniformly distributed in $[-1, 1]$, the top $n\tau$ fraction of all scores is uniformly distributed in $[1 - 2\tau, 1]$. Therefore the threshold is $t = 1 - \tau$. Then, the value of the objective function is

$$L(w_1) \approx \int_0^1 \max\{0, 1 + (1 - \tau - s)\} ds = \int_0^1 (2 - \tau - s) ds = \frac{3}{2} - \tau,$$

Pat&Mat formulation (2.13):

- For $w_0 = (0, 0)^\top$, we have

$$\tau = \frac{1}{n} \sum_{i \in \mathcal{I}} \max\{0, 1 + \vartheta(0 - t)\} = \frac{1}{n} \sum_{i \in \mathcal{I}} (1 - \vartheta t) = 1 - \vartheta t,$$

which implies that threshold t equals

$$t = \frac{1 - \tau}{\vartheta}. \quad (\text{B.3})$$

Consequently, the value of the objective function is

$$L(w_0) = \frac{1}{n_+} \sum_{i \in \mathcal{I}_+} \max\{0, 1 + (t - 0)\} = \frac{1}{n_+} \sum_{i \in \mathcal{I}_+} (1 + t) = 1 + t, \quad (\text{B.4})$$

where the last equality follows the fact that $t \geq 0$.

- For $w_1 = (1, 0)^\top$, the computation is similar. All scores are uniformly distributed in $[-1, 1]$. Then, if the scaling parameter ϑ satisfies $\vartheta \leq \tau$, we have

$$\tau = \frac{1}{n} \sum_{i \in \mathcal{I}} \max\{0, 1 + \vartheta(s_i - t)\} \approx \frac{1}{2} \int_{-1}^1 \max\{0, 1 + \vartheta(s - t)\} ds = \frac{1}{2} \int_{-1}^1 (1 + \vartheta(s - t)) ds = 1 - \vartheta t,$$

which again implies that threshold t is $t = \frac{1}{\vartheta}(1 - \tau)$. Note that we could ignore the max operator in the relation above, since

$$1 + \vartheta(s - t) \geq 1 + \vartheta(-1 - t) = 1 + \vartheta\left(-1 - \frac{1 - \tau}{\vartheta}\right) = \tau - \vartheta \geq 0,$$

where the last inequality follows from the assumption $\vartheta \leq \tau$. Finally, since positive scores are uniformly distributed in $[0, 1]$, the value of the objective function is

$$L(w_1) = \frac{1}{n_+} \sum_{i \in \mathcal{I}_+} \max\{0, 1 + (t - s_i)\} \approx \int_0^1 \max\{0, 1 + t - s\} ds = \int_0^1 (1 + t - s) ds = \frac{1}{2} + t$$

Grill-NP formulation (2.18):

- For $w_0 = (0, 0)^\top$, the threshold and objective function is the same as for *Grill*.
- For $w_1 = (1, 0)^\top$, negative scores are uniformly distributed in $[-1, 0]$ and the top τ -quantile of negative score equals $t = -\tau$. Then, the value of the objective function is

$$\begin{aligned} L(w_1) &\approx \int_0^1 \max\{0, 1 + (-\tau - s)\} ds + \int_{-1}^0 \max\{0, 1 + (s + \tau)\} ds \\ &= \int_0^{1-\tau} (1 - \tau - s) ds + \int_{-1}^0 (1 + \tau + s) ds = 1 + \frac{1}{2}\tau^2 \end{aligned}$$

 τ -FPL formulation (2.20):

- For $w_0 = (0, 0)^\top$, the threshold and objective function is the same as for *TopPushK*.
- For $w_1 = (1, 0)^\top$, the threshold is the mean of $n_- \tau$ largest negative scores. Since negative scores are uniformly distributed in $[-1, 0]$, top $n_- \tau$ fraction of negative scores is uniformly distributed in $[-\tau, 0]$. Therefore the threshold is $t = -\frac{1}{2}\tau$. Then, the value of the objective function is

$$L(w_1) \approx \int_0^1 \max\left\{0, 1 + \left(-\frac{1}{2}\tau - s\right)\right\} ds = \int_0^{1-\frac{1}{2}\tau} \left(1 - \frac{1}{2}\tau - s\right) ds = \frac{1}{2} - \frac{1}{8}\tau(4 + \tau)$$

Pat&Mat-NP formulation (2.22):

- For $w_0 = (0, 0)^\top$, we have

$$\tau = \frac{1}{n_-} \sum_{i \in \mathcal{I}_-} \max\{0, 1 + \vartheta(0 - t)\} = \frac{1}{n_-} \sum_{i \in \mathcal{I}_-} (1 - \vartheta t) = 1 - \vartheta t,$$

which implies that threshold is $t = \frac{1-\tau}{\vartheta}$. Consequently, the value of the objective function is

$$L(w_0) = \frac{1}{n_+} \sum_{i \in \mathcal{I}_+} \max\{0, 1 + (t - 0)\} = \frac{1}{n_+} \sum_{i \in \mathcal{I}_+} (1 + t) = 1 + t,$$

where the last equality follows the fact that $t \geq 0$.

- For $w_1 = (1, 0)^\top$, the computation is similar. Negative scores are uniformly distributed in $[-1, 0]$. Then, if the scaling parameter ϑ satisfies $\vartheta \leq 2\tau$, we have

$$\begin{aligned} \tau &= \frac{1}{n_-} \sum_{i \in \mathcal{I}_-} \max\{0, 1 + \vartheta(s_i - t)\} \approx \int_{-1}^0 \max\{0, 1 + \vartheta(s - t)\} ds \\ &= \int_{-1}^0 (1 + \vartheta(s - t)) ds = 1 - \vartheta t - \frac{1}{2}\vartheta. \end{aligned}$$

which implies that threshold is $t = \frac{1}{\vartheta}(1 - \tau) - \frac{1}{2}$. Note that we could ignore the max operator in the relation above, since

$$1 + \vartheta(s - t) \geq 1 + \vartheta(-1 - t) = 1 + \vartheta\left(-1 - \frac{1-\tau}{\vartheta} + \frac{1}{2}\right) = \tau - \frac{1}{2}\vartheta \geq 0,$$

where the last inequality follows from the assumption $\vartheta \leq 2\tau$. Finally, since positive scores are uniformly distributed in $[0, 1]$, the value of the objective function is

$$L(w_1) = \frac{1}{n_+} \sum_{i \in \mathcal{I}_+} \max\{0, 1 + (t - s_i)\} \approx \int_0^1 \max\{0, 1 + t - s\} ds = \int_0^1 (1 + t - s) ds = \frac{1}{2} + t.$$

Theorem 3.5

Consider any of these formulations: *TopPush*, *TopPushK*, *TopMeanK* or τ -FPL. Fix any w and denote the corresponding objective function $L(w)$ and threshold $t(w)$. If we have

$$t(w) \geq \frac{1}{n_+} \sum_{i \in \mathcal{I}_+} w^\top x_i, \quad (3.1)$$

then $L(0) \leq L(w)$. Specifically, using Notation 2.2 we get the following implications

$$\begin{aligned} s_{[1]}^- &\geq \frac{1}{n_+} \sum_{i=1}^{n_+} s_i^+ &\implies L(0) \leq L(w) \text{ for } TopPush, \\ \frac{1}{K} \sum_{i=1}^K s_{[i]}^- &\geq \frac{1}{n_+} \sum_{i=1}^{n_+} s_i^+ &\implies L(0) \leq L(w) \text{ for } TopPushK, \\ \frac{1}{K} \sum_{i=1}^K s_{[i]}^- &\geq \frac{1}{n_+} \sum_{i=1}^{n_+} s_i^+ &\implies L(0) \leq L(w) \text{ for } TopMeanK, \\ \frac{1}{n_- \tau} \sum_{i=1}^{n_- \tau} s_{[i]}^- &\geq \frac{1}{n_+} \sum_{i=1}^{n_+} s_i^+ &\implies L(0) \leq L(w) \text{ for } \tau\text{-FPL}. \end{aligned}$$

Proof of Theorem 3.5 on page 30:

All mentioned formulations use a surrogate approximation of the false-negative rate as the objective function L . The objective function has the following form

$$L(w) = \frac{1}{n_+} \sum_{i \in \mathcal{I}_+} l(t - w^\top x_i)$$

Due to $l(0) = 1$ and the convexity of l , we have $l(s) \geq 1 + cs$, where c equals to the derivative of l at 0. Then we have

$$L(w) \geq \frac{1}{n_+} \sum_{i \in \mathcal{I}_+} (1 + c(t - w^\top x_i)) = 1 + c \left(t - \frac{1}{n_+} \sum_{i \in \mathcal{I}_+} w^\top x_i \right) \geq 1,$$

where the last inequality follows from assumption (3.1). Now we realize that for any formulation from the statement, the corresponding threshold for $w = 0$ equals to $t = 0$, and thus $L(0) = 1$. But it implies that $L(0) \leq L(w)$. The second part of the result follows from the form of thresholds $t(w)$. ■

Theorem 3.8

Consider the *Pat&Mat* or *Pat&Mat-NP* formulation with the hinge loss as a surrogate and no regularization. Assume that for some w we have

$$\frac{1}{n_+} \sum_{i \in \mathcal{I}_+} w^\top x_i > \frac{1}{n_-} \sum_{j \in \mathcal{I}_-} w^\top x_j. \quad (3.2)$$

Then there exists a scaling parameter ϑ_0 for the surrogate top τ -quantile (2.12) or (2.21) such that $L(w) < L(0)$ for all $\vartheta \in (0, \vartheta_0)$.

Proof of Theorem 3.8 on page 31:

Recall that we use linear model and Notation 2.2 and let us define the following auxiliary variables

$$s_{\min} = \min_{i \in I} s_i, \quad s_{\max} = \max_{i \in I} s_i, \quad \bar{s} = \frac{1}{n} \sum_{i \in I} s_i.$$

Using the definition of \bar{s} we get the following relation

$$\bar{s} = \frac{1}{n} \sum_{i \in \mathcal{I}_+} s_i + \frac{1}{n} \sum_{i \in \mathcal{I}_-} s_i < \frac{1}{n} \sum_{i \in \mathcal{I}_+} s_i + \frac{n_-}{nn_+} \sum_{i \in \mathcal{I}_+} s_i = \frac{1}{n_+} \sum_{i \in \mathcal{I}_+} s_i, \quad (\text{B.5})$$

where the inequality follows from (3.2), and the last equality follows from

$$\frac{1}{n} + \frac{n_-}{nn_+} = \frac{1}{n} \left(1 + \frac{n_-}{n_+} \right) = \frac{1}{n} \frac{n_+ + n_-}{n_+} = \frac{1}{n} \frac{n}{n_+} = \frac{1}{n_+}.$$

Since the average of all elements of a vector is smaller or equal to its maximum, we get the following relation

$$\bar{s} < \frac{1}{n_+} \sum_{i \in \mathcal{I}_+} s_i \leq \max_{i \in \mathcal{I}_+} s_i \leq \max_{i \in I} s_i = s_{\max}$$

where the first inequality follows from (B.5). The lower bound for \bar{s} can be computed in a similar way.

Combining all results above, we have $s_{\min} < \bar{s} < s_{\max}$. Then we can define

$$\vartheta_0 = \min \left\{ \frac{\tau}{\bar{s} - s_{\min}}, \frac{1 - \tau}{s_{\max} - \bar{s}}, \tau \right\}.$$

Note that $\vartheta_0 > 0$. Now we fix any $\vartheta \in (0, \vartheta_0)$ and define

$$t = \frac{1 - \tau}{\vartheta} + \bar{s}.$$

Then for any $i \in \mathcal{I}$, we obtain

$$1 + \vartheta(s_i - t) \geq 1 + \vartheta(s_{\min} - t) = 1 + \vartheta \left(s_{\min} - \frac{1 - \tau}{\vartheta} - \bar{s} \right) = \tau - \vartheta(\bar{s} - s_{\min}),$$

where the first equality follows from the definition of t . From the definition ϑ_0 we deduce

$$0 < \vartheta \leq \vartheta_0 \leq \frac{\tau}{\bar{s} - s_{\min}}.$$

Since $\bar{s} - s_{\min} > 0$, we get the following inequality

$$1 + \vartheta(s_i - t) \geq \tau - \vartheta(\bar{s} - s_{\min}) \geq \tau - \frac{\tau}{\bar{s} - s_{\min}}(\bar{s} - s_{\min}) = 0 \quad (\text{B.6})$$

Combining the definition of the hinge loss function from Notation 2.1 and the inequality above, we have

$$l(\vartheta(s_i - t)) = \max\{0, 1 + \vartheta(s_i - t), 0\} = 1 + \vartheta(s_i - t).$$

Finally, replacing the hinge loss in the left-hand side of (2.12) leads to

$$\frac{1}{n} \sum_{i \in \mathcal{I}} l(\vartheta(s_i - t)) = \frac{1}{n} \sum_{i \in \mathcal{I}} (1 + \vartheta(s_i - t)) = 1 - \vartheta t + \frac{\vartheta}{n} \sum_{i \in \mathcal{I}} s_i = 1 - \vartheta \left(\frac{1 - \tau}{\vartheta} + \bar{s} \right) + \vartheta \bar{s} = \tau,$$

where the third equality employs the definition of \bar{s} and t . But this means that t is the threshold corresponding to w , i.e. it solves (2.12).

In the same way, as we derived (B.6), we get

$$1 + t - s_i \geq 1 + t - s_{\max} = 1 + \frac{1 - \tau}{\vartheta} + \bar{s} - s_{\max} \geq \frac{1 - \tau}{\vartheta} + \bar{s} - s_{\max} \geq 0, \quad (\text{B.7})$$

where the last inequality follows from the definition of ϑ_0 . Then for the objective, we have

$$L(w) = \frac{1}{n_+} \sum_{i \in \mathcal{I}_+} l(t - s_i) = \frac{1}{n_+} \sum_{i \in \mathcal{I}_+} (1 + t - s_i) = 1 + t - \frac{1}{n_+} \sum_{i \in \mathcal{I}_+} s_i < 1 + \left(\frac{1 - \tau}{\vartheta} + \bar{s} \right) - \bar{s} = 1 + \frac{1 - \tau}{\vartheta},$$

where the second equality follows from (B.7), the only inequality from (B.5). Using (B.3) and (B.4), we finally get

$$L(w) < 1 + \frac{1 - \tau}{\vartheta} = L(0).$$

Thus, we finished the proof for *Pat&Mat*. The proof for *Pat&Mat-NP* can be performed identically. ■

B.4 Stochastic Gradient Descent

The proof of convergence of stochastic gradient descent for *Pat&Mat* and *Pat&Mat-NP* is divided into three parts. In Section B.4.1, we prove a general statement for convergence of stochastic gradient descent with a convex objective function. In Section B.4.2 we apply it to Theorem 3.9. Finally, in Section B.4.3, we provide auxiliary results.

B.4.1 General Results

Consider a differentiable objective function L and the optimization method

$$w^{k+1} = w^k - \alpha^k g(w^k), \quad (\text{B.8})$$

where $\alpha^k > 0$ is a stepsize and $g(w^k)$ is an approximation of the gradient $\nabla L(w^k)$. Assume the following:

- (A1) L is differentiable, convex, and attains a global minimum;
- (A2) $\|g(w^k)\| \leq B$ for all k ;
- (A3) the stepsize is non-increasing and satisfies $\sum_{k=0}^{\infty} \alpha^k = \infty$;
- (A4) the stepsize satisfies $\sum_{k=0}^{\infty} (\alpha^k)^2 < \infty$;
- (A5) the stepsize satisfies $\sum_{k=0}^{\infty} \|\alpha^{k+1} - \alpha^k\| < \infty$.

Assumptions (A3)-(A5) are satisfied for example for a stepsize defined by

$$\alpha^k = \frac{\alpha^0}{k+1}.$$

Theorem B.7

Assume that the assumptions (A1)-(A4) are satisfied. If there exists some C such that for a global minimizer w^* of L we have

$$\sum_{k=0}^{\infty} \alpha^k \langle g(w^k) - \nabla L(w^k), w^* - w^k \rangle \leq C, \quad (\text{B.9})$$

then the sequence $\{w^k\}$ generated by (B.8) is bounded and $L(w^k) \rightarrow L(w^*)$. Thus, all its convergent subsequences converge to some global minimum of L .

Proof:

Note first that the convexity of L from (A1) implies

$$\langle \nabla L(w^k), w^* - w^k \rangle \leq L(w^*) - L(w^k). \quad (\text{B.10})$$

Then we have

$$\begin{aligned} \|w^{k+1} - w^*\|^2 &= \|w^k - \alpha^k g(w^k) - w^*\|^2 \\ &= \|w^k - w^*\|^2 + 2\alpha^k \langle g(w^k), w^* - w^k \rangle + (\alpha^k)^2 \|g(w^k)\|^2 \\ &\leq \|w^k - w^*\|^2 + 2\alpha^k \langle g(w^k), w^* - w^k \rangle + (\alpha^k)^2 B^2 \\ &= \|w^k - w^*\|^2 + 2\alpha^k \langle g(w^k) + \nabla L(w^k) - \nabla L(w^k), w^* - w^k \rangle + (\alpha^k)^2 B^2 \\ &\leq \|w^k - w^*\|^2 + 2\alpha^k \langle g(w^k) - \nabla L(w^k), w^* - w^k \rangle + 2\alpha^k (L(w^*) - L(w^k)) + (\alpha^k)^2 B^2, \end{aligned}$$

where the first inequality follows from assumption (A2) and the second one from the properties of inner product and (B.10). Summing this expression for all k and using (B.9) leads to

$$\limsup_{k \rightarrow \infty} \|w^k - w^*\|^2 \leq \|w^0 - w^*\|^2 + 2C + 2 \sum_{k=0}^{\infty} \alpha^k (L(w^*) - L(w^k)) + \sum_{k=0}^{\infty} (\alpha^k)^2 B^2.$$

Using assumption (A4) results in the existence of some \hat{C} such that

$$\limsup_{k \rightarrow \infty} \|w^k - w^*\|^2 + 2 \sum_{k=0}^{\infty} \alpha^k (L(w^k) - L(w^*)) \leq 2\hat{C}. \quad (\text{B.11})$$

Since $\alpha^k > 0$ and $L(w^k) \geq L(w^*)$ as w^* is a global minimizer of L , we infer that sequence $\{w^k\}$ is bounded and (B.11) implies

$$\sum_{k=0}^{\infty} \alpha^k (L(w^k) - L(w^*)) \leq \hat{C}.$$

Since $L(w^k) - L(w^*) \geq 0$, due to assumption (A3) we obtain

$$\lim_{k \rightarrow \infty} L(w^k) = L(w^*),$$

which implies the theorem statement. ■

B.4.2 Proof of Theorem 3.9

For the proof of Theorem 3.9, we consider a general surrogate function l that satisfies:



Figure B.1: Comparison of the hinge loss and its smoothed version with $\varepsilon = 0.25$, $\varepsilon = 0.5$, and $\varepsilon = 0.75$.

- (S1) $l(s) \geq 0$ for all $s \in \mathbb{R}$, $l(0) = 1$ and $l(s) \rightarrow 0$ as $s \rightarrow -\infty$;
- (S2) l is convex and strictly increasing function on $(s_0, +\infty)$, where $s_0 := \sup\{s \mid l(s) = 0\}$;
- (S3) $\frac{l'}{l}$ is a decreasing function on $(s_0, +\infty)$;
- (S4) l' is a bounded function;
- (S5) l' is a Lipschitz continuous function with Lipschitz constant D .

For simplicity, we also assume that the scaling parameter for the threshold in the *Pat&Mat* formulation is $\vartheta = 1$, and regularization parameter is $\lambda = 1$. All requirements above are satisfied for the hinge loss smoothed on an ε -neighborhood of -1

$$l(s) = \begin{cases} 0 & \text{for } s < -1 - \varepsilon, \\ \frac{1}{4\varepsilon}(1 + s + \varepsilon)^2 & \text{for } -1 - \varepsilon \leq s < -1 + \varepsilon, \\ 1 + s & \text{otherwise.} \end{cases}$$

Figure B.1 shows the comparison of the hinge loss and its smoothed version with different ε .

Theorem 3.9

Consider the *Pat&Mat* formulation, stepsizes $\alpha^k = \frac{1}{k+1}\alpha^0$, and piecewise disjoint mini-batches $\mathcal{I}_{\text{mb}}^1, \mathcal{I}_{\text{mb}}^2, \dots, \mathcal{I}_{\text{mb}}^m$ which cycle periodically $\mathcal{I}_{\text{mb}}^{k+m} = \mathcal{I}_{\text{mb}}^k$. If l is the smoothed hinge function defined by

$$l(s) = \begin{cases} 0 & \text{for } s < -1 - \varepsilon, \\ \frac{1}{4\varepsilon}(1 + s + \varepsilon)^2 & \text{for } -1 - \varepsilon \leq s < -1 + \varepsilon, \\ 1 + s & \text{otherwise,} \end{cases} \quad (3.11)$$

where $\varepsilon > 0$, then Algorithm 2 converges to the global minimum of (2.13).

Proof of Theorem 3.9 on page 33:

We intend to apply Theorem B.7 and thus, we need to verify its assumptions. Recall the form of the objective function

$$L(w^k) = \frac{1}{2} \|w^k\|^2 + \frac{1}{n_+} \sum_{i \in \mathcal{I}_+} l(t(w^k) - x_i^\top w^k).$$

The objective is a combination of squared norm of weights, which is strictly convex function, and a surrogate approximation of false-negative rate, which is convex function due to Theorem 3.2. Therefore, the objective L is a strictly convex function. Moreover, it is also differentiable due to Theorem 3.3 and differentiability of smoothed hinge loss l . As a result, Assumption (A1) is satisfied.

Lemma B.10 says that $\|g(w^k)\| \leq \|w^k\| + \hat{B}$ for all k . To show that Assumption (A2) is satisfied, we have to show, that $\|w^k\|$ is uniformly bounded. Consider sufficiently large k such that $\alpha^k < 1$. Then

$$\begin{aligned} \|w^{k+1}\| &= \|w^k - \alpha^k g(w^k)\| = \left\| (1 - \alpha^k)w^k - \alpha^k \frac{1}{n_{\text{mb},+}^k} \sum_{i \in \mathcal{I}_{\text{mb},+}^k} l'(t^k - s_i^k)(\nabla t^k - x_i) \right\| \\ &\leq (1 - \alpha^k) \|w^k\| + \alpha^k \left\| \frac{1}{n_{\text{mb},+}^k} \sum_{i \in \mathcal{I}_{\text{mb},+}^k} l'(t^k - s_i^k)(\nabla t^k - x_i) \right\| \leq (1 - \alpha^k) \|w^k\| + \alpha^k \hat{B}, \end{aligned}$$

where the first inequality follows from the triangle inequality and the last from the proof of Lemma B.10. Now we have two possible cases

- If $\|w^k\| \leq \hat{B}$, then we get

$$\|w^{k+1}\| \leq (1 - \alpha^k) \|w^k\| + \alpha^k \hat{B} \leq (1 - \alpha^k) \hat{B} + \alpha^k \hat{B} = \hat{B}.$$

- If $\|w^k\| > \hat{B}$, then we get

$$\|w^{k+1}\| \leq (1 - \alpha^k) \|w^k\| + \alpha^k B < (1 - \alpha^k) \|w^k\| + \alpha^k \|w^k\| = \|w^k\|.$$

Therefore, for sufficiently large k , we have $\|w^k\| \leq \max\{\hat{B}, \|w^0\|\}$. Combining this with Lemma B.10, we get $\|g(w^k)\| \leq B$, for some B , and Assumption (A2) is satisfied.

Assumptions (A3)-(A5) are imposed directly in the statement of this theorem.

It remains to verify (B.9). For simplicity, we will do so only for $\vartheta = 1$ and for 2 minibatches of the same size. However, the proof would be identical for different ϑ and more minibatches. From the assumptions, we have two minibatches $\mathcal{I}_{\text{mb}}^k$ and $\mathcal{I}_{\text{mb}}^{k+1}$, which are pairwise disjoint and cover all samples. Moreover, for all k , we have $\mathcal{I}_{\text{mb}}^k = \mathcal{I}_{\text{mb}}^{k+2}$. Furthermore, the assumptions imply that the number of positive samples in each minibatch is equal to $n_{\text{mb},+}^k = \frac{1}{2} n_+$, where n_+ is the total number of positive samples.

First we estimate the difference between s_i^k defined in (3.6) and $x_i^\top w^k$. For any $i \in \mathcal{I}_{\text{mb}}^k$ we have $s_i^k = x_i^\top w^k$. Since we have two disjoint minibatches, due to the construction (3.6) we get

$$\begin{aligned} s_i^{k-1} &= s_i^{k-2} = x_i^\top w^{k-2} = x_i^\top (w^k + \alpha^{k-2} g(w^{k-2}) + \alpha^{k-1} g(w^{k-1})) \\ &= x_i^\top w^k + \alpha^{k-2} x_i^\top g(w^{k-2}) + \alpha^{k-1} x_i^\top g(w^{k-1}). \end{aligned} \tag{B.12}$$

Similarly, due to the construction of s_i^k from (3.6), we have for $i \notin \mathcal{I}_{\text{mb}}^k$

$$s_i^k = s_i^{k-1} = \mathbf{x}_i^\top \mathbf{w}^{k-1} = \mathbf{x}_i^\top (\mathbf{w}^k + \alpha^{k-1} g(\mathbf{w}^{k-1})) = \mathbf{x}_i^\top \mathbf{w}^k + \alpha^{k-1} \mathbf{x}_i^\top g(\mathbf{w}^{k-1}). \quad (\text{B.13})$$

Recall that we already verified (A1)-(A5). Combining (A2) with (B.12) and (B.13) yields the existence of some C_2 such that for all $i \in \mathcal{I}$ we have

$$\|s_i^k - \mathbf{x}_i^\top \mathbf{w}^k\| \leq C_2 \alpha^{k-1}, \quad \|s_i^{k-1} - \mathbf{x}_i^\top \mathbf{w}^k\| \leq C_2 (\alpha^{k-1} + \alpha^{k-2}). \quad (\text{B.14})$$

This also immediately implies

$$\|t^k - t(\mathbf{w}^k)\| \leq C_2 \alpha^{k-1}, \quad \|t^{k-1} - t(\mathbf{w}^k)\| \leq C_2 (\alpha^{k-1} + \alpha^{k-2}). \quad (\text{B.15})$$

Moreover, we know that l' is Lipschitz continuous with Lipschitz constant D according to (S5). Then due to (B.14) and (B.15) we get

$$\|l'(t^k - s_i^k) - l'(t(\mathbf{w}^k) - \mathbf{x}_i^\top \mathbf{w}^k)\| \leq D \|t^k - s_i^k - t(\mathbf{w}^k) + \mathbf{x}_i^\top \mathbf{w}^k\| \leq 2C_2 D \alpha^{k-1}. \quad (\text{B.16})$$

In an identical way, we can derive the following relations

$$\begin{aligned} \|l'(t^{k-1} - s_i^{k-1}) - l'(t(\mathbf{w}^k) - \mathbf{x}_i^\top \mathbf{w}^k)\| &\leq 2C_2 D (\alpha^{k-1} + \alpha^{k-2}), \\ \|l'(s_i^k - t^k) - l'(\mathbf{x}_i^\top \mathbf{w}^k - t(\mathbf{w}^k))\| &\leq 2C_2 D \alpha^{k-1}, \\ \|l'(s_i^{k-1} - t^{k-1}) - l'(\mathbf{x}_i^\top \mathbf{w}^k - t(\mathbf{w}^k))\| &\leq 2C_2 D (\alpha^{k-1} + \alpha^{k-2}). \end{aligned} \quad (\text{B.17})$$

Now we need to estimate the distance between $\nabla t(\mathbf{w}^k)$ and ∇t^k . By plugging (3.9) into (3.10), we get

$$\nabla t^k = \frac{\sum_{i \in \mathcal{I}_{\text{mb}}^k} l'(s_i^k - t^k) \mathbf{x}_i + \sum_{i \in \mathcal{I}_{\text{mb}}^{k-1}} l'(s_i^{k-1} - t^{k-1}) \mathbf{x}_i}{\sum_{i \in \mathcal{I}} l'(s_i^k - t^k)}.$$

Moreover, using Theorem 3.3 and the fact that we have only two minibatches and therefore for any k we have $\mathcal{I} = \mathcal{I}_{\text{mb}}^k \cup \mathcal{I}_{\text{mb}}^{k-1}$, we get

$$\nabla t(\mathbf{w}^k) = \frac{\sum_{i \in \mathcal{I}_{\text{mb}}^k} l'(\mathbf{x}_i^\top \mathbf{w}^k - t(\mathbf{w}^k)) \mathbf{x}_i + \sum_{i \in \mathcal{I}_{\text{mb}}^{k-1}} l'(\mathbf{x}_i^\top \mathbf{w}^k - t(\mathbf{w}^k)) \mathbf{x}_i}{\sum_{i \in \mathcal{I}} l'(\mathbf{x}_i^\top \mathbf{w}^k - t(\mathbf{w}^k))}.$$

From Lemma B.9 we deduce that the denominators in the relations above are bounded away from zero uniformly in k . Assumption (A4) implies $\alpha^k \rightarrow 0$. This allows us to use Lemma B.11 which together with (B.17) implies that there is some C_3 such that for all sufficiently large k we have

$$\|\nabla t^k - \nabla t(\mathbf{w}^k)\| \leq C_3 (\alpha^{k-1} + \alpha^{k-2}). \quad (\text{B.18})$$

Using the assumptions above, we can simplify the terms for $g(\mathbf{w}^k)$ from (3.8) and $\nabla L(\mathbf{w}^k)$

from (3.5) to

$$\begin{aligned}
 g(\mathbf{w}^k) &= \mathbf{w}^k + \frac{2}{n_+} \sum_{i \in \mathcal{I}_{\text{mb},+}^k} l'(t^k - s_i^k)(\nabla t^k - \mathbf{x}_i), \\
 g(\mathbf{w}^{k+1}) &= \mathbf{w}^{k+1} + \frac{2}{n_+} \sum_{i \in \mathcal{I}_{\text{mb},+}^{k+1}} l'(t^{k+1} - s_i^{k+1})(\nabla t^{k+1} - \mathbf{x}_i), \\
 \nabla L(\mathbf{w}^k) &= \mathbf{w}^k + \frac{1}{n_+} \sum_{i \in \mathcal{I}_+} l'(t(\mathbf{w}^k) - \mathbf{x}_i^\top \mathbf{w}^k)(\nabla t(\mathbf{w}^k) - \mathbf{x}_i), \\
 \nabla L(\mathbf{w}^{k+1}) &= \mathbf{w}^{k+1} + \frac{1}{n_+} \sum_{i \in \mathcal{I}_+} l'(t(\mathbf{w}^{k+1}) - \mathbf{x}_i^\top \mathbf{w}^{k+1})(\nabla t(\mathbf{w}^{k+1}) - \mathbf{x}_i).
 \end{aligned}$$

Due to the assumptions, we have $\mathcal{I}_+ = \mathcal{I}_{\text{mb},+}^k \cup \mathcal{I}_{\text{mb},+}^{k+1}$ and $\emptyset = \mathcal{I}_{\text{mb},+}^k \cap \mathcal{I}_{\text{mb},+}^{k+1}$, which allows us to write

$$n_+(g(\mathbf{w}^k) + g(\mathbf{w}^{k+1}) - \nabla L(\mathbf{w}^k) - \nabla L(\mathbf{w}^{k+1})) \quad (\text{B.19a})$$

$$= \sum_{i \in \mathcal{I}_{\text{mb},+}^k} l'(t^k - s_i^k)(\nabla t^k - \mathbf{x}_i) - \sum_{i \in \mathcal{I}_{\text{mb},+}^k} l'(t(\mathbf{w}^k) - \mathbf{x}_i^\top \mathbf{w}^k)(\nabla t(\mathbf{w}^k) - \mathbf{x}_i) \quad (\text{B.19b})$$

$$+ \sum_{i \in \mathcal{I}_{\text{mb},+}^k} l'(t^k - s_i^k)(\nabla t^k - \mathbf{x}_i) - \sum_{i \in \mathcal{I}_{\text{mb},+}^k} l'(t(\mathbf{w}^{k+1}) - \mathbf{x}_i^\top \mathbf{w}^{k+1})(\nabla t(\mathbf{w}^{k+1}) - \mathbf{x}_i) \quad (\text{B.19c})$$

$$+ \sum_{i \in \mathcal{I}_{\text{mb},+}^{k+1}} l'(t^{k+1} - s_i^{k+1})(\nabla t^{k+1} - \mathbf{x}_i) - \sum_{i \in \mathcal{I}_{\text{mb},+}^{k+1}} l'(t(\mathbf{w}^k) - \mathbf{x}_i^\top \mathbf{w}^k)(\nabla t(\mathbf{w}^k) - \mathbf{x}_i) \quad (\text{B.19d})$$

$$+ \sum_{i \in \mathcal{I}_{\text{mb},+}^{k+1}} l'(t^{k+1} - s_i^{k+1})(\nabla t^{k+1} - \mathbf{x}_i) - \sum_{i \in \mathcal{I}_{\text{mb},+}^{k+1}} l'(t(\mathbf{w}^{k+1}) - \mathbf{x}_i^\top \mathbf{w}^{k+1})(\nabla t(\mathbf{w}^{k+1}) - \mathbf{x}_i). \quad (\text{B.19e})$$

Then relations (B.16) and (B.18) applied to Lemma B.12 imply

$$\left\| \sum_{i \in \mathcal{I}_{\text{mb},+}^k} l'(t^k - s_i^k)(\nabla t^k - \mathbf{x}_i) - \sum_{i \in \mathcal{I}_{\text{mb},+}^k} l'(t(\mathbf{w}^k) - \mathbf{x}_i^\top \mathbf{w}^k)(\nabla t(\mathbf{w}^k) - \mathbf{x}_i) \right\| \leq C_4(\alpha^{k-1} + \alpha^{k-2})$$

for some C_4 , which gives a bound for (B.19b). Bound for (B.19e) is obtained by increasing k by one. Bounds for (B.19c) and (B.19d) can be find similarly using (B.17). Altogether, we showed

$$\|g(\mathbf{w}^k) + g(\mathbf{w}^{k+1}) - \nabla L(\mathbf{w}^k) - \nabla L(\mathbf{w}^{k+1})\| \leq C_1(\alpha^{k-2} + \alpha^{k-1} + \alpha^k + \alpha^{k+1}) \quad (\text{B.20})$$

for some C_1 .

We now estimate

$$\begin{aligned}
 &\alpha^k \langle g(\mathbf{w}^k) - \nabla L(\mathbf{w}^k), \mathbf{w}^* - \mathbf{w}^k \rangle + \alpha^{k+1} \langle g(\mathbf{w}^{k+1}) - \nabla L(\mathbf{w}^{k+1}), \mathbf{w}^* - \mathbf{w}^{k+1} \rangle \\
 &= \langle g(\mathbf{w}^k) - \nabla L(\mathbf{w}^k), \alpha^k(\mathbf{w}^* - \mathbf{w}^k) \rangle + \langle g(\mathbf{w}^{k+1}) - \nabla L(\mathbf{w}^{k+1}), \alpha^{k+1}(\mathbf{w}^* - \mathbf{w}^{k+1}) \rangle \\
 &= \langle g(\mathbf{w}^k) - \nabla L(\mathbf{w}^k) + g(\mathbf{w}^{k+1}) - \nabla L(\mathbf{w}^{k+1}), \alpha^k(\mathbf{w}^* - \mathbf{w}^k) \rangle \\
 &\quad + \langle g(\mathbf{w}^{k+1}) - \nabla L(\mathbf{w}^{k+1}), \alpha^{k+1}(\mathbf{w}^* - \mathbf{w}^{k+1}) - \alpha^k(\mathbf{w}^* - \mathbf{w}^k) \rangle.
 \end{aligned} \quad (\text{B.21})$$

To estimate the second part of the right hand side of (B.21), we make use of Lemma B.10 to

obtain the existence of some C_5 such that

$$\begin{aligned}
 & \langle g(w^{k+1}) - \nabla L(w^{k+1}), \alpha^{k+1}(w^* - w^{k+1}) - \alpha^k(w^* - w^k) \rangle \\
 & \leq 2B \|\alpha^{k+1}(w^* - w^{k+1}) - \alpha^k(w^* - w^k)\| \\
 & = 2B \|\alpha^{k+1}(w^* - w^k + \alpha^k g(w^k)) - \alpha^k(w^* - w^k)\| \\
 & = 2B \|(\alpha^{k+1} - \alpha^k)w^* + (\alpha^k - \alpha^{k+1})w^k + \alpha^k \alpha^{k+1} g(w^k)\| \\
 & \leq C_5 \|\alpha^{k+1} - \alpha^k\| + C_5 (\alpha^k)^2 + C_5 (\alpha^{k+1})^2.
 \end{aligned} \tag{B.22}$$

In the last inequality we used the inequality $2ab \leq a^2 + b^2$. To estimate the first part of the right hand side of (B.21), we can apply (B.20) together with the boundedness of $\{w^k\}$ to obtain the existence of some C_6 such that

$$\begin{aligned}
 & \langle g(w^k) - \nabla L(w^k) + g(w^{k+1}) - \nabla L(w^{k+1}), \alpha^k(w^* - w^k) \rangle \\
 & \leq C_6 (\alpha^{k-2})^2 + C_6 (\alpha^{k-1})^2 + C_6 (\alpha^k)^2 + C_6 (\alpha^{k+1})^2.
 \end{aligned} \tag{B.23}$$

Plugging (B.22) and (B.23) into (B.21) and summing the terms yields (B.9). Then the assumptions of Theorem B.7 are verified and the theorem statement follows. \blacksquare

B.4.3 Auxiliary Results

Lemma B.9

Let l satisfy (S1)-(S3). Then there exists some $\hat{C} > 0$ such that for all k we have

$$\hat{C} \leq \sum_{i \in \mathcal{I}} l'(s_i^k - t^k), \quad \hat{C} \leq \sum_{i \in \mathcal{I}} l'(x_i^\top w^k - t(w^k)).$$

Proof:

First, we will find an upper bound of $s_i^k - t^k$. Fix any index i_0 . Since l is nonnegative due to (S1), equation (3.7) implies

$$n\tau = \sum_{i \in \mathcal{I}} l(s_i^k - t^k) \geq l(s_{i_0}^k - t^k).$$

Since l is a strictly increasing function due to (S2) and $n\tau > 0$, we get

$$l^{-1}(n\tau) \geq s_{i_0}^k - t^k. \tag{B.24}$$

Since i_0 was an arbitrary index, it holds true for all indices. Then (S3) which leads to a further estimate

$$\sum_{i \in \mathcal{I}} l'(s_i^k - t^k) = \sum_{i \in \mathcal{I}} l(s_i^k - t^k) \frac{l'(s_i^k - t^k)}{l(s_i^k - t^k)} \geq \sum_{i \in \mathcal{I}} l(s_i^k - t^k) \frac{l'(l^{-1}(n\tau))}{l(l^{-1}(n\tau))} = n\tau \frac{l'(l^{-1}(n\tau))}{l(l^{-1}(n\tau))} = l'(l^{-1}(n\tau)),$$

where the inequality follows from (B.24) and the following equality from (3.7). Due to (S2) we obtain that $l'(l^{-1}(n\tau))$ is a positive number, which finishes the proof of the first part. The second part can be obtained in an identical way. \blacksquare

Lemma B.10

Let l satisfy (S1)-(S4). Then there exists some \hat{B} such that for all k we have

$$\|\nabla L(w^k)\| \leq \|w^k\| + \hat{B}, \quad \|g(w^k)\| \leq \|w^k\| + \hat{B}.$$

Proof:

By applying norm to the gradient (3.5) of the objective function L , we get

$$\|\nabla L(w^k)\| \leq \|w^k\| + \left\| \frac{1}{n_+} \sum_{i \in \mathcal{I}_+} l'(t(w^k) - x_i^\top w^k)(\nabla t(w^k) - x_i) \right\|,$$

where the inequality follows from the triangle inequality. Due to (S4) the derivative l' is bounded by some \hat{C}_1 . Then Theorem 3.3 and Lemma B.9 imply

$$\|\nabla t(w^k)\| \leq \frac{\hat{C}_1 \sum_{i \in \mathcal{I}} \|x_i\|}{\sum_{i \in \mathcal{I}} l'(x_i^\top w^k - t(w^k))} \leq \frac{\hat{C}_1}{\hat{C}_2} \sum_{i \in \mathcal{I}} \|x_i\|,$$

which is independent of k . Then (3.5) and again the boundedness of l' imply the existence of some \hat{B} such that $\|\nabla L(w^k)\| \leq \|w^k\| + \hat{B}$ for all k . The proof for $g(w^k)$ can be performed identically. ■

Lemma B.11

Consider uniformly bounded positive sequences $c_1^k, c_2^k, d_1^k, d_2^k, \alpha^k$ and positive constants C_1, C_2 such that for all k we have

$$\|c_1^k - c_2^k\| \leq C_1 \alpha^k, \quad \|d_1^k - d_2^k\| \leq C_1 \alpha^k, \quad d_1^k \geq C_2, \quad d_2^k \geq C_2.$$

If $\alpha^k \rightarrow 0$, then there exists a constant C_3 such that for all sufficiently large k we have

$$\left\| \frac{c_1^k}{d_1^k} - \frac{c_2^k}{d_2^k} \right\| \leq C_3 \alpha^k.$$

Proof:

Since d_1^k and d_2^k are bounded away from zero and since $\alpha^k \rightarrow 0$, we have

$$\left\| \frac{c_1^k}{d_1^k} - \frac{c_2^k}{d_2^k} \right\| \leq \max \left\{ \frac{c_1^k}{d_1^k} - \frac{c_1^k + C_1 \alpha^k}{d_1^k - C_1 \alpha^k}, \frac{c_1^k}{d_1^k} - \frac{c_1^k - C_1 \alpha^k}{d_1^k + C_1 \alpha^k} \right\}.$$

The first term can be estimated as

$$\left\| \frac{c_1^k}{d_1^k} - \frac{c_1^k + C_1 \alpha^k}{d_1^k - C_1 \alpha^k} \right\| = \left\| \frac{(c_1^k + d_1^k) C_1 \alpha^k}{d_1^k (d_1^k - C_1 \alpha^k)} \right\| \leq \frac{(c_1^k + d_1^k) C_1 \alpha^k}{C_2 |d_1^k - C_1 \alpha^k|}.$$

Since $\alpha^k \rightarrow 0$ by assumption, for large k we have $\|d_1^k - C_1 \alpha^k\| \geq \frac{1}{2} C_2$. Since the sequences are uniformly bounded, the statement follows. ■

Lemma B.12

Consider scalars a_i, c_i and vectors b_i, d_i . If there is some \hat{C} such that $|a_i| \leq \hat{C}$ and $\|d_i\| \leq \hat{C}$, then

$$\left\| \sum_{i=1}^n a_i b_i - \sum_{i=1}^n c_i d_i \right\| \leq \hat{C} \sum_{i=1}^n (|a_i - c_i| + \|b_i - d_i\|).$$

Proof:

It is simple to verify

$$\left\| \sum_{i=1}^n a_i b_i - \sum_{i=1}^n c_i d_i \right\| \leq \sum_{i=1}^n \|d_i\| |a_i - c_i| + \sum_{i=1}^n |a_i| \|b_i - d_i\|,$$

from which the statement follows. ■

Appendix for Chapter 4

C.1 Derivation of Dual Problems

C.1.1 Family of *TopPushK* Formulations

Theorem 4.3: Dual formulation for *TopPushK* family

Consider Notation 4.2, surrogate function l , and formulation (4.4). Then the corresponding dual problem has the following form

$$\begin{aligned} \underset{\alpha, \beta}{\text{maximize}} \quad & -\frac{1}{2} \begin{pmatrix} \alpha \\ \beta \end{pmatrix}^\top \mathbb{K} \begin{pmatrix} \alpha \\ \beta \end{pmatrix} - C \sum_{i=1}^{n_+} l^* \left(\frac{\alpha_i}{C} \right) \end{aligned} \quad (4.5a)$$

$$\text{subject to} \quad \sum_{i=1}^{n_+} \alpha_i = \sum_{j=1}^{\tilde{n}} \beta_j, \quad (4.5b)$$

$$0 \leq \beta_j \leq \frac{1}{K} \sum_{i=1}^{n_+} \alpha_i, \quad j = 1, 2, \dots, \tilde{n}, \quad (4.5c)$$

where l^* is conjugate function of l and

	K	\mathbb{K}	\tilde{n}	$\tilde{\mathbf{x}}_j$
<i>TopPush</i>	1	\mathbb{K}^-	n_-	\mathbf{x}_j^-
<i>TopPushK</i>	K	\mathbb{K}^-	n_-	\mathbf{x}_j^-
<i>TopMeanK</i>	$n\tau$	\mathbb{K}^\pm	n	\mathbf{x}_j
τ -FPL	$n_- \tau$	\mathbb{K}^-	n_-	\mathbf{x}_j^-

If $K = 1$, the upper bound in the second constraint (4.5c) vanishes due to the first constraint. Finally, the primal variables w can be computed from dual variables as follows

$$w = \sum_{i=1}^{n_+} \alpha_i \mathbf{x}_i^+ - \sum_{j=1}^{\tilde{n}} \beta_j \tilde{\mathbf{x}}_j. \quad (4.6)$$

Proof:

We show the proof only for *TopPushK* formulation, i.e., the decision threshold is computed only from negative samples. The proof for the remaining formulations is identical. Firstly, we derive an alternative formulation to formulation (4.4). Using Lemma 1 from [75], we can rewrite the formula for the decision threshold to the following form

$$\sum_{j=1}^K s_{[j]}^- = \min_t \left\{ Kt + \sum_{j=1}^{n_-} \max\{0, s_j^- - t\} \right\}.$$

By substituting this formula into the objective function of (4.4), we get

$$\begin{aligned} \sum_{i=1}^{n_+} l \left(\frac{1}{K} \sum_{j=1}^K s_{[j]}^- - s_i^+ \right) &= \sum_{i=1}^{n_+} l \left(\frac{1}{K} \min_t \left\{ Kt + \sum_{j=1}^{n_-} \max\{0, s_j^- - t\} \right\} - s_i^+ \right) \\ &= \min_t \sum_{i=1}^{n_+} l \left(t + \frac{1}{K} \sum_{j=1}^{n_-} \max\{0, s_j^- - t\} - s_i^+ \right). \end{aligned}$$

where the last equality follows from the fact that the surrogate function l is non-decreasing. The max operator can be replaced using an auxiliary variable $\mathbf{z} \in \mathbb{R}^{n_-}$ that fulfills $z_j \geq s_j^- - t$ and $z_j \geq 0$ for all $j = 1, \dots, n_-$. Furthermore, we use auxiliary variable $\mathbf{y} \in \mathbb{R}^{n_+}$ defined for all $i = 1, \dots, n_+$ as

$$y_i = t + \frac{1}{K} \sum_{j=1}^{n_-} z_j - s_i^+.$$

The combination of all the above relations and the use of a linear model yields to

$$\begin{aligned} \underset{\mathbf{w}, t, \mathbf{y}, \mathbf{z}}{\text{minimize}} \quad & \frac{1}{2} \|\mathbf{w}\|_2^2 + C \sum_{i=1}^{n_+} l(y_i) \\ \text{subject to} \quad & y_i = t + \frac{1}{K} \sum_{j=1}^{n_-} z_j - \mathbf{w}^\top \mathbf{x}_i^+, \quad i = 1, 2, \dots, n_+, \\ & z_j \geq \mathbf{w}^\top \mathbf{x}_j^- - t, \quad j = 1, 2, \dots, n_-, \\ & z_j \geq 0, \quad j = 1, 2, \dots, n_-, \end{aligned}$$

The Lagrangian of this formulation is defined as

$$\begin{aligned} \mathcal{L}(\mathbf{w}, t, \mathbf{y}, \mathbf{z}; \alpha, \beta, \gamma) &= \frac{1}{2} \|\mathbf{w}\|_2^2 + C \sum_{i=1}^{n_+} l(y_i) + \sum_{i=1}^{n_+} \alpha_i \left(t + \frac{1}{K} \sum_{j=1}^{n_-} z_j - \mathbf{w}^\top \mathbf{x}_i^+ - y_i \right) \\ &\quad + \sum_{j=1}^{n_-} \beta_j (\mathbf{w}^\top \mathbf{x}_j^- - t - z_j) - \sum_{j=1}^{n_-} \gamma_j z_j, \end{aligned}$$

with feasibility conditions $\beta_j \geq 0$ and $\gamma_j \geq 0$ for all $j = 1, \dots, n_-$. Since the Lagrangian \mathcal{L} is separable in primal variables, it can be minimized with respect to each variable separately.

Then the dual objective function (to be maximized) reads

$$g(\alpha, \beta, \gamma) = \min_w \frac{1}{2} \|w\|_2^2 - w^\top \left(\sum_{i=1}^{n_+} \alpha_i x_i^+ - \sum_{j=1}^{n_-} \beta_j x_j^- \right) \quad (\text{C.1a})$$

$$+ \min_t t \left(\sum_{i=1}^{n_+} \alpha_i - \sum_{j=1}^{n_-} \beta_j \right) \quad (\text{C.1b})$$

$$+ \min_y C \sum_{i=1}^{n_+} \left(l(y_i) - \frac{\alpha_i}{C} y_i \right) \quad (\text{C.1c})$$

$$+ \min_z \sum_{j=1}^{n_-} \left(\frac{1}{K} \sum_{i=1}^{n_+} \alpha_i - \beta_j - \gamma_j \right) z_j \quad (\text{C.1d})$$

From optimality conditions with respect to w , we deduce

$$w = \sum_{i=1}^{n_+} \alpha_i x_i^+ - \sum_{j=1}^{n_-} \beta_j x_j^- = \begin{pmatrix} \mathbb{X}^+ \\ -\mathbb{X}^- \end{pmatrix}^\top \begin{pmatrix} \alpha \\ \beta \end{pmatrix} \Rightarrow \frac{1}{2} \|w\|_2^2 - w^\top \left(\sum_{i=1}^{n_+} \alpha_i x_i^+ - \sum_{j=1}^{n_-} \beta_j x_j^- \right) = -\frac{1}{2} \begin{pmatrix} \alpha \\ \beta \end{pmatrix}^\top \mathbb{K} \begin{pmatrix} \alpha \\ \beta \end{pmatrix},$$

where we use Notation 4.2. It mean, that we get the first part of the objective function (4.5a), and we also get the relation (4.6) between primal and dual variables.

Optimality condition with respect to t reads

$$\sum_{i=1}^{n_+} \alpha_i - \sum_{j=1}^{n_-} \beta_j = 0,$$

and implies constrain (4.5b).

Similarly, optimality condition of (C.1d) with respect to z reads for all $j = 1, \dots, n_-$ as

$$\frac{1}{K} \sum_{i=1}^{n_+} \alpha_i - \beta_j - \gamma_j = 0.$$

Plugging the feasibility condition $\gamma_j \geq 0$ into this equality and combining it with the feasibility conditions $\beta_j \geq 0$, yields constraint (4.5c).

Finally, the second part of the objective function (4.5a) follows from Definition 4.1 of the conjugate function. Using the definition, minimization of (C.1c) with respect to y yields

$$C \min_{y_i} \left(l(y_i) - \frac{\alpha_i}{C} y_i \right) = -C l^* \left(\frac{\alpha_i}{C} \right),$$

for all $i = 1, \dots, n_+$, which finishes the proof for *TopPushK*. For *TopPush*, we have $K = 1$. From (4.5b) and non-negativity of β_j we deduce that the upper bound in (4.5c) is always fulfilled and can be omitted. ■

C.1.2 Family of *Pat&Mat* Formulations

Theorem 4.4: Dual formulation for *Pat&Mat* family

Consider Notation 4.2, surrogate function l , and formulation (4.7). Then the corresponding dual problem has the following form

$$\underset{\alpha, \beta, \delta}{\text{maximize}} \quad -\frac{1}{2} \begin{pmatrix} \alpha \\ \beta \end{pmatrix}^\top \mathbb{K} \begin{pmatrix} \alpha \\ \beta \end{pmatrix} - C \sum_{i=1}^{n_+} l^\star\left(\frac{\alpha_i}{C}\right) - \delta \sum_{j=1}^{\tilde{n}} l^\star\left(\frac{\beta_j}{\delta \vartheta}\right) - \delta \tilde{n} \tau \quad (4.8a)$$

$$\text{subject to} \quad \sum_{i=1}^{n_+} \alpha_i = \sum_{j=1}^{\tilde{n}} \beta_j, \quad (4.8b)$$

$$\delta \geq 0, \quad (4.8c)$$

where l^\star is conjugate function of l , $\vartheta > 0$ is a scaling parameter and

	\mathbb{K}	\tilde{n}	$\tilde{\mathbf{x}}_j$
<i>Pat&Mat</i>	\mathbb{K}^\pm	n	\mathbf{x}_j
<i>Pat&Mat-NP</i>	\mathbb{K}^-	n_-	\mathbf{x}_j^-

Finally, the primal variables \mathbf{w} can be computed from dual variables as follows

$$\mathbf{w} = \sum_{i=1}^{n_+} \alpha_i \mathbf{x}_i^+ - \sum_{j=1}^{\tilde{n}} \beta_j \tilde{\mathbf{x}}_j. \quad (4.9)$$

Proof:

For simplicity, we show the proof only for *Pat&Mat-NP*, i.e. the threshold is computed only from negative samples. Let us first realize that formulation (4.7) is equivalent to the following formulation

$$\begin{aligned} \underset{\mathbf{w}, t, \mathbf{y}, \mathbf{z}}{\text{minimize}} \quad & \frac{1}{2} \|\mathbf{w}\|_2^2 + C \sum_{i=1}^{n_+} l(y_i) \\ \text{subject to} \quad & \sum_{j=1}^{n_-} l(\vartheta z_j) \leq n_- \tau, \\ & y_i = t - \mathbf{w}^\top \mathbf{x}_i^+, \quad i = 1, 2, \dots, n_+, \\ & z_j = \mathbf{w}^\top \mathbf{x}_j^- - t, \quad j = 1, 2, \dots, n_-. \end{aligned}$$

The corresponding Lagrangian then reads

$$\begin{aligned} \mathcal{L}(\mathbf{w}, t, \mathbf{y}, \mathbf{z}; \alpha, \beta, \delta) = & \frac{1}{2} \|\mathbf{w}\|_2^2 + C \sum_{i=1}^{n_+} l(y_i) + \sum_{i=1}^{n_+} \alpha_i (t - \mathbf{w}^\top \mathbf{x}_i^+ - y_i) \\ & + \sum_{j=1}^{n_-} \beta_j (\mathbf{w}^\top \mathbf{x}_j^- - t - z_j) + \delta \left(\sum_{j=1}^{n_-} l(\vartheta z_j) - n_- \tau \right). \end{aligned}$$

with feasibility condition $\delta \geq 0$. Since the Lagrangian \mathcal{L} is separable in primal variables, it can be minimized with respect to each variable separately. Then the dual objective function

(to be maximized) can be rewritten as follows

$$g(\alpha, \beta, \delta) = \min_w \frac{1}{2} \|w\|_2^2 - w^\top \left(\sum_{i=1}^{n_+} \alpha_i x_i^+ - \sum_{j=1}^{n_-} \beta_j x_j^- \right) \quad (\text{C.2a})$$

$$+ \min_t t \left(\sum_{i=1}^{n_+} \alpha_i - \sum_{j=1}^{n_-} \beta_j \right) \quad (\text{C.2b})$$

$$+ \min_y C \sum_{i=1}^{n_+} \left(l(y_i) - \frac{\alpha_i}{C} y_i \right) \quad (\text{C.2c})$$

$$+ \min_z \delta \sum_{j=1}^{n_-} \left(l(\vartheta z_j) - \frac{\beta_j}{\delta} z_j \right) \quad (\text{C.2d})$$

$$- \delta n_- \tau. \quad (\text{C.2e})$$

Note that the resulting dual function is very similar to one (C.1) for *TopPushK*. In fact, the first three parts of (C.1) and (C.2) are identical. Therefore, we only have to show how to minimize (C.2) with respect to z . For that, we can use the conjugate function as in the case of minimization of (C.1) with respect to y . Then, for all $j = 1, \dots, n_-$, we get

$$\delta \min_z \left(l(\vartheta z_j) - \frac{\beta_j}{\delta \vartheta} \vartheta z_j \right) = -\delta l^* \left(\frac{\beta_j}{\delta \vartheta} \right),$$

where the equality follows from Definition 4.1 of a conjugate function. Plugging this back into (C.2d) yields the third part of the objective function (4.8a), which finishes the proof. ■

C.2 Coordinate Descent Algorithm

C.2.1 Family of *TopPushK* Formulations

Hinge Loss

Proposition 4.7: Update rule (4.14a) for problem (4.16)

Consider problem (4.16), update rule (4.14a), indices $1 \leq k \leq n_+$ and $1 \leq l \leq n_+$ and Notation 4.6. Then the optimal solution Δ^* is given by (4.15) where

$$\begin{aligned} \Delta_{lb} &= \max\{-\alpha_{\hat{k}}, \alpha_{\hat{l}} - C\}, \\ \Delta_{ub} &= \min\{C - \alpha_{\hat{k}}, \alpha_{\hat{l}}\}, \\ \gamma &= -\frac{s_k - s_l}{\mathbb{K}_{kk} + \mathbb{K}_{ll} - \mathbb{K}_{kl} - \mathbb{K}_{lk}}. \end{aligned}$$

Proof of Proposition 4.7 on page 43:

Constraint (4.16b) is always satisfied from the definition of the update rule (4.14a), and constraint (4.16d) is always satisfied since no β_j was updated and the sum of all α_i did not change. Constraint (4.16c) reads

$$\begin{aligned} 0 \leq \alpha_{\hat{k}} + \Delta \leq C &\implies -\alpha_{\hat{k}} \leq \Delta \leq C - \alpha_{\hat{k}}, \\ 0 \leq \alpha_{\hat{l}} - \Delta \leq C &\implies \alpha_{\hat{l}} - C \leq \Delta \leq \alpha_{\hat{l}}, \end{aligned}$$

which gives the lower and upper bound of Δ .

Using the update rule (4.14a), objective function (4.16a) can be rewritten as a quadratic function with respect to Δ

$$-\frac{1}{2}[\mathbb{K}_{kk} + \mathbb{K}_{ll} - \mathbb{K}_{kl} - \mathbb{K}_{lk}]\Delta^2 - [s_k - s_l]\Delta - c(\alpha, \beta).$$

Finally, the optimal solution Δ^* is given by (4.15). ■

Proposition 4.8: Update rule (4.14b) for problem (4.16)

Consider problem (4.16), update rule (4.14b), indices $1 \leq k \leq n_+$ and $n_+ + 1 \leq l \leq \tilde{n}$ and Notation 4.6. Let us define

$$\beta_{\max} = \max_{j \in \{1, 2, \dots, \tilde{n}\} \setminus \{l\}} \beta_j.$$

Then the optimal solution Δ^* is given by (4.15) where

$$\begin{aligned} \Delta_{lb} &= \begin{cases} \max\{-\alpha_{\hat{k}}, -\beta_{\hat{l}}\} & K = 1, \\ \max\{-\alpha_{\hat{k}}, -\beta_{\hat{l}}, K\beta_{\max} - \sum_{i=1}^{n_+} \alpha_i\} & \text{otherwise,} \end{cases} \\ \Delta_{ub} &= \begin{cases} C - \alpha_{\hat{k}} & K = 1, \\ \min\left\{C - \alpha_{\hat{k}}, \frac{1}{K-1} \left(\sum_{i=1}^{n_+} \alpha_i - K\beta_{\hat{l}}\right)\right\} & \text{otherwise.} \end{cases} \\ \gamma &= -\frac{s_k + s_l - 1}{\mathbb{K}_{kk} + \mathbb{K}_{ll} + \mathbb{K}_{kl} + \mathbb{K}_{lk}}. \end{aligned}$$

Proof of Proposition 4.8 on page 44:

Constraint (4.16b) is always satisfied from the definition of the update rule (4.14b). Constraint (4.16c) reads $-\alpha_{\hat{k}} \leq \Delta \leq C - \alpha_{\hat{k}}$. Using the definition of β_{\max} , constraint (4.16d) for any $K \geq 2$ reads

$$\begin{aligned} 0 \leq \beta_{\max} \leq \frac{1}{K} \sum_{i=1}^{n_+} \alpha_i + \frac{\Delta}{K} &\implies K\beta_{\max} - \sum_{i=1}^{n_+} \alpha_i \leq \Delta, \\ 0 \leq \beta_{\hat{l}} + \Delta \leq \frac{1}{K} \sum_{i=1}^{n_+} \alpha_i + \frac{\Delta}{K} &\implies -\beta_{\hat{l}} \leq \Delta \quad \wedge \quad \Delta \leq \frac{1}{K-1} \left(\sum_{i=1}^{n_+} \alpha_i - K\beta_{\hat{l}} \right). \end{aligned}$$

The combination of these bounds yields the lower bound Δ_{lb} and upper bound Δ_{ub} . If $K = 1$, the upper bound in (4.16d) is always satisfied due to (4.16b) and the lower and upper bound of Δ can be simplified.

Using the update rule (4.14b), objective function (4.16a) can be rewritten as a quadratic function with respect to Δ

$$-\frac{1}{2}[\mathbb{K}_{kk} + \mathbb{K}_{ll} + \mathbb{K}_{kl} + \mathbb{K}_{lk}]\Delta^2 - [s_k + s_l - 1]\Delta - c(\alpha, \beta).$$

Finally, the optimal solution Δ^* is given by (4.15). ■

Proposition 4.9: Update rule (4.14c) for problem (4.16)

Consider problem (4.16), update rule (4.14c), indices $n_+ + 1 \leq k \leq \tilde{n}$ and $n_+ + 1 \leq l \leq \tilde{n}$ and Notation 4.6. Then the optimal solution Δ^* is given by (4.15) where

$$\begin{aligned}\Delta_{lb} &= \begin{cases} -\beta_{\hat{k}} & K = 1, \\ \max\{-\beta_{\hat{k}}, \beta_{\hat{l}} - \frac{1}{K} \sum_{i=1}^{n_+} \alpha_i\} & \text{otherwise,} \end{cases} \\ \Delta_{ub} &= \begin{cases} \beta_{\hat{l}} & K = 1, \\ \min\{\frac{1}{K} \sum_{i=1}^{n_+} \alpha_i - \beta_{\hat{k}}, \beta_{\hat{l}}\} & \text{otherwise.} \end{cases} \\ \gamma &= -\frac{s_k - s_l}{\mathbb{K}_{kk} + \mathbb{K}_{ll} - \mathbb{K}_{kl} - \mathbb{K}_{lk}}.\end{aligned}$$

Proof of Proposition 4.9 on page 44:

Constraint (4.16b) is always satisfied from the definition of the update rule (4.14c), and constraint (4.16c) is satisfied since no α_i is updated. Constraint (4.16d) for any $K \geq 2$ reads

$$\begin{aligned}0 \leq \beta_{\hat{k}} + \Delta \leq \frac{1}{K} \sum_{i=1}^{n_+} \alpha_i &\implies -\beta_{\hat{k}} \leq \Delta \leq \frac{1}{K} \sum_{i=1}^{n_+} \alpha_i - \beta_{\hat{k}}, \\ 0 \leq \beta_{\hat{l}} - \Delta \leq \frac{1}{K} \sum_{i=1}^{n_+} \alpha_i &\implies \beta_{\hat{l}} - \frac{1}{K} \sum_{i=1}^{n_+} \alpha_i \leq \Delta \leq \beta_{\hat{l}},\end{aligned}$$

which gives the lower and upper bound of Δ . If $K = 1$, the upper bound in (4.16d) is always satisfied due to (4.16b) and the lower and upper bound of Δ can be simplified.

Using the update rule (4.14c), objective function (4.16a) can be rewritten as a quadratic function with respect to Δ

$$-\frac{1}{2}[\mathbb{K}_{kk} + \mathbb{K}_{ll} - \mathbb{K}_{kl} - \mathbb{K}_{lk}]\Delta^2 - [s_k - s_l]\Delta - c(\alpha, \beta).$$

Finally, the optimal solution Δ^* is given by (4.15). ■

Quadratic Hinge Loss

The second considered surrogate function is the quadratic hinge loss from Notation 2.1. Plugging the conjugate (4.2) of the quadratic hinge loss into the dual formulation (4.5) yields

$$\underset{\alpha, \beta}{\text{maximize}} \quad -\frac{1}{2} \begin{pmatrix} \alpha \\ \beta \end{pmatrix}^\top \mathbb{K} \begin{pmatrix} \alpha \\ \beta \end{pmatrix} + \sum_{i=1}^{n_+} \alpha_i - \frac{1}{4C} \sum_{i=1}^{n_+} \alpha_i^2 \quad (\text{C.3a})$$

$$\text{subject to} \quad \sum_{i=1}^{n_+} \alpha_i = \sum_{j=1}^{\tilde{n}} \beta_j, \quad (\text{C.3b})$$

$$0 \leq \alpha_i, \quad i = 1, 2, \dots, n_+, \quad (\text{C.3c})$$

$$0 \leq \beta_j \leq \frac{1}{K} \sum_{i=1}^{n_+} \alpha_i, \quad j = 1, 2, \dots, \tilde{n}, \quad (\text{C.3d})$$

Similarly to the previous case, the form of \mathbb{K} and \tilde{n} depends on the used formulation and the upper bound in (C.3d) can be omitted for $K = 1$.

Proposition C.6: Update rule (4.14a) for problem (C.3)

Consider problem (C.3), update rule (4.14a), indices $1 \leq k \leq n_+$ and $1 \leq l \leq n_+$ and Notation 4.6. Then the optimal solution Δ^* is given by (4.15) where

$$\Delta_{lb} = -\alpha_{\hat{k}}, \quad \Delta_{ub} = \alpha_{\hat{l}}, \quad \gamma = -\frac{s_k - s_l + \frac{1}{2C}(\alpha_{\hat{k}} - \alpha_{\hat{l}})}{\mathbb{K}_{kk} + \mathbb{K}_{ll} - \mathbb{K}_{kl} - \mathbb{K}_{lk} + \frac{1}{C}}.$$

Proof:

Constraint (C.3b) is always satisfied from the definition of the update rule (4.14a). Constraint (C.3d) is also always satisfied since no β_j was updated and the sum of all α_i did not change. Constraint (C.3c) reads

$$\begin{aligned} 0 \leq \alpha_{\hat{k}} + \Delta &\implies -\alpha_{\hat{k}} \leq \Delta, \\ 0 \leq \alpha_{\hat{l}} - \Delta &\implies \Delta \leq \alpha_{\hat{l}}, \end{aligned}$$

which gives the lower and upper bound of Δ .

Using the update rule (4.14a), objective function (C.3a) can be rewritten as a quadratic function with respect to Δ

$$-\frac{1}{2} \left[\mathbb{K}_{kk} + \mathbb{K}_{ll} - \mathbb{K}_{kl} - \mathbb{K}_{lk} + \frac{1}{C} \right] \Delta^2 - \left[s_k - s_l + \frac{1}{2C}(\alpha_{\hat{k}} - \alpha_{\hat{l}}) \right] \Delta - c(\alpha, \beta).$$

Finally, the optimal solution Δ^* is given by (4.15). ■

Proposition C.7: Update rule (4.14b) for problem (C.3)

Consider problem (C.3), update rule (4.14b), indices $1 \leq k \leq n_+$ and $n_+ + 1 \leq l \leq \tilde{n}$ and Notation 4.6. Let us define

$$\beta_{\max} = \max_{j \in \{1, 2, \dots, \tilde{n}\} \setminus \{\hat{l}\}} \beta_j.$$

Then the optimal solution Δ^* is given by (4.15) where

$$\begin{aligned} \Delta_{lb} &= \begin{cases} \max\{-\alpha_{\hat{k}}, -\beta_{\hat{l}}\} & K = 1, \\ \max\{-\alpha_{\hat{k}}, -\beta_{\hat{l}}, K\beta_{\max} - \sum_{i=1}^{n_+} \alpha_i\} & \text{otherwise,} \end{cases} \\ \Delta_{ub} &= \begin{cases} +\infty & K = 1, \\ \frac{1}{K-1} \left(\sum_{i=1}^{n_+} \alpha_i - K\beta_{\hat{l}} \right) & \text{otherwise,} \end{cases} \\ \gamma &= -\frac{s_k + s_l - 1 + \frac{1}{2C}\alpha_{\hat{k}}}{\mathbb{K}_{kk} + \mathbb{K}_{ll} + \mathbb{K}_{kl} + \mathbb{K}_{lk} + \frac{1}{2C}}. \end{aligned}$$

Proof:

Constraint (C.3b) is always satisfied from the definition of the update rule (4.14b). Constraint (C.3c) reads $-\alpha_{\hat{k}} \leq \Delta$. Using the definition of β_{\max} , constraint (C.3d) for any $K \geq 2$ reads

$$\begin{aligned} 0 \leq \beta_{\max} \leq \frac{1}{K} \sum_{i=1}^{n_+} \alpha_i + \frac{\Delta}{K} &\implies K\beta_{\max} - \sum_{i=1}^{n_+} \alpha_i \leq \Delta, \\ 0 \leq \beta_{\hat{l}} + \Delta \leq \frac{1}{K} \sum_{i=1}^{n_+} \alpha_i + \frac{\Delta}{K} &\implies -\beta_{\hat{l}} \leq \Delta \quad \wedge \quad \Delta \leq \frac{1}{K-1} \left(\sum_{i=1}^{n_+} \alpha_i - K\beta_{\hat{l}} \right). \end{aligned}$$

The combination of these bounds yields the lower bound Δ_{lb} and upper bound Δ_{ub} . If $K = 1$, the upper bound in (C.3d) is always satisfied due to (C.3b) and the lower and upper bound of Δ can be simplified.

Using the update rule (4.14b), objective function (C.3a) can be rewritten as a quadratic function with respect to Δ

$$-\frac{1}{2} \left[\mathbb{K}_{kk} + \mathbb{K}_{ll} + \mathbb{K}_{kl} + \mathbb{K}_{lk} + \frac{1}{2C} \right] \Delta^2 - \left[s_k + s_l - 1 + \frac{1}{2C} \alpha_{\hat{k}} \right] \Delta - c(\alpha, \beta).$$

Finally, the optimal solution Δ^* is given by (4.15). ■

Proposition C.8: Update rule (4.14c) for problem (C.3)

Consider problem (C.3), update rule (4.14c), indices $n_+ + 1 \leq k \leq \tilde{n}$ and $n_+ + 1 \leq l \leq \tilde{n}$ and Notation 4.6. Then the optimal solution Δ^* is given by (4.15) where

$$\begin{aligned} \Delta_{lb} &= \begin{cases} -\beta_{\hat{k}} & K = 1, \\ \max\left\{-\beta_{\hat{k}}, \beta_{\hat{l}} - \frac{1}{K} \sum_{i=1}^{n_+} \alpha_i\right\} & \text{otherwise,} \end{cases} \\ \Delta_{ub} &= \begin{cases} \beta_{\hat{l}} & K = 1, \\ \min\left\{\beta_{\hat{l}}, \frac{1}{K} \sum_{i=1}^{n_+} \alpha_i - \beta_{\hat{k}}\right\} & \text{otherwise,} \end{cases} \\ \gamma &= -\frac{s_k - s_l}{\mathbb{K}_{kk} + \mathbb{K}_{ll} - \mathbb{K}_{kl} - \mathbb{K}_{lk}}. \end{aligned}$$

Proof:

Constraint (C.3b) is always satisfied from the definition of the update rule (4.14c). Constraint (C.3c) is also always satisfied since no α_i is updated. Constraint (C.3d) for any $K \geq 2$ reads

$$\begin{aligned} 0 \leq \beta_{\hat{k}} + \Delta \leq \frac{1}{K} \sum_{i=1}^{n_+} \alpha_i &\implies -\beta_{\hat{k}} \leq \Delta \leq \frac{1}{K} \sum_{i=1}^{n_+} \alpha_i - \beta_{\hat{k}}, \\ 0 \leq \beta_{\hat{l}} - \Delta \leq \frac{1}{K} \sum_{i=1}^{n_+} \alpha_i &\implies \beta_{\hat{l}} - \frac{1}{K} \sum_{i=1}^{n_+} \alpha_i \leq \Delta \leq \beta_{\hat{l}}, \end{aligned}$$

which gives the lower and upper bound of Δ . If $K = 1$, the upper bound in (C.3d) is always satisfied due to (C.3b) and the lower and upper bound of Δ can be simplified.

Using the update rule (4.14c), objective function (C.3a) can be rewritten as a quadratic function with respect to Δ

$$-\frac{1}{2} [\mathbb{K}_{kk} + \mathbb{K}_{ll} - \mathbb{K}_{kl} - \mathbb{K}_{lk}] \Delta^2 - [s_k - s_l] \Delta - c(\alpha, \beta).$$

Finally, the optimal solution Δ^* is given by (4.15). ■

Initialization

Theorem 4.10

Consider problem (4.17), some initial solution α^0, β^0 and denote the sorted version (in non-decreasing order) of β^0 as $\beta_{[\cdot]}^0$. Then if the following condition holds

$$\sum_{j=1}^K \left(\beta_{[\tilde{n}-K+j]}^0 + \max_{i=1, \dots, n_+} \alpha_i^0 \right) \leq 0, \quad (4.18)$$

the optimal solution of (4.17) amounts to $\alpha = \beta = \mathbf{0}$. In the opposite case, the following system of two equations

$$\sum_{i=1}^{n_+} \text{clip}_{[0, C]} \left(\alpha_i^0 - \lambda + \frac{1}{K} \sum_{j=1}^{\tilde{n}} \text{clip}_{[0, +\infty)} (\beta_j^0 + \lambda - \mu) \right) - K\mu = 0, \quad (4.19a)$$

$$\sum_{j=1}^{\tilde{n}} \text{clip}_{[0, \mu]} (\beta_j^0 + \lambda) - K\mu = 0, \quad (4.19b)$$

has a solution (λ, μ) with $\mu > 0$, and the optimal solution of (4.17) is equal to

$$\begin{aligned} \alpha_i &= \text{clip}_{[0, C]} \left(\alpha_i^0 - \lambda + \frac{1}{K} \sum_{j=1}^{\tilde{n}} \text{clip}_{[0, +\infty)} (\beta_j^0 + \lambda - \mu) \right), \\ \beta_j &= \text{clip}_{[0, \mu]} (\beta_j^0 + \lambda). \end{aligned}$$

Proof of Theorem 4.10 on page 45:

The Lagrangian of (4.17) reads

$$\begin{aligned} \mathcal{L}(\alpha, \beta; \lambda, p, q, u, v) &= \frac{1}{2} \|\alpha - \alpha^0\|^2 + \frac{1}{2} \|\beta - \beta^0\|^2 + \lambda \left(\sum_{i=1}^{n_+} \alpha_i - \sum_{j=1}^{\tilde{n}} \beta_j \right) \\ &\quad - \sum_{i=1}^{n_+} p_i \alpha_i + \sum_{i=1}^{n_+} q_i (\alpha_i - C_1) - \sum_{j=1}^{\tilde{n}} u_j \beta_j + \sum_{j=1}^{\tilde{n}} v_j \left(\beta_j - \frac{1}{K} \sum_{i=1}^{n_+} \alpha_i \right). \end{aligned}$$

The KKT conditions then amount to

$$\frac{\partial \mathcal{L}}{\partial \alpha_i} = \alpha_i - \alpha_i^0 + \lambda - p_i + q_i - \frac{1}{K} \sum_{j=1}^{\tilde{n}} v_j = 0, \quad i = 1, 2, \dots, n_+, \quad (C.4a)$$

$$\frac{\partial \mathcal{L}}{\partial \beta_j} = \beta_j - \beta_j^0 - \lambda - u_j + v_j = 0, \quad j = 1, 2, \dots, \tilde{n}, \quad (C.4b)$$

the primal feasibility conditions (4.17), the dual feasibility conditions $\lambda \in \mathbb{R}, p_i \geq 0, q_i \geq 0$,

$u_j \geq 0, v_j \geq 0$ and finally the complementarity conditions

$$p_i \alpha_i = 0, \quad i = 1, 2, \dots, n_+, \quad (\text{C.4c})$$

$$q_i(\alpha_i - C_1) = 0, \quad i = 1, 2, \dots, n_+, \quad (\text{C.4d})$$

$$u_j \beta_j = 0, \quad j = 1, 2, \dots, \tilde{n}, \quad (\text{C.4e})$$

$$v_j \left(\beta_j - \frac{1}{K} \sum_{i=1}^{n_+} \alpha_i \right) = 0, \quad j = 1, 2, \dots, \tilde{n}. \quad (\text{C.4f})$$

Case 1: The first case concerns when the optimal solution satisfies $\sum_i \alpha_i = 0$. From the primal feasibility conditions, we immediately get $\alpha_i = 0$ for all i and $\beta_j = 0$ for all j . Then (C.4d) implies $q_i = 0$ for all i and all complementarity conditions are satisfied. Moreover, optimality condition (C.4a) implies

$$\lambda = \alpha_i^0 + p_i + \frac{1}{K} \sum_{j=1}^{\tilde{n}} v_j.$$

Since the only condition on p_i is the non-negativity, this implies

$$\lambda \geq \max_{i=1, \dots, n_+} \alpha_i^0 + \frac{1}{K} \sum_{j=1}^{\tilde{n}} v_j.$$

Similarly, from optimality condition (C.4b) we deduce

$$v_j = \beta_j^0 + \lambda + u_j \geq \beta_j^0 + \lambda \geq \beta_j^0 + \max_{i=1, \dots, n_+} \alpha_i^0 + \frac{1}{K} \sum_{i=1}^{\tilde{n}} v_i.$$

Since we need to fulfill $v_j \geq 0$, this amounts to

$$v_j \geq \text{clip}_{[0, +\infty)} \left(\beta_j^0 + \max_{i=1, \dots, n_+} \alpha_i^0 + \frac{1}{K} \sum_{i=1}^{\tilde{n}} v_i \right).$$

Summing this with respect to j and using the substitution $\bar{v} = \frac{1}{K} \sum_i v_i$ results in

$$K \bar{v} - \sum_{j=1}^{\tilde{n}} \text{clip}_{[0, +\infty)} \left(\beta_j^0 + \max_{i=1, \dots, n_+} \alpha_i^0 + \bar{v} \right) \geq 0. \quad (\text{C.5})$$

Denote by $\beta_{[j]}^0$ the sorted version of β_j^0 . Then the function on the left-hand side of (C.5) as a function of \bar{v} is increasing on $(-\infty, -\beta_{[n_+-K+1]}^0 - \max_i \alpha_i^0]$ and non-increasing otherwise. Thus, (C.5) can be satisfied if and only if its function value at $-\beta_{[n_+-K+1]}^0 - \max_i \alpha_i^0$ is non-negative

$$\begin{aligned} & K \left(-\beta_{[n_+-K+1]}^0 - \max_{i=1, \dots, n_+} \alpha_i^0 \right) - \sum_{j=1}^{\tilde{n}} \text{clip}_{[0, +\infty)} \left(\beta_j^0 + \max_{i=1, \dots, n_+} \alpha_i^0 - \beta_{[n_+-K+1]}^0 - \max_{i=1, \dots, n_+} \alpha_i^0 \right) \\ &= K \left(-\beta_{[n_+-K+1]}^0 - \max_{i=1, \dots, n_+} \alpha_i^0 \right) - \sum_{j=1}^K \left(\beta_{[n_+-K+j]}^0 - \beta_{[n_+-K+1]}^0 \right) = - \sum_{j=1}^K \left(\beta_{[n_+-K+j]}^0 + \max_{i=1, \dots, n_+} \alpha_i^0 \right) \geq 0, \end{aligned}$$

which is precisely condition (4.18).

Case 2: If (4.18) holds true, then from the discussion above we obtain that the optimal solution satisfies $\sum_i \alpha_i > 0$. For simplicity, we define

$$\bar{\alpha} = \frac{1}{K} \sum_{i=1}^{n_+} \alpha_i, \quad \bar{\beta} = \frac{1}{K} \sum_{j=1}^{\tilde{n}} \beta_j, \quad \bar{v} = \frac{1}{K} \sum_{j=1}^{\tilde{n}} v_j.$$

For any fixed i , the standard trick is to combine the optimality condition (C.4a) with the primal feasibility condition $0 \leq \alpha_i \leq C_1$, the dual feasibility conditions $p_i \geq 0$, $q_i \geq 0$ and the complementarity conditions (C.4c, C.4d) to obtain

$$\alpha_i = \text{clip}_{[0, C_1]}(\alpha_i^0 - \lambda + \bar{v}). \quad (\text{C.6})$$

Similarly for any fixed j , we combine the optimality condition (C.4b) with the primal feasibility condition $0 \leq \beta_j \leq \bar{\alpha}$, the dual feasibility conditions $u_j \geq 0$, $v_j \geq 0$ and the complementarity conditions (C.4e, C.4f) to obtain

$$\beta_j = \text{clip}_{[0, \bar{\alpha}]}(\beta_j^0 + \lambda), \quad (\text{C.7})$$

$$v_j = \text{clip}_{[0, +\infty)}(\beta_j^0 + \lambda - \bar{\alpha}). \quad (\text{C.8})$$

Summing equations (C.6), (C.7) and (C.8) respectively with respect to i and j results in

$$K\bar{\alpha} = \sum_{i=1}^{n_+} \text{clip}_{[0, C_1]}(\alpha_i^0 - \lambda + \bar{v}), \quad (\text{C.9a})$$

$$K\bar{\beta} = \sum_{j=1}^{\tilde{n}} \text{clip}_{[0, \bar{\alpha}]}(\beta_j^0 + \lambda), \quad (\text{C.9b})$$

$$K\bar{v} = \sum_{j=1}^{\tilde{n}} \text{clip}_{[0, +\infty)}(\beta_j^0 + \lambda - \bar{\alpha}). \quad (\text{C.9c})$$

We denote $\mu = \bar{\alpha}$. Then (4.19a) results by plugging (C.9c) into (C.9a) while (4.19b) follows from (C.9b) and $\sum_i \alpha_i = \sum_j \beta_j$. ■

Lemma 4.11

Even though $\lambda(\mu)$ is not unique, function h from (4.20) is well-defined in the sense that it gives the same value for every choice of $\lambda(\mu)$. Moreover, h is decreasing in μ on $(0, +\infty)$.

Proof of Lemma 4.11 on page 46:

Recall that based on (4.19b) we defined

$$g(\lambda; \mu) := \sum_{j=1}^{\tilde{n}} \text{clip}_{[0, \mu]}(\beta_j^0 + \lambda) - K\mu,$$

and solutions of $g(\lambda; \mu) = 0$ for a fixed μ are denoted by $\lambda(\mu)$.

Let us first consider the case, when the solution to $g(\lambda) = 0$ is not unique. Since function $g(\cdot; \mu)$ is non-decreasing and K is an integer, it can happen only if the solution $\lambda(\mu)$ satisfies

$$\beta_{[j]}^0 + \lambda(\mu) \begin{cases} \geq \mu & \text{for } j = \tilde{n} - K + 1, \dots, \tilde{n}, \\ \leq 0 & \text{otherwise.} \end{cases}$$

Here, we again denote $\beta_{[\cdot]}^0$ to be the sorted version of β_j^0 . Then h defined in (4.20) equals to

$$\begin{aligned} h(\mu) &= \sum_{i=1}^{n_+} \text{clip}_{[0, C_1]} \left(\alpha_i^0 - \lambda(\mu) + \frac{1}{K} \sum_{j=\tilde{n}-K+1}^{\tilde{n}} (\beta_j^0 + \lambda(\mu) - \mu) \right) - K\mu \\ &= \sum_{i=1}^{n_+} \text{clip}_{[0, C_1]} \left(\alpha_i^0 - \mu + \frac{1}{K} \sum_{j=\tilde{n}-K+1}^{\tilde{n}} \beta_j^0 \right) - K\mu. \end{aligned}$$

This implies the first statement of the lemma that h is independent of the choice of $\lambda(\mu)$.

In the previous paragraph, we prove, that h gives the same value for every choice of $\lambda(\mu)$. Now we need to show that h is a decreasing function for the arbitrary choice of $\lambda(\mu)$. Fix any $\mu_2 > \mu_1 > 0$. From (4.19b) we have

$$\sum_{j=1}^{\tilde{n}} \text{clip}_{[0, \mu_1]} (\beta_j^0 + \lambda(\mu_1)) - K\mu_1 = 0, \quad (\text{C.10})$$

$$\sum_{j=1}^{\tilde{n}} \text{clip}_{[0, \mu_2]} (\beta_j^0 + \lambda(\mu_2)) - K\mu_2 = 0. \quad (\text{C.11})$$

Equation (C.10) implies that at most K values of $\beta_j^0 + \lambda(\mu_1)$ are greater or equal than μ_1 . If we increase the upper bound in the projection, at most K values can increase, which results in

$$\sum_{j=1}^{\tilde{n}} \text{clip}_{[0, \mu_2]} (\beta_j^0 + \lambda(\mu_1)) \leq \sum_{j=1}^{\tilde{n}} \text{clip}_{[0, \mu_1]} (\beta_j^0 + \lambda(\mu_1)) + K(\mu_2 - \mu_1) = K\mu_2, \quad (\text{C.12})$$

where the equality follows from (C.10). Comparing (C.11) and (C.12) yields $\lambda(\mu_2) \geq \lambda(\mu_1)$.

Now define

$$J = \{j \mid \beta_j^0 + \lambda(\mu_1) \geq 0\}$$

and observe that due to (C.10) we have $|J| \geq K$. Moreover, the definition of J and (C.10) yields

$$\sum_{j \in J} \text{clip}_{[0, \mu_1]} (\beta_j^0 + \lambda(\mu_1)) - K\mu_1 = \sum_{j=1}^{\tilde{n}} \text{clip}_{[0, \mu_1]} (\beta_j^0 + \lambda(\mu_1)) - K\mu_1 = 0. \quad (\text{C.13})$$

Then we have

$$\begin{aligned} \sum_{j=1}^{\tilde{n}} \text{clip}_{[0, \mu_2]} (\beta_j^0 + \lambda(\mu_1) + \mu_2 - \mu_1) &\geq \sum_{j \in J} \text{clip}_{[0, \mu_2]} (\beta_j^0 + \lambda(\mu_1) + \mu_2 - \mu_1) \\ &= \sum_{j \in J} \text{clip}_{[\mu_2 - \mu_1, \mu_2]} (\beta_j^0 + \lambda(\mu_1) + \mu_2 - \mu_1) \\ &= \sum_{j \in J} \text{clip}_{[0, \mu_1]} (\beta_j^0 + \lambda(\mu_1)) + |J|(\mu_2 - \mu_1) \\ &= K\mu_1 + |J|(\mu_2 - \mu_1) \geq K\mu_1 + K(\mu_2 - \mu_1) = K\mu_2, \end{aligned}$$

where the first equality follows from the definition of J and the second equality is a shift by a $\mu_2 - \mu_1$. The third equality follows from (C.13) and finally, the last inequality follows from $|J| \geq K$. The chain above together with (C.11) implies $\lambda(\mu_2) - \mu_2 \leq \lambda(\mu_1) - \mu_1$. Combining this with $\mu_2 > \mu_1$ and $\lambda(\mu_2) \geq \lambda(\mu_1)$, this implies that h from (4.20) is non-increasing which is precisely the lemma statement. ■

C.2.2 Family of *Pat&Mat* Formulations

In this section, we derive a coordinate descent algorithm for solving dual formulation (4.8) for the family of *Pat&Mat* formulations. We follow the same approach as for *TopPushK* family in Section 4.3.1, i.e. we use update rules (4.14). In this case, we must also consider the third primary variable δ . Then the dual formulation (4.8) can be rewritten as a one-dimensional quadratic problem

$$\begin{aligned} & \underset{\Delta}{\text{maximize}} && -\frac{1}{2}a(\alpha, \beta, \delta)\Delta^2 - b(\alpha, \beta, \delta)\Delta - c(\alpha, \beta, \delta) \\ & \text{subject to} && \Delta_{lb}(\alpha, \beta, \delta) \leq \Delta \leq \Delta_{ub}(\alpha, \beta, \delta) \end{aligned}$$

where $a, b, c, \Delta_{lb}, \Delta_{ub}$ are constants with respect to Δ . The form of the optimal solution is the same as for problem (4.5) and reads

$$\Delta^* = \text{clip}_{[\Delta_{lb}, \Delta_{ub}]}(\gamma).$$

Since we assume one of the update rule (4.14), the constrain (4.8b) is always satisfied after the update. The exact form of the update rules depends on the surrogate function. Moreover, the form of optimal δ also depends on the surrogate function. The upcoming text follows the same order as in the previous section. Therefore, we introduce concrete forms of update rules for hinge and quadratic hinge loss function and then show how to find an initial feasible solution.

Hinge Loss

We again start with the hinge loss function from Notation 2.1. Plugging the conjugate (4.2) of the hinge loss into the dual formulation (4.8) yields

$$\underset{\alpha, \beta, \delta}{\text{maximize}} \quad -\frac{1}{2} \begin{pmatrix} \alpha \\ \beta \end{pmatrix}^\top \mathbb{K} \begin{pmatrix} \alpha \\ \beta \end{pmatrix} + \sum_{i=1}^{n_+} \alpha_i + \frac{1}{\vartheta} \sum_{j=1}^{\tilde{n}} \beta_j - \delta \tilde{n} \tau \quad (\text{C.14a})$$

$$\text{subject to} \quad \sum_{i=1}^{n_+} \alpha_i = \sum_{j=1}^{\tilde{n}} \beta_j, \quad (\text{C.14b})$$

$$0 \leq \alpha_i \leq C, \quad i = 1, 2, \dots, n_+, \quad (\text{C.14c})$$

$$0 \leq \beta_j \leq \delta \vartheta, \quad j = 1, 2, \dots, \tilde{n}, \quad (\text{C.14d})$$

$$\delta \geq 0. \quad (\text{C.14e})$$

Since we know the form of the optimal solution (4.15), we only need to show how to compute Δ_{lb}, Δ_{ub} and γ for all update rules (4.14). However, in this case, constants Δ_{lb}, Δ_{ub} and γ also depend on the third dual variable δ . We do not perform a joint maximization in $(\alpha_k, \beta_l, \delta)$ but perform a maximization with respect to (α_k, β_l) , update these two values and then optimize the objective with respect to δ . Then for fixed feasible solution α and β , maximizing objective function (C.14a) with respect to δ yields

$$\begin{aligned} & \underset{\delta}{\text{maximize}} && -\tilde{n} \tau \delta \\ & \text{subject to} && 0 \leq \beta_j \leq \delta \vartheta, \quad j = 1, 2, \dots, \tilde{n}, \\ & && \delta \geq 0. \end{aligned}$$

Since $\tilde{n} \tau \geq 0$, we have to find the smallest possible δ that satisfies constraints above. Such δ is in the following form

$$\delta^* = \frac{1}{\vartheta} \max_{j \in \{1, 2, \dots, \tilde{n}\}} \beta_j. \quad (\text{C.15})$$

The following three propositions provide closed-form formulae for all three update rules.

Proposition C.11: Update rule (4.14a) for problem (C.14)

Consider problem (C.14), update rule (4.14a), indices $1 \leq k \leq n_+$ and $1 \leq l \leq n_+$ and Notation 4.6. Then the optimal solution Δ^* is given by (4.15) where

$$\begin{aligned}\Delta_{lb} &= \min\{-\alpha_{\hat{k}}, \alpha_{\hat{l}} - C\}, & \Delta_{ub} &= \max\{C - \alpha_{\hat{k}}, \alpha_{\hat{l}}\}, \\ \gamma &= -\frac{s_k - s_l}{\mathbb{K}_{kk} + \mathbb{K}_{ll} - \mathbb{K}_{kl} - \mathbb{K}_{lk}}, & \delta^* &= \delta.\end{aligned}$$

Proof:

Constraint (C.14b) is always satisfied from the definition of the update rule (4.14a). Constraint (C.14d) is also always satisfied since no β_j was updated and the sum of all α_i did not change. Constraint (C.14c) reads

$$\begin{aligned}0 \leq \alpha_{\hat{k}} + \Delta \leq C &\implies -\alpha_{\hat{k}} \leq \Delta \leq C - \alpha_{\hat{k}} \\ 0 \leq \alpha_{\hat{l}} - \Delta \leq C &\implies \alpha_{\hat{l}} - C \leq \Delta \leq \alpha_{\hat{l}}\end{aligned}$$

which gives the lower and upper bound of Δ .

Using the update rule (4.14a), objective function (C.14a) can be rewritten as a quadratic function with respect to Δ

$$-\frac{1}{2}[\mathbb{K}_{kk} + \mathbb{K}_{ll} - \mathbb{K}_{kl} - \mathbb{K}_{lk}]\Delta^2 - [s_k - s_l]\Delta - c(\alpha, \beta).$$

The optimal solution Δ^* is given by (4.15). Finally, since optimal δ is given by (C.15) and no β_j was updated, the optimal δ does not change. ■

Proposition C.12: Update rule (4.14b) for problem (C.14)

Consider problem (C.14), update rule (4.14b), indices $1 \leq k \leq n_+$ and $n_+ + 1 \leq l \leq \tilde{n}$ and Notation 4.6. Let us define

$$\beta_{\max} = \max_{j \in \{1, 2, \dots, \tilde{n}\} \setminus \{\hat{l}\}} \beta_j.$$

Then the bounds from (4.15) are defined as $\Delta_{lb} = \max\{-\alpha_{\hat{k}}, -\beta_{\hat{l}}\}$ and $\Delta_{ub} = C - \alpha_{\hat{k}}$ and there are two possible solutions

1. Δ_1^* is feasible if $\beta_{\hat{l}} + \Delta_1^* \leq \beta_{\max}$ and is given by (4.15) where

$$\gamma = -\frac{s_k + s_l - 1 - \frac{1}{\vartheta}}{\mathbb{K}_{kk} + \mathbb{K}_{ll} + \mathbb{K}_{kl} + \mathbb{K}_{lk}}, \quad \delta_1^* = \frac{\beta_{\max}}{\vartheta}.$$

2. Δ_2^* is feasible if $\beta_{\hat{l}} + \Delta_2^* \geq \beta_{\max}$ and is given by (4.15) where

$$\gamma = -\frac{s_k + s_l - 1 - \frac{1 - \tilde{n}\tau}{\vartheta}}{\mathbb{K}_{kk} + \mathbb{K}_{ll} + \mathbb{K}_{kl} + \mathbb{K}_{lk}}, \quad \delta_2^* = \frac{\beta_{\hat{l}} + \Delta_2^*}{\vartheta}.$$

The optimal solution Δ^* is equal to one of them, which maximizes the original objective and is feasible.

Proof:

Constraint (C.14b) is always satisfied from the definition of the update rule (4.14b). Constraint (C.14c) reads $-\alpha_{\hat{k}} \leq \Delta \leq C - \alpha_{\hat{k}}$. Using the definition of β_{\max} , constraint (C.14d)

reads $\beta_{\max} \leq \delta\vartheta$ and $0 \leq \beta_{\hat{l}} + \Delta \leq \delta\vartheta$. Since the optimal δ is given by (C.15), there are only two possible choices: $\delta_1^* = \frac{\beta_{\max}}{\vartheta}$ and $\delta_2^* = \frac{\beta_{\hat{l}} + \Delta}{\vartheta}$. If δ is feasible, all upper bounds in constraint (C.14d) hold. Therefore, we can simplify the constraints to $-\beta_{\hat{l}} \leq \Delta$, which in combination with bounds for $\alpha_{\hat{k}}$ gives the lower and upper bound of Δ . Now let us discuss how to select optimal δ :

1. Using δ_1^* and the update rule (4.14b), objective function (C.14a) can be rewritten as a quadratic function with respect to Δ as

$$-\frac{1}{2}[\mathbb{K}_{kk} + \mathbb{K}_{ll} + \mathbb{K}_{kl} + \mathbb{K}_{lk}]\Delta^2 - \left[s_k + s_l - 1 - \frac{1}{\vartheta}\right]\Delta - c(\alpha, \beta).$$

The optimal solution Δ_1^* is given by (4.15) and is feasible if $\beta_{\hat{l}} + \Delta_1^* \leq \beta_{\max}$.

2. Using δ_2^* and the update rule (4.14b), objective function (C.14a) can be rewritten as a quadratic function with respect to Δ as

$$-\frac{1}{2}[\mathbb{K}_{kk} + \mathbb{K}_{ll} + \mathbb{K}_{kl} + \mathbb{K}_{lk}]\Delta^2 - \left[s_k + s_l - 1 - \frac{1 - \tilde{n}\tau}{\vartheta}\right]\Delta - c(\alpha, \beta).$$

The optimal solution Δ_2^* is given by (4.15) and is feasible if $\beta_{\hat{l}} + \Delta_2^* \geq \beta_{\max}$.

The optimal solution is the one, which maximizes the objective (C.14a) and is feasible. ■

Proposition C.13: Update rule (4.14c) for problem (C.14)

Consider problem (C.14), update rule (4.14c), indices $n_+ + 1 \leq k \leq \tilde{n}$ and $n_+ + 1 \leq l \leq \tilde{n}$ and Notation 4.6. Let us define

$$\beta_{\max} = \max_{j \in \{1, 2, \dots, \tilde{n}\} \setminus \{\hat{k}, \hat{l}\}} \beta_j.$$

Then the bounds from (4.15) are defined as $\Delta_{lb} = -\beta_{\hat{k}}$ and $\Delta_{ub} = \beta_{\hat{l}}$ and there are three possible solutions

1. Δ_1^* is feasible if $\beta_{\max} \geq \max\{\beta_{\hat{k}} + \Delta_1^*, \beta_{\hat{l}} - \Delta_1^*\}$ and is given by (4.15) where

$$\gamma = -\frac{s_k - s_l}{\mathbb{K}_{kk} + \mathbb{K}_{ll} - \mathbb{K}_{kl} - \mathbb{K}_{lk}}, \quad \delta_1^* = \frac{\beta_{\max}}{\vartheta}.$$

2. Δ_2^* is feasible if $\beta_{\hat{k}} + \Delta_2^* \geq \max\{\beta_{\max}, \beta_{\hat{l}} - \Delta_2^*\}$ and is given by (4.15) where

$$\gamma = -\frac{s_k - s_l + \frac{\tilde{n}\tau}{\vartheta}}{\mathbb{K}_{kk} + \mathbb{K}_{ll} - \mathbb{K}_{kl} - \mathbb{K}_{lk}}, \quad \delta_2^* = \frac{\beta_{\hat{k}} + \Delta_2^*}{\vartheta}.$$

3. Δ_3^* is feasible if $\beta_{\hat{l}} - \Delta_3^* \geq \max\{\beta_{\hat{k}} + \Delta_3^*, \beta_{\max}\}$ and is given by (4.15) where

$$\gamma = -\frac{s_k - s_l - \frac{\tilde{n}\tau}{\vartheta}}{\mathbb{K}_{kk} + \mathbb{K}_{ll} - \mathbb{K}_{kl} - \mathbb{K}_{lk}}, \quad \delta_3^* = \frac{\beta_{\hat{l}} - \Delta_3^*}{\vartheta}.$$

The optimal solution Δ^* is equal to one of them, which maximizes the original objective and is feasible.

Proof:

Constraint (C.14b) is always satisfied from the definition of the update rule (4.14c). Constraint (C.14c) is also always satisfied since no α_i is updated. Using the definition of β_{\max} ,

constraint (C.14d) reads

$$\begin{aligned}\beta_{\max} &\leq \delta \vartheta, \\ 0 &\leq \beta_{\hat{k}} + \Delta \leq \delta \vartheta, \\ 0 &\leq \beta_{\hat{l}} - \Delta \leq \delta \vartheta.\end{aligned}$$

Since the optimal δ is given by (C.15), there are only two possible choices

$$\delta_1^* = \frac{\beta_{\max}}{\vartheta}, \quad \delta_2^* = \frac{\beta_{\hat{k}} + \Delta}{\vartheta}, \quad \delta_3^* = \frac{\beta_{\hat{l}} - \Delta}{\vartheta}. \quad (\text{C.16})$$

If we use any of these choices which is feasible, all upper bounds in constraint (C.14d) hold, i.e. we can simplify the constraints to

$$\begin{aligned}0 \leq \beta_{\hat{k}} + \Delta &\implies -\beta_{\hat{k}} \leq \Delta, \\ 0 \leq \beta_{\hat{l}} - \Delta &\implies \Delta \leq \beta_{\hat{l}},\end{aligned}$$

which gives the lower and upper bound of Δ . Now let us discuss how to select optimal δ :

1. Using δ_1^* from (C.16) and the update rule (4.14c), objective function (C.14a) can be rewritten as a quadratic function with respect to Δ as

$$-\frac{1}{2}[\mathbb{K}_{kk} + \mathbb{K}_{ll} - \mathbb{K}_{kl} - \mathbb{K}_{lk}]\Delta^2 - [s_k - s_l]\Delta - c(\alpha, \beta).$$

The optimal solution Δ_1^* is given by (4.15) and is feasible if

$$\beta_{\max} \geq \max\{\beta_{\hat{k}} + \Delta_1^*, \beta_{\hat{l}} - \Delta_1^*\}.$$

2. Using δ_2^* from (C.16) and the update rule (4.14c), objective function (C.14a) can be rewritten as a quadratic function with respect to Δ as

$$-\frac{1}{2}[\mathbb{K}_{kk} + \mathbb{K}_{ll} - \mathbb{K}_{kl} - \mathbb{K}_{lk}]\Delta^2 - \left[s_k - s_l + \frac{\tilde{n}\tau}{\vartheta}\right]\Delta - c(\alpha, \beta).$$

The optimal solution Δ_2^* is given by (4.15) and is feasible if

$$\beta_{\hat{k}} + \Delta_2^* \geq \max\{\beta_{\max}, \beta_{\hat{l}} - \Delta_2^*\}.$$

3. Using δ_3^* from (C.16) and the update rule (4.14c), objective function (C.14a) can be rewritten as a quadratic function with respect to Δ as

$$-\frac{1}{2}[\mathbb{K}_{kk} + \mathbb{K}_{ll} - \mathbb{K}_{kl} - \mathbb{K}_{lk}]\Delta^2 - \left[s_k - s_l - \frac{\tilde{n}\tau}{\vartheta}\right]\Delta - c(\alpha, \beta).$$

The optimal solution Δ_3^* is given by (4.15) and is feasible if

$$\beta_{\hat{l}} - \Delta_3^* \geq \max\{\beta_{\max}, \beta_{\hat{k}} + \Delta_3^*\}.$$

The optimal solution is the one, which maximizes the objective (C.14a) and is feasible. ■

Quadratic Hinge Loss

The second considered surrogate function is the quadratic hinge loss from Notation 2.1. Plugging the conjugate (4.3) of the quadratic hinge loss into the dual formulation (4.8) yields

$$\underset{\alpha, \beta, \delta}{\text{maximize}} \quad -\frac{1}{2} \begin{pmatrix} \alpha \\ \beta \end{pmatrix}^\top \mathbb{K} \begin{pmatrix} \alpha \\ \beta \end{pmatrix} + \sum_{i=1}^{n_+} \alpha_i - \frac{1}{4C} \sum_{i=1}^{n_+} \alpha_i^2 \quad (\text{C.17a})$$

$$+ \frac{1}{\vartheta} \sum_{j=1}^{\tilde{n}} \beta_j - \frac{1}{4\delta\vartheta^2} \sum_{j=1}^{\tilde{n}} \beta_j^2 - \delta\tilde{n}\tau \quad (\text{C.17b})$$

$$\text{subject to} \quad \sum_{i=1}^{n_+} \alpha_i = \sum_{j=1}^{\tilde{n}} \beta_j, \quad (\text{C.17c})$$

$$\alpha_i \geq 0, \quad i = 1, 2, \dots, n_+, \quad (\text{C.17d})$$

$$\beta_j \geq 0, \quad j = 1, 2, \dots, \tilde{n}, \quad (\text{C.17e})$$

$$\delta \geq 0, \quad (\text{C.17f})$$

Similar to the previous case, we perform maximization only with respect to (α_k, β_l) . Then for fixed feasible solution α, β , we need to maximize the objective function (C.17a-C.17b) with respect to δ , which leads to the following problem

$$\underset{\delta}{\text{maximize}} \quad -(\tilde{n}\tau)\delta - \left(\frac{1}{4\vartheta^2} \sum_{j=1}^{\tilde{n}} \beta_j^2 \right) \frac{1}{\delta}$$

$$\text{subject to} \quad \delta \geq 0,$$

with the optimal solution that equals to

$$\delta^* = \sqrt{\frac{1}{4\vartheta^2 \tilde{n}\tau} \sum_{j=1}^{\tilde{n}} \beta_j^2}. \quad (\text{C.18})$$

The following three propositions provide closed-form formulae for all three update rules.

Proposition C.14: Update rule (4.14a) for problem (C.17)

Consider problem (C.17), update rule (4.14a), indices $1 \leq k \leq n_+$ and $1 \leq l \leq n_+$ and Notation 4.6. Then the optimal solution Δ^* is given by (4.15) where

$$\begin{aligned} \Delta_{lb} &= -\alpha_k, \\ \Delta_{ub} &= \alpha_l, \\ \gamma &= -\frac{s_k - s_l + \frac{1}{2C}(\alpha_k - \alpha_l)}{\mathbb{K}_{kk} + \mathbb{K}_{ll} - \mathbb{K}_{kl} - \mathbb{K}_{lk} + \frac{1}{C}}, \\ \delta^* &= \delta. \end{aligned}$$

Proof:

Constraint (C.17c) is always satisfied from the definition of the update rule (4.14a). Constraint (C.17e) is also always satisfied since no β_j was updated. Constraint (C.17d) reads

$$\begin{aligned} 0 \leq \alpha_k + \Delta &\implies -\alpha_k \leq \Delta, \\ 0 \leq \alpha_l - \Delta &\implies \Delta \leq \alpha_l, \end{aligned}$$

which gives the lower and upper bound of Δ .

Using the update rule (4.14a), objective function (C.17a-C.17b) can be rewritten as a quadratic function with respect to Δ

$$-\frac{1}{2} \left[\mathbb{K}_{kk} + \mathbb{K}_{ll} - \mathbb{K}_{kl} - \mathbb{K}_{lk} + \frac{1}{C} \right] \Delta^2 - \left[s_k - s_l + \frac{1}{2C} (\alpha_{\hat{k}} - \alpha_{\hat{l}}) \right] \Delta - c(\alpha, \beta).$$

The optimal solution Δ^* is given by (4.15). Finally, since optimal δ is given by (C.18) and no β_j was updated, the optimal δ does not change. ■

Proposition C.15: Update rule (4.14b) for problem (C.17)

Consider problem (C.17), update rule (4.14b), indices $1 \leq k \leq n_+$ and $n_+ + 1 \leq l \leq \tilde{n}$ and Notation 4.6. Then the optimal solution Δ^* is given by (4.15) where

$$\begin{aligned} \Delta_{lb} &= \max\{-\alpha_{\hat{k}}, -\beta_{\hat{l}}\}, \\ \Delta_{ub} &= +\infty, \\ \gamma &= -\frac{s_k + s_l - 1 + \frac{\alpha_{\hat{k}}}{2C} - \frac{1}{\vartheta} + \frac{\beta_{\hat{l}}}{2\delta\vartheta^2}}{\mathbb{K}_{kk} + \mathbb{K}_{ll} + \mathbb{K}_{kl} + \mathbb{K}_{lk} + \frac{1}{2C} + \frac{1}{2\delta\vartheta^2}}, \\ \delta^* &= \sqrt{\delta^2 + \frac{1}{4\vartheta^2\tilde{n}\tau} (\Delta^{*2} + 2\Delta^*\beta_{\hat{l}})}. \end{aligned}$$

Proof:

Constraint (C.17c) is always satisfied from the definition of the update rule (4.14b). Constraints (C.17d) and (C.17e) reads

$$\begin{aligned} 0 \leq \alpha_{\hat{k}} + \Delta &\implies -\alpha_{\hat{k}} \leq \Delta, \\ 0 \leq \beta_{\hat{l}} + \Delta &\implies -\beta_{\hat{l}} \leq \Delta, \end{aligned}$$

which gives the lower bound of Δ . In this case, Δ has no upper bound.

Using the update rule (4.14b), objective function (C.17a-C.17b) can be rewritten as a quadratic function with respect to Δ

$$\begin{aligned} &-\frac{1}{2} \left[\mathbb{K}_{kk} + \mathbb{K}_{ll} + \mathbb{K}_{kl} + \mathbb{K}_{lk} + \frac{1}{2C} + \frac{1}{2\delta\vartheta^2} \right] \Delta^2 \\ &\quad - \left[s_k + s_l - 1 + \frac{\alpha_{\hat{k}}}{2C} - \frac{1}{\vartheta} + \frac{\beta_{\hat{l}}}{2\delta\vartheta^2} \right] \Delta - c(\alpha, \beta). \end{aligned}$$

The optimal solution Δ^* is given by (4.15). We know that the optimal δ^* is given by (C.18), then

$$\delta^* = \sqrt{\frac{1}{4\vartheta^2\tilde{n}\tau} \left(\sum_{j \neq \hat{l}} \beta_j^2 + (\beta_{\hat{l}} + \Delta^*)^2 \right)} = \sqrt{\delta^2 + \frac{1}{4\vartheta^2\tilde{n}\tau} (\Delta^{*2} + 2\Delta^*\beta_{\hat{l}})}.$$

Proposition C.16: Update rule (4.14c) for problem (C.17)

Consider problem (C.17), update rule (4.14c) indices $n_+ + 1 \leq k \leq \tilde{n}$ and $n_+ + 1 \leq l \leq \tilde{n}$ and Notation 4.6. Then the optimal solution Δ^* is given by (4.15) where

$$\begin{aligned}\Delta_{lb} &= -\beta_{\hat{k}}, \\ \Delta_{ub} &= \beta_{\hat{l}}, \\ \gamma &= -\frac{s_k - s_l + \frac{1}{2\delta\vartheta^2}(\beta_{\hat{k}} - \beta_{\hat{l}})}{\mathbb{K}_{kk} + \mathbb{K}_{ll} - \mathbb{K}_{kl} - \mathbb{K}_{lk} + \frac{1}{\delta\vartheta^2}}, \\ \delta^* &= \sqrt{\delta^2 + \frac{1}{2\vartheta^2\tilde{n}\tau}(\Delta^{*2} + \Delta^*(\beta_{\hat{k}} - \beta_{\hat{l}}))}.\end{aligned}$$

Proof:

Constraint (C.17c) is always satisfied from the definition of the update rule (4.14c). Constraint (C.17d) is also always satisfied since no α_i is updated. Constraint (C.17e) reads

$$\begin{aligned}0 \leq \beta_{\hat{k}} + \Delta &\implies -\beta_{\hat{k}} \leq \Delta, \\ 0 \leq \beta_{\hat{l}} - \Delta &\implies \Delta \leq \beta_{\hat{l}},\end{aligned}$$

which gives the lower and upper bound of Δ .

Using the update rule (4.14c), objective function (C.17a-C.17b) can be rewritten as a quadratic function with respect to Δ as

$$-\frac{1}{2}\left[\mathbb{K}_{kk} + \mathbb{K}_{ll} - \mathbb{K}_{kl} - \mathbb{K}_{lk} + \frac{1}{\delta\vartheta^2}\right]\Delta^2 - \left[s_k - s_l + \frac{1}{2\delta\vartheta^2}(\beta_{\hat{k}} - \beta_{\hat{l}})\right]\Delta - c(\alpha, \beta).$$

The optimal solution Δ^* is given by (4.15). We know that the optimal δ^* is given by (C.18), then

$$\delta^* = \sqrt{\frac{1}{4\vartheta^2\tilde{n}\tau}\left(\sum_{j \notin \{\hat{l}, \hat{k}\}} \beta_j^2 + (\beta_{\hat{k}} + \Delta^*)^2 + (\beta_{\hat{l}} - \Delta^*)^2\right)} = \sqrt{\delta^2 + \frac{1}{2\vartheta^2\tilde{n}\tau}(\Delta^{*2} + \Delta^*(\beta_{\hat{k}} - \beta_{\hat{l}}))}.$$

■

Initialization

As in the case of problem (4.5), all update rules (4.14) assume that the current solution α, β, δ is feasible. So to create an iterative algorithm that solves problem (C.14) or (C.17), we need to have a way how to obtain an initial feasible solution. Such a task can be formally written as a projection of random variables $\alpha^0, \beta^0, \delta^0$ to the feasible set of solutions

$$\begin{aligned}\text{minimize}_{\alpha, \beta, \delta} \quad & \frac{1}{2}\|\alpha - \alpha^0\|^2 + \frac{1}{2}\|\beta - \beta^0\|^2 + \frac{1}{2}(\delta - \delta^0)^2 \\ \text{subject to} \quad & \sum_{i=1}^{n_+} \alpha_i = \sum_{j=1}^{\tilde{n}} \beta_j, \\ & 0 \leq \alpha_i \leq C_1, \quad i = 1, 2, \dots, n_+, \\ & 0 \leq \beta_j \leq C_2\delta, \quad j = 1, 2, \dots, \tilde{n}, \\ & \delta \geq 0,\end{aligned}\tag{C.19}$$

where the upper bounds in the second and third constraints depend on the used surrogate function and are defined as follows

$$C_1 = \begin{cases} C & \text{for hinge loss,} \\ +\infty & \text{for quadratic hinge loss,} \end{cases} \quad C_2 = \begin{cases} \vartheta & \text{for hinge loss,} \\ +\infty & \text{for quadratic hinge loss.} \end{cases}$$

We show the way how to solve (C.19) only for hinge loss, since it is trivial to solve it for quadratic hinge. Again, we will follow the same approach as in [47] to solve this optimization problem. In the following theorem, we show that problem (C.19) can be written as a system of two equations of two variables λ and μ . The theorem also shows the concrete form of feasible solution α , β , δ that depends only on λ and μ .

Theorem C.17

Consider problem (C.19) and some initial solution α^0 , β^0 and δ^0 . Then if the following condition holds

$$\delta^0 \leq -C_2 \sum_{j=1}^{\tilde{n}} \text{clip}_{[0, +\infty)}(\beta_j^0 + \max_{i=1, \dots, n_+} \alpha_i^0). \quad (\text{C.20})$$

the optimal solution of (C.19) amounts to $\alpha = \beta = \mathbf{0}$ and $\delta^0 = 0$. In the opposite case, the following system of two equations

$$0 = \sum_{i=1}^{n_+} \text{clip}_{[0, C_1]}(\alpha_i^0 - \lambda) - \sum_{j=1}^{\tilde{n}} \text{clip}_{[0, \lambda + \mu]}(\beta_j^0 + \lambda), \quad (\text{C.21a})$$

$$\lambda = C_2 \delta^0 + C_2^2 \sum_{j=1}^{\tilde{n}} \text{clip}_{[0, +\infty)}(\beta_j^0 - \mu) - \mu. \quad (\text{C.21b})$$

has a solution (λ, μ) with $\lambda + \mu > 0$ and the optimal solution of (C.19) is equal to

$$\begin{aligned} \alpha_i &= \text{clip}_{[0, C_1]}(\alpha_i^0 - \lambda), \\ \beta_j &= \text{clip}_{[0, \lambda + \mu]}(\beta_j^0 + \lambda), \\ C_2 \delta &= \lambda + \mu. \end{aligned}$$

Proof:

The Lagrangian of (C.19) reads

$$\begin{aligned} \mathcal{L}(\alpha, \beta; \lambda, p, q, u, v) &= \frac{1}{2} \|\alpha - \alpha^0\|^2 + \frac{1}{2} \|\beta - \beta^0\|^2 + \frac{1}{2} (\delta - \delta^0)^2 + \lambda \left(\sum_{i=1}^{n_+} \alpha_i - \sum_{j=1}^{\tilde{n}} \beta_j \right) \\ &\quad - \sum_{i=1}^{n_+} p_i \alpha_i + \sum_{i=1}^{n_+} q_i (\alpha_i - C_1) - \sum_{j=1}^{\tilde{n}} u_j \beta_j + \sum_{j=1}^{\tilde{n}} v_j (\beta_j - C_2 \delta). \end{aligned}$$

The KKT conditions then amount to the optimality conditions

$$\frac{\partial \mathcal{L}}{\partial \alpha_i} = \alpha_i - \alpha_i^0 + \lambda - p_i + q_i = 0, \quad i = 1, 2, \dots, n_+, \quad (\text{C.22a})$$

$$\frac{\partial \mathcal{L}(\cdot)}{\partial \beta_j} = \beta_j - \beta_j^0 - \lambda - u_j + v_j = 0, \quad j = 1, 2, \dots, \tilde{n}, \quad (\text{C.22b})$$

$$\frac{\partial \mathcal{L}(\cdot)}{\partial \delta} = \delta - \delta^0 - C_2 \sum_{j=1}^{\tilde{n}} v_j = 0, \quad (\text{C.22c})$$

the primal feasibility conditions (C.19), the dual feasibility conditions $\lambda \in \mathbb{R}$, $p_i \geq 0$, $q_i \geq 0$, $u_j \geq 0$, $v_j \geq 0$ and finally the complementarity conditions

$$p_i \alpha_i = 0, \quad i = 1, 2, \dots, n_+, \quad (\text{C.22d})$$

$$q_i (\alpha_i - C_1) = 0, \quad i = 1, 2, \dots, n_+, \quad (\text{C.22e})$$

$$u_j \beta_j = 0, \quad j = 1, 2, \dots, \tilde{n}, \quad (\text{C.22f})$$

$$v_j (\beta_j - C_2 \delta) = 0, \quad j = 1, 2, \dots, \tilde{n}. \quad (\text{C.22g})$$

Case 1: The first case concerns when the optimal solution satisfies $\delta = 0$. From the primal feasibility conditions, we immediately get $\alpha_i = 0$ for all i and $\beta_j = 0$ for all j . Then (C.22e) implies $q_i = 0$ and all complementarity conditions are satisfied. Moreover, (C.22a) implies for all i

$$\lambda = \alpha_i^0 + p_i.$$

Since the only condition on p_i is the non-negativity, this implies $\lambda \geq \max_i \alpha_i^0$.

Similarly, from (C.22b) we deduce

$$v_j = \beta_j^0 + \lambda + u_j \geq \beta_j^0 + \lambda \geq \beta_j^0 + \max_{i=1, \dots, n_+} \alpha_i^0.$$

Since we also have the non-negativity constraint on v_j , this implies

$$v_j \geq \text{clip}_{[0, +\infty)} \left(\beta_j^0 + \max_{i=1, \dots, n_+} \alpha_i^0 \right).$$

Condition (C.22c) implies

$$\delta^0 = -C_2 \sum_{j=1}^{\tilde{n}} v_j \leq -C_2 \sum_{j=1}^{\tilde{n}} \text{clip}_{[0, +\infty)} \left(\beta_j^0 + \max_{i=1, \dots, n_+} \alpha_i^0 \right),$$

which is precisely condition (C.20).

Case 2: If (C.20) holds true, then from the discussion above we obtain that the optimal solution satisfies $\delta > 0$. For any fixed i , the standard trick is to combine the optimality condition (C.22a) with the primal feasibility condition $0 \leq \alpha_i \leq C_1$, the dual feasibility conditions $p_i \geq 0$, $q_i \geq 0$ and the complementarity conditions (C.22d, C.22e) to obtain

$$\alpha_i = \text{clip}_{[0, C_1]} (\alpha_i^0 - \lambda). \quad (\text{C.23})$$

Similarly for any fixed j , we combine the optimality condition (C.22b) with the primal feasibility condition $0 \leq \beta_j \leq C_2\delta$, the dual feasibility conditions $u_j \geq 0$, $v_j \geq 0$ and the complementarity conditions (C.22f, C.22g) to obtain

$$\beta_j = \text{clip}_{[0, C_2\delta]}(\beta_j^0 + \lambda), \quad (\text{C.24})$$

$$v_j = \text{clip}_{[0, +\infty)}(\beta_j^0 + \lambda - C_2\delta). \quad (\text{C.25})$$

Note that we now obtain the following system

$$\begin{aligned} \sum_{i=1}^{n_+} \text{clip}_{[0, C_1]}(\alpha_i^0 - \lambda) - \sum_{j=1}^{\tilde{n}} \text{clip}_{[0, C_2\delta]}(\beta_j^0 + \lambda) &= 0, \\ \delta - \delta^0 - C_2 \sum_{j=1}^{\tilde{n}} \text{clip}_{[0, +\infty)}(\beta_j^0 + \lambda - C_2\delta) &= 0. \end{aligned}$$

Here, the first equation follows from plugging (C.23) and (C.24) into the feasibility condition $\sum_i \alpha_i = \sum_j \beta_j$ while the second equation follows from plugging (C.25) into (C.22c). Finally, system (C.21) follows after making the substitution $C_2\delta = \lambda + \mu$. ■

System (C.21) is relatively simple to solve, since equation (C.21b) provides an explicit formula for λ . Let us denote it as $\lambda(\mu)$, then we denote the right-hand side of (C.21a) as

$$h(\mu) := \sum_{i=1}^{n_+} \text{clip}_{[0, C_1]}(\alpha_i^0 - \lambda(\mu)) - \sum_{j=1}^{\tilde{n}} \text{clip}_{[0, \lambda(\mu)+\mu]}(\beta_j^0 + \lambda(\mu)). \quad (\text{C.26})$$

Then the system of equations (C.21) is equivalent to solving $h(\mu) = 0$. The following lemma states that h is a non-decreasing function in μ on $(0, \infty)$ and thus the equation $h(\mu) = 0$ is simple to solve using any root-finding method. Note that if $\delta^0 < 0$, then it may happen that $\lambda + \mu < 0$ if the initial μ is chosen large. In such a case, it suffices to decrease μ until $\lambda + \mu$ is positive.

Lemma C.18

Function h is non-decreasing in μ on $(0, \infty)$.

Proof of Lemma C.18 on page 119:

Consider any $\mu_1 < \mu_2$. Then from (C.21b) we obtain both $\lambda(\mu_1) \geq \lambda(\mu_2)$ and $\mu_1 + \lambda(\mu_1) \geq \mu_2 + \lambda(\mu_2)$. The statement then follows from the definition of h in (C.26). ■

Appendix for Chapter 5

Lemma 5.3

Let j^\star be unique. Assume that the selection of positive and negative samples into the minibatch is independent and that the threshold is computed from negative samples while the objective is computed from positive samples. Then the conditional expectation of the sampled gradient satisfies

$$\mathbb{E}[\nabla \hat{L}(w) | j_{\text{mb}}^\star = j^\star] = \nabla L(w).$$

Proof of Lemma 5.3 on page 53:

If j^\star is unique, then the true threshold t is a differentiable function of weights w . The differentiability of L and \hat{L} follows from the chain rule. If $j_{\text{mb}}^\star = j^\star$ holds, then the sampled gradient equals to

$$\nabla \hat{L}(w) = \lambda w + \frac{1}{n_{\text{mb},+}} \sum_{i \in \mathcal{I}_{\text{mb},+}} l'(t - f(x_i; w)) (\nabla f(x_{j^\star}; w) - \nabla f(x_i; w)). \quad (\text{D.1})$$

The summands are identical to the ones in (5.2). Since the sum is performed with respect to positive samples, the threshold is computed from negative samples, the lemma statement follows. ■

Theorem 5.4

Under the assumptions of Lemma 5.3, the bias of the sampled gradient from (5.4) satisfies

$$\text{bias}(w) = \mathbb{P}[j_{\text{mb}}^\star \neq j^\star] (\nabla L(w) - \mathbb{E}[\nabla \hat{L}(w) | j_{\text{mb}}^\star \neq j^\star]). \quad (5.8)$$

Proof of Theorem 5.4 on page 53:

The law of total expectation implies

$$\mathbb{E} \nabla \hat{L}(w) = \mathbb{P}[j_{\text{mb}}^\star = j^\star] \mathbb{E}[\nabla \hat{L}(w) | j_{\text{mb}}^\star = j^\star] + \mathbb{P}[j_{\text{mb}}^\star \neq j^\star] \mathbb{E}[\nabla \hat{L}(w) | j_{\text{mb}}^\star \neq j^\star],$$

from where the statement follows due to definition (5.4) and Lemma 5.3. ■

Bibliography

- [1] Tom M Mitchell and Tom M Mitchell. *Machine learning*, volume 1. McGraw-hill New York, 1997.
- [2] Charu C Aggarwal. *Artificial Intelligence-A Textbook*. Springer, 2021.
- [3] Vaibhav Swaminathan, Shrey Arora, Ravi Bansal, and R Rajalakshmi. Autonomous driving system with road sign recognition using convolutional neural networks. In *2019 International Conference on Computational Intelligence in Data Science (ICCIDS)*, pages 1–4, 2019.
- [4] Giuseppe Viale. The current state of breast cancer classification. *Annals of Oncology*, 23:207–210, 2012.
- [5] Daniel Lévy and Arzav Jain. Breast mass classification from mammograms using deep convolutional neural networks. *arXiv preprint arXiv:1612.00542*, 2016.
- [6] Patrick Pantel, Dekang Lin, et al. Spamcop: A spam classification & organization program. In *Proceedings of AAAI-98 Workshop on Learning for Text Categorization*, pages 95–98, 1998.
- [7] Martin Grill and Tomáš Pevný. Learning combination of anomaly detectors for security domain. *Computer Networks*, 107:55–63, 2016.
- [8] Karen Scarfone, Peter Mell, et al. Guide to intrusion detection and prevention systems (idps). *NIST special publication*, 800(2007):94, 2007.
- [9] Giorgio Giacinto and Fabio Roli. Intrusion detection in computer networks by multiple classifier systems. In *Object recognition supported by user interaction for service robots*, volume 2, pages 390–393. IEEE, 2002.
- [10] Shashank Shanbhag and Tilman Wolf. Accurate anomaly detection through parallelism. *IEEE network*, 23(1):22–28, 2009.
- [11] Frederick Kaefer, Carrie M Heilman, and Samuel D Ramenofsky. A neural network application to consumer classification to improve the timing of direct marketing activities. *Computers & Operations Research*, 32(10):2595–2615, 2005.
- [12] Xi-Zheng Zhang. Building personalized recommendation system in e-commerce using association rule-based mining and classification. In *2007 International Conference on Machine Learning and Cybernetics*, volume 7, pages 4113–4118. IEEE, 2007.
- [13] Tom Fawcett. An introduction to roc analysis. *Pattern recognition letters*, 27(8):861–874, 2006.
- [14] Charles E Metz. Basic principles of roc analysis. In *Seminars in nuclear medicine*, volume 8, pages 283–298. Elsevier, 1978.

- [15] Kay Henning Brodersen, Cheng Soon Ong, Klaas Enno Stephan, and Joachim M Buhmann. The balanced accuracy and its posterior distribution. In *2010 20th international conference on pattern recognition*, pages 3121–3124. IEEE, 2010.
- [16] Mohammad Hossin and Md Nasir Sulaiman. A review on evaluation metrics for data classification evaluations. *International journal of data mining & knowledge management process*, 5(2):1, 2015.
- [17] James P Egan and James Pendleton Egan. *Signal detection theory and ROC-analysis*. Academic press, 1975.
- [18] Andrew P Bradley. The use of the area under the roc curve in the evaluation of machine learning algorithms. *Pattern recognition*, 30(7):1145–1159, 1997.
- [19] James A Hanley and Barbara J McNeil. The meaning and use of the area under a receiver operating characteristic (roc) curve. *Radiology*, 143(1):29–36, 1982.
- [20] Corinna Cortes and Mehryar Mohri. AUC optimization vs. error rate minimization. *Advances in neural information processing systems*, 16, 2003.
- [21] Yoav Freund, Raj Iyer, Robert E Schapire, and Yoram Singer. An efficient boosting algorithm for combining preferences. *The Journal of machine learning research*, 4:933–969, 2003.
- [22] Yoav Freund and Robert E Schapire. A decision-theoretic generalization of on-line learning and an application to boosting. *Journal of computer and system sciences*, 55(1):119–139, 1997.
- [23] Cynthia Rudin. The p-norm push: A simple convex ranking algorithm that concentrates at the top of the list. *J. Mach. Learn. Res.*, 10:2233–2271, December 2009.
- [24] Shivani Agarwal. The infinite push: A new support vector ranking algorithm that directly optimizes accuracy at the absolute top of the list. In *Proceedings of the 2011 SIAM International Conference on Data Mining*, pages 839–850. SIAM, 2011.
- [25] Corinna Cortes and Vladimir Vapnik. Support-vector networks. *Machine learning*, 20(3):273–297, 1995.
- [26] Nan Li, Rong Jin, and Zhi-Hua Zhou. Top rank optimization in linear time. In *Advances in neural information processing systems*, NIPS’14, pages 1502–1510, Cambridge, MA, USA, 2014. MIT Press.
- [27] Stephen Boyd, Corinna Cortes, Mehryar Mohri, and Ana Radovanovic. Accuracy at the top. In *Advances in neural information processing systems*, pages 953–961, 2012.
- [28] Thorsten Joachims. A support vector method for multivariate performance measures. In *Proceedings of the 22nd International Conference on Machine Learning*, ICML ’05, pages 377–384, New York, NY, USA, 2005. ACM.
- [29] Elad ET Eban, Mariano Schain, Alan Mackey, Ariel Gordon, Rif A Saurous, and Gal Elidan. Scalable learning of non-decomposable objectives. In *Artificial Intelligence and Statistics*, pages 832–840, 2017.
- [30] Dirk Tasche. A plug-in approach to maximising precision at the top and recall at the top. *arXiv preprint arXiv:1804.03077*, 2018.

- [31] Jerzy Neyman and Egon Sharpe Pearson. On the problem of the most efficient tests of statistical hypotheses. *Philosophical Transactions of the Royal Society of London. Series A, Containing Papers of a Mathematical or Physical Character*, 231(694-706):289–337, 1933.
- [32] Maksim Lapin, Matthias Hein, and Bernt Schiele. Top-k multiclass svm. In *Advances in Neural Information Processing Systems*, pages 325–333, 2015.
- [33] Ao Zhang, Nan Li, Jian Pu, Jun Wang, Junchi Yan, and Hongyuan Zha. *tau-fpl*: Tolerance-constrained learning in linear time. *arXiv preprint arXiv:1801.04701*, 2018.
- [34] Lukáš Adam, Václav Mácha, Václav Šmídl, and Tomáš Pevný. General framework for binary classification on top samples. *Optimization Methods and Software*, pages 1–32, 2021.
- [35] Stephen Boyd and Lieven Vandenberghe. *Convex optimization*. Cambridge university press, 2004.
- [36] Mark Schmidt, Nicolas Le Roux, and Francis Bach. Minimizing finite sums with the stochastic average gradient. *Mathematical Programming*, 162(1-2):83–112, 2017.
- [37] Václav Mácha, Lukáš Adam, and Václav Šmídl. Nonlinear classifiers for ranking problems based on kernelized svm. *arXiv preprint arXiv:2002.11436*, 2020.
- [38] Alan Mackey, Xiyang Luo, and Elad Eban. Constrained classification and ranking via quantiles. *arXiv preprint arXiv:1803.00067*, 2018.
- [39] Lukáš Adam and Martin Branda. Machine learning approach to chance-constrained problems: An algorithm based on the stochastic gradient descent. *arXiv preprint arXiv:1905.10986*, 2019.
- [40] Bernhard Scholkopf and Alexander J Smola. *Learning with kernels: support vector machines, regularization, optimization, and beyond*. MIT press, 2001.
- [41] Shai Shnlev-Shwartz and Tong Zhang. Accelerated proximal stochastic dual coordinate ascent for regularized loss minimization. In *31st International Conference on Machine Learning, ICML 2014*, volume 1, page 111, 2014.
- [42] Takafumi Kanamori, Akiko Takeda, and Taiji Suzuki. Conjugate relation between loss functions and uncertainty sets in classification problems. *The Journal of Machine Learning Research*, 14(1):1461–1504, 2013.
- [43] Kai-Wei Chang, Cho-Jui Hsieh, and Chih-Jen Lin. Coordinate descent method for large-scale l2-loss linear support vector machines. *Journal of Machine Learning Research*, 9(Jul):1369–1398, 2008.
- [44] Cho-Jui Hsieh, Kai-Wei Chang, Chih-Jen Lin, S Sathiya Keerthi, and Sellamanickam Sundararajan. A dual coordinate descent method for large-scale linear svm. In *Proceedings of the 25th international conference on Machine learning*, pages 408–415. ACM, 2008.
- [45] Zeynep Batmaz, Ali Yurekli, Alper Bilge, and Cihan Kaleli. A review on deep learning for recommender systems: challenges and remedies. *Artificial Intelligence Review*, 52(1):1–37, 2019.
- [46] Tino Werner. A review on ranking problems in statistical learning. *arXiv preprint arXiv:1909.02998*, 2019.
- [47] Lukáš Adam and V Mácha. Projections onto the canonical simplex with additional linear inequalities. *Optimization Methods and Software*, pages 1–29, 2020.

- [48] Léon Bottou, Frank E Curtis, and Jorge Nocedal. Optimization methods for large-scale machine learning. *Siam Review*, 60(2):223–311, 2018.
- [49] Peter W. Glynn. Importance sampling for monte carlo estimation of quantiles. In *Proc. 2nd St. Petersburg Workshop on Simulation*, pages 180–185, St Petersburg, Russia, 1996. Publishing House of Saint Petersburg University.
- [50] Yang You, Jing Li, Sashank Reddi, Jonathan Hseu, Sanjiv Kumar, Srinadh Bhojanapalli, Xiaodan Song, James Demmel, Kurt Keutzer, and Cho-Jui Hsieh. Large batch optimization for deep learning: Training bert in 76 minutes. *arXiv preprint arXiv:1904.00962*, 2019.
- [51] Jorge Nocedal and Stephen Wright. *Numerical optimization*. Springer Science & Business Media, 2006.
- [52] Bernhard E Boser, Isabelle M Guyon, and Vladimir N Vapnik. A training algorithm for optimal margin classifiers. In *Proceedings of the fifth annual workshop on Computational learning theory*, pages 144–152, 1992.
- [53] Chih-Chung Chang and Chih-Jen Lin. Libsvm: a library for support vector machines. *ACM transactions on intelligent systems and technology (TIST)*, 2(3):1–27, 2011.
- [54] Milton Friedman. A comparison of alternative tests of significance for the problem of m rankings. *The Annals of Mathematical Statistics*, 11(1):86–92, 1940.
- [55] Janez Demšar. Statistical comparisons of classifiers over multiple data sets. *Journal of Machine learning research*, 7:1–30, 2006.
- [56] Peter Bjorn Nemenyi. *Distribution-free multiple comparisons*. Princeton University, 1963.
- [57] Jeff Bezanson, Alan Edelman, Stefan Karpinski, and Viral B Shah. Julia: A fresh approach to numerical computing. *SIAM review*, 59(1):65–98, 2017.
- [58] Mike Innes. Flux: Elegant machine learning with julia. *Journal of Open Source Software*, 2018.
- [59] Michael Innes, Elliot Saba, Keno Fischer, Dhairya Gandhi, Marco Concetto Rudilosso, Neethu Mariya Joy, Tejan Karmali, Avik Pal, and Viral Shah. Fashionable modelling with flux. *CoRR*, abs/1811.01457, 2018.
- [60] Li Deng. The mnist database of handwritten digit images for machine learning research. *IEEE Signal Processing Magazine*, 29(6):141–142, 2012.
- [61] Han Xiao, Kashif Rasul, and Roland Vollgraf. Fashion-mnist: a novel image dataset for benchmarking machine learning algorithms. *arXiv preprint arXiv:1708.07747*, 2017.
- [62] Alex Krizhevsky, Geoffrey Hinton, et al. *Learning multiple layers of features from tiny images*. Citeseer, 2009.
- [63] Yuval Netzer, Tao Wang, Adam Coates, Alessandro Bissacco, Bo Wu, and Andrew Y Ng. Reading digits in natural images with unsupervised feature learning. In *Advances in neural information processing systems*, NIPS’11, pages 1502–1510, 2011.
- [64] Diederik Kingma and Jimmy Ba. Adam: A method for stochastic optimization. *arXiv preprint arXiv:1412.6980*, 2014.
- [65] Vincent G Sigillito, Simon P Wing, Larrie V Hutton, and Kile B Baker. Classification of radar returns from the ionosphere using neural networks. *Johns Hopkins APL Technical Digest*, 10(3):262–266, 1989.

- [66] Tayana Morkel, Jan HP Eloff, and Martin S Olivier. An overview of image steganography. In *ISSA*, number 2, pages 1–11, 2005.
- [67] Joshua Silman. Steganography and steganalysis: an overview. *Sans Institute*, 3:61–76, 2001.
- [68] Jessica Fridrich, Tomáš Pevný, and Jan Kodovský. Statistically undetectable jpeg steganography: dead ends challenges, and opportunities. In *Proceedings of the 9th workshop on Multimedia & security*, pages 3–14, 2007.
- [69] Rémi Cigranne, Quentin Giboulot, and Patrick Bas. Steganography by minimizing statistical detectability: The cases of jpeg and color images. In *Proceedings of the 2020 ACM Workshop on Information Hiding and Multimedia Security*, pages 161–167, 2020.
- [70] Jan Kodovský and Jessica Fridrich. Steganalysis of jpeg images using rich models. In *Media Watermarking, Security, and Forensics 2012*, volume 8303, pages 81–93. SPIE, 2012.
- [71] The Independent JPEG Group’s JPEG software. *Libjpeg*, 2014.
- [72] Mingxing Tan and Quoc Le. Efficientnet: Rethinking model scaling for convolutional neural networks. In *International Conference on Machine Learning*, pages 6105–6114. PMLR, 2019.
- [73] Tomáš Pevný and Petr Somol. Using neural network formalism to solve multiple-instance problems. In *International Symposium on Neural Networks*, pages 135–142. Springer, 2017.
- [74] Simon Mandlik, Matej Racinsky, Viliam Lisy, and Tomas Pevny. Mill. jl and jsongrinder. jl: automated differentiable feature extraction for learning from raw json data. *arXiv preprint arXiv:2105.09107*, 2021.
- [75] Włodzimierz Ogryczak and Arie Tamir. Minimizing the sum of the k largest functions in linear time. *Information Processing Letters*, 85(3):117–122, 2003.